ALEX(01)-TR-76-02

PRELIMINARY EVALUATION OF THE SEISMIC RESEARCH OBSERVATORIES

TECHNICAL REPORT NO. 2

VELA NETWORK EVALUATION AND AUTOMATIC PROCESSING RESEARCH

Prepared by
Alan C. Strauss

TEXAS INSTRUMENTS INCORPORATED
Equipment Group
Post Office Box 6015
Dallas, Texas 75222

Prepared for

AIR FORCE TECHNICAL APPLICATIONS CENTER
Alexandria, Virginia 22314

Sponsored by

ADVANCED RESEARCH PROJECTS AGENCY
Nuclear Monitoring Research Office
ARPA Program Code No. 6F10
ARPA Order No. 2551

29 October 1976

Acknowledgment: This research was supported by the Advanced Research Projects Agency, Nuclear Monitoring Research Office, under Project VELA-UNIFORM, and accomplished under the technical direction of the Air Force Technical Applications Center under Contract Number F08606-76-C-0011.

APPROVED FOR PUBLIC RELEASE, DISTRIBUTION UNLIMITED

ALEX(01)-TR-76-02

PRELIMINARY EVALUATION OF THE SEISMIC RESEARCH OBSERVATORIES

TECHNICAL REPORT NO. 2

VELA NETWORK EVALUATION AND AUTOMATIC PROCESSING RESEARCH

Prepared by
Alan C. Strauss

TEXAS INSTRUMENTS INCORPORATED
Equipment Group
Post Office Box 6015
Dallas, Texas 75222

Prepared for

AIR FORCE TECHNICAL APPLICATIONS CENTER
Alexandria, Virginia 22314

Sponsored by

ADVANCED RESEARCH PROJECTS AGENCY
Nuclear Monitoring Research Office
ARPA Program Code No. 6F10
ARPA Order No. 2551

29 October 1976

Acknowledgment: This research was supported by the Advanced Research Projects Agency, Nuclear Monitoring Research Office, under Project VELA-UNIFORM, and accomplished under the technical direction of the Air Force Technical Applications Center under Contract Number F08606-76-C-0011.

(See 1473)

UNCLASSIFIED

SECURITY CLASSIFICATION OF THIS PAGE (When Data Entered)

REPORT DOCUMENTATION PAGE		READ INSTRUCTIONS BEFORE COMPLETING FORM
1. REPORT NUMBER	2. GOVT ACCESSION NO.	3. RECIPIENT'S CATALOG NUMBER
4. TITLE (and Subtitle) PRELIMINARY EVALUATION OF THE SEISMIC RESEARCH OBSERVATORIES.		5. TYPE OF REPORT & PERIOD COVERED Technical rept.,
		6. PERFORMING ORG. REPORT NUMBER TI-ALEX(01)-TR-76-02
7. AUTHOR(s) Alan C. Strauss		8. CONTRACT OR GRANT NUMBER(s) F08606-76-C-0011, ARPA Order-2551
9. PERFORMING ORGANIZATION NAME AND ADDRESS Texas Instruments Incorporated Equipment Group Dallas, Texas 75222		10. PROGRAM ELEMENT, PROJECT, TASK AREA & WORK UNIT NUMBERS VELA T/6705/B/ETR
11. CONTROLLING OFFICE NAME AND ADDRESS Advanced Research Projects Agency Nuclear Monitoring Research Office Arlington, Virginia 22209		12. REPORT DATE 29 Oct[redacted]76
		13. NUMBER OF PAGES 116 117p.
14. MONITORING AGENCY NAME & ADDRESS (if different from Controlling Office) Air Force Technical Applications Center VELA Seismological Center Alexandria, Virginia 22314		15. SECURITY CLASS. (of this report) UNCLASSIFIED
		15a. DECLASSIFICATION/DOWNGRADING SCHEDULE

16. DISTRIBUTION STATEMENT (of this Report)

APPROVED FOR PUBLIC RELEASE, DISTRIBUTION UNLIMITED

17. DISTRIBUTION STATEMENT (of the abstract entered in Block 20, if different from Report)

18. SUPPLEMENTARY NOTES

ARPA Order No. 2551

19. KEY WORDS (Continue on reverse side if necessary and identify by block number)

Seismic Research Observatories
Data Quality
RMS Noise Levels
Noise Spectral Content
Detection Capability
Discrimination Capability
M_s - m_b Relationships

20. ABSTRACT (Continue on reverse side if necessary and identify by block number)

This report describes the preliminary evaluation of five of the projected ten Seismic Research Observatories (SRO). This evaluation was performed by Texas Instruments Incorporated at the Seismic Data Analysis Center in Alexandria, Virginia.

The major areas of study in the evaluation were as follows:

over

405076

DD FORM 1 JAN 73 1473 EDITION OF 1 NOV 65 IS OBSOLETE

UNCLASSIFIED

SECURITY CLASSIFICATION OF THIS PAGE (When Data Entered)

20. continued

- Analysis of RMS noise levels, RMS noise trends, and noise spectral content.
- Estimation of the detection capability of the individual stations.
- Analysis of $M_s - m_b$ relationships.

Conclusions regarding the above points and plans regarding necessary future work are presented in this report.

M sub s - m sub b

ABSTRACT

This report describes the preliminary evaluation of five of the projected ten Seismic Research Observatories (SRO). This evaluation was performed by Texas Instruments Incorporated at the Seismic Data Analysis Center in Alexandria, Virginia.

The major areas of study in the evaluation were as follows:

- Analysis of RMS noise levels, RMS noise trends, and noise spectral content.
- Estimation of the detection capability of the individual stations.
- Analysis of $M_s - m_b$ relationships.

Conclusions regarding the above points and plans regarding necessary future work are presented in this report.

TABLE OF CONTENTS

TABLE OF CONTENTS
(continued)

LIST OF FIGURES

LIST OF FIGURES
(continued)

LIST OF FIGURES
(continued)

LIST OF TABLES

SECTION I
INTRODUCTION

It has been noted that a significant amount of long-period seismic data recorded at surface-sited instruments is degraded or obscured by wind-induced earth tilts. Tests and theoretical data indicated that this noise could be avoided by locating the sensors at a depth of 100 meters or more. This report presents the results of the work conducted to date on the evaluation of the Seismic Research Observatories, which were built to implement this observation.

The specific goals of this evaluation are as follows:

- To evaluate the quality of the short-period and long-period data recorded at each SRO.
- To investigate the short-period and long-period noise field at each SRO.
- To estimate the detection capability of each SRO.
- To estimate the discrimination capability of each SRO.

Since this is the initial evaluation of the SRO system, we shall briefly describe the operation of an arbitrary station, the concept of the automatic short-period processor, and the digital recording format.

Sufficient data was available from five SRO stations to permit this evaluation in terms of the points listed above. These stations are Albuquerque, New Mexico (ANMO); Guam, Marianas Islands (GUMO); Mashhad, Iran (MAIO); Narrogin, Western Australia (NWAO); and Wellington, New Zealand (SNZO).

In Section II of this report we briefly describe the operation of a Seismic Research Observatory. The data base is described in Section III. The noise field analysis is described in Section IV. Details of the detection and discrimination capability evaluation are presented in Sections V and VI. Section VII summarizes results, presents conclusions, and suggests possible areas of further investigation utilizing SRO data.

SECTION II

OPERATION OF THE SEISMIC RESEARCH OBSERVATORIES

In this section we shall briefly describe the design and operation of a Seismic Research Observatory, with notes on the digital tape format and operation of the short-period automatic detector.

A. THE SEISMIC RESEARCH OBSERVATORY

Each Seismic Research Observatory produces four seismograms daily and a digital magnetic tape about every two weeks. Vertical, north, and east components of long-period motion are recorded in analog form on Helicorders and in digital form on tape. Vertical-component short-period motion is recorded continuously on a Helicorder, with selected time segments also recorded in digital form on tape.

The SRO borehole seismometer contains three sensor modules, a module leveling device, and electronics for control and signal conditioning. Normal depth of installation is 100 meters. The sensors are force-balance accelerometers having closed loop periods of 1 second. Output is flat to earth acceleration over the period range of 1 to 50 seconds. These broadband signals are filtered in a well-head terminal to produce conventional short-period and long-period outputs that are treated independently in the recording process. The well-head terminal also contains the controls needed to lock, unlock, level, and calibrate the sensors.

The digital portion of the SRO recording system consists of anti-aliasing filters, a gain-ranging analog-to-digital converter, two nine-track synchronous-type tape drives, a digital clock, and a mini-computer with 8K core memory. The operator communicates with the central processor through a teletypewriter, and the printout serves as a log of station operations. A digital data monitor is provided so that the operator can check the validity of the digital data. Long-period signals are sampled once each second and short-period signals are sampled twenty times each second. Long-period data are quantized at 5 computer counts per millimicron of ground motion. Short-period data are quantized at 2000 computer counts per millimicron of ground motion at 1 second period with the following exceptions. Beginning 1 May 1976 at the Guam SRO, 14 April 1976 at the Wellington, New Zealand SRO, and the operational date at the Taipei, Taiwan SRO, the data are quantized at 2 computer counts per millimicron. The data samples are gain-ranged and counted to 11 data bits, a sign bit, and 4 bits defining a gain factor.

Each SRO station is furnished with a power subsystem consisting of a battery charger, 20 lead-cadmium batteries, and an inverter. The batteries will power the station for 8 hours in the event of a line power failure. At some of the SRO stations, the seismometer is installed at a remote site to avoid cultural noise. The data are first digitized, then transmitted by telephone circuit or radio to the recording location.

B. THE SHORT-PERIOD EVENT DETECTION PROCESSOR

The SRO software includes a short-period event detection processor. The design of this detector is illustrated by Figure II-1 and may be summarized as follows. The short-period data format consists of a 12-bit integer quantity and a 4-bit scaling exponent. At the input to the detector, the gain-ranged seismic data is converted to integer 12-bit data. This data is then passed through a band-limiting bandpass filter. The output from the filter is rectified and processed through a short-term exponential averager with a time constant of one second. The output from the short-term averager is

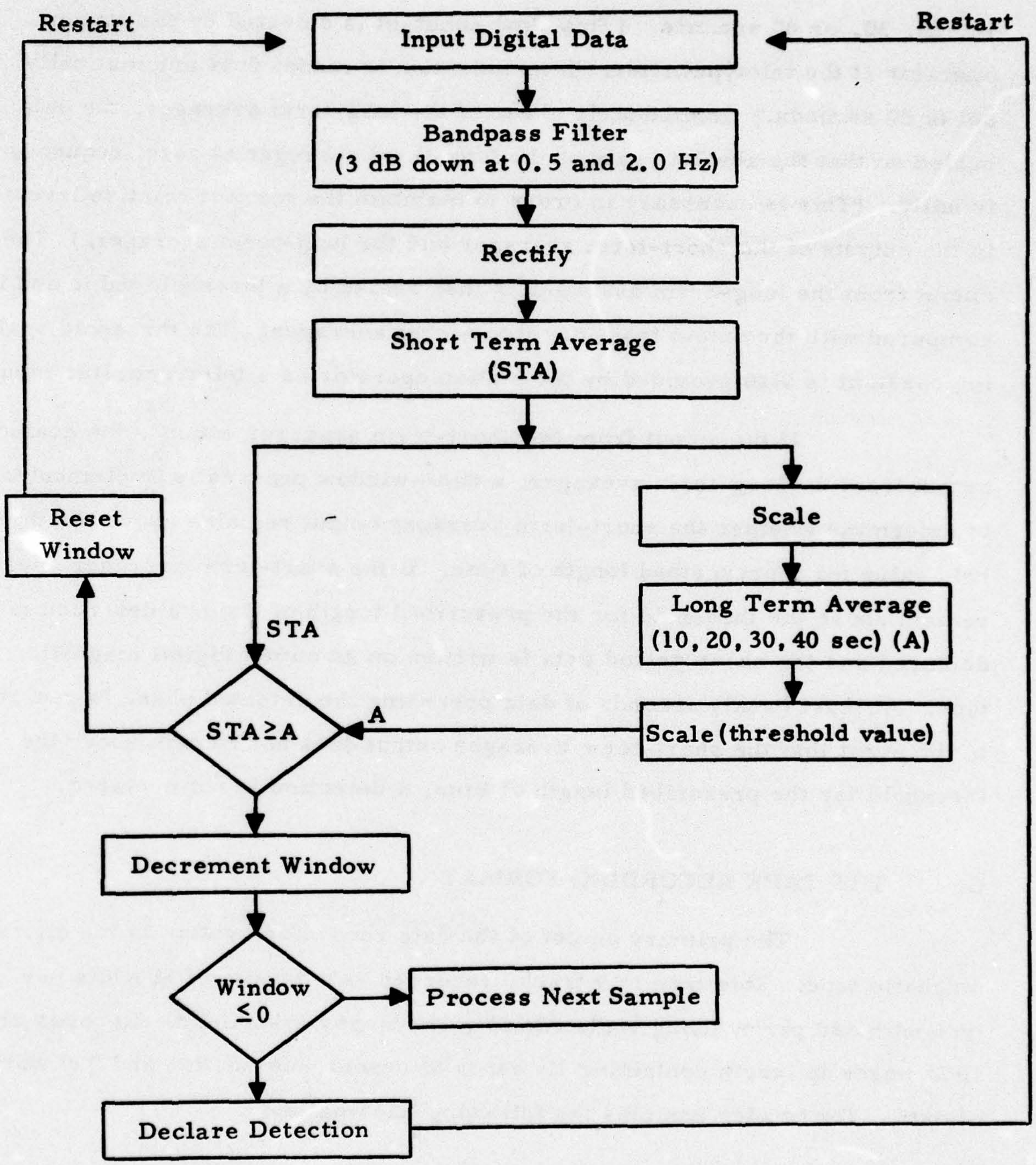

FIGURE II-1
SHORT-PERIOD DETECTOR CONCEPT

processed through a long-term exponential averager with a time constant of 10, 20, 30, or 40 seconds. (This time constant is selected by the station operator at the teletypewriter. If no selection is made, it is automatically set to 20 seconds.) Immediately ahead of the long-term averager, the data is scaled so that the absolute gain of the long-term averager at zero frequency is unity. (This is necessary in order to maintain the correct relative levels in the outputs of the short-term averager and the long-term averager.) The output from the long-term averager is then scaled by a threshold value and is compared with the output from the short-term averager. The threshold scaling constant is also provided by the station operator as a teletypewriter input.

If the output from the short-term averager exceeds the scaled output from the long-term averager, a time-window process is implemented to determine whether the short-term averager output remains above the threshold value for a prescribed length of time. If the short-term averager does remain above the threshold for the prescribed length of time, a detection is declared and the short-period data is written on an output digital magnetic tape. At least twenty seconds of data preceding the detected phase is recorded. In the event that the short-term averager output does not remain above the threshold for the prescribed length of time, a detection is not declared.

C. THE TAPE RECORDING FORMAT

The primary output of the data recording system is the digital magnetic tape. This tape is 9 track, recorded at a density of 800 bits per inch with odd parity using two's complement binary arithmetic. Records are 1000 words in length containing 10 words of header information and 990 words of data. The header contains the following information:

- A two-digit station identifier.
- The data sample rate.

- Time of the first data sample in the record to the nearest deciseconds.

- A two-digit number specifying the number of channels which are multiplexed in the record.

- Eight status or flag bits.

- Five blank words reserved for future use.

The remaining 990 words in the tape record are used for storage of sampled data. The data consists of consecutive frames, where each frame consists of one sample from each long-period channel formatted, beginning with channel one. No record is allowed to contain a partial frame at the end of the record. Thus, the number of data samples in each record may be slightly smaller than 990, depending on the number of channels multiplexed in the record. The number of valid data samples N is:

$$N = NCH \left[\frac{990}{NCH} \right] ,$$

where NCH denotes the number of channels multiplexed and the brackets denote "largest integer" of the enclosed quantity. Figure II-2 illustrates the tape format for the case where four channels are multiplexed.

The SRO data word format consists of two bytes containing eight bits each in the following format:

- Byte 1- The four most significant bits define the gain factor. The following bit defines the sign of the mantissa. The three least significant bits of this byte are the three most significant bits of the mantissa.

- Byte 2- These eight bits are the least significant eight bits of the mantissa.

CPU WORD 1	MS Byte	10's STA ID (BCD)	1's STA ID (BCD)
	LS Byte	Sample Rate	
CPU WORD 2	MS Byte	Year (BCD)	100's DAYS (BCD)
	LS Byte	10's DAYS (BCD)	1's DAYS (BCD)
CPU WORD 3	MS Byte	10's HR (BCD)	1's HR (BCD)
	LS Byte	10's MIN (BCD)	1's MIN (BCD)
CPU WORD 4	MS Byte	10's SEC (BCD)	1's SEC (BCD)
	LS Byte	100's MS (BCD)	10's MS (BCD)
CPU WORD 5	MS Byte	10's NCH (BCD)	1's NCH (BCD)
	LS Byte	Status (Flag) Byte	
Five Unspecified (Blank) Words			
CPU WORD 11	MS Byte	Data Word 1 (CH1)	
	LS Byte		
CPU WORD 12	MS Byte	Data Word 2 (CH2)	
	LS Byte		
CPU WORD 13	MS Byte	Data Word 3 (CH3)	
	LS Byte		
CPU WORD 14	MS Byte	Data Word 4 (CH4)	
	LS Byte		
CPU WORD 997	MS Byte	Data Word 987 (CH3)	
	LS Byte		
CPU WORD 998	MS Byte	Data Word 988 (CH4)	
	LS Byte		
CPU WORD 999	MS Byte	Data Word 989 (Dummy)	
	LS Byte		
CPU WORD 1000	MS Byte	Data Word 990 (Dummy)	
	LS Byte		

FIGURE II-2

FORMAT OF THE SRO 1000-WORD TAPE RECORDS;
NUMBER OF MULTIPLEXED CHANNELS IN THIS EXAMPLE IS FOUR

The gain factor is an unsigned integer having a value from zero to ten. The mantissa is an integer with negative values expressed in two's complement binary arithmetic. The absolute value of a data word in digital counts is:

$$\text{Amplitude} = \text{Mantissa} * 2^{(10\text{-gain factor})}.$$

The maximum possible amplitude of the SRO data is 2,097,152 digital counts.

A more detailed discussion of the SRO system can be found in the operation and maintenance manual for the Seismic Research Observatory data recording system.

SECTION III
THE DATA BASE

A. DATA AVAILABILITY

The Seismic Research Observatory network, when fully operational, will consist of the ten stations listed in Table III-1 and shown in Figure III-1. During the contract period covered by this report, data were available from five of these ten stations: Albuquerque, New Mexico (ANMO); Mashhad, Iran (MAIO); Guam, Marianas Islands (GUMO); Mundaring (Narrogin), Western Australia (NWAO); and Wellington (South Karori), New Zealand (SNZO). April 5, 1976, was set as the cutoff date for data to be included in this report. Table III-2 lists the data availability up to this cutoff date.

Since the start-up dates of these five stations are different, it was not possible to process a suite of events common to all five. Therefore, the original data base used for stations ANMO, GUMO, and MAIO was extended to cover the time period for which data was available from SNZO and NWAO. Thus, stations ANMO, GUMO, and MAIO share a common data base, and SNZO and NWAO share a second common data base.

The data base was created from the Norwegian Seismic Array (NORSAR) seismic event lists. Events which would clearly be mixed with other larger events at two or more stations and all but the largest events of earthquake swarms were deleted from these lists, with the remaining events being incorporated in the data base. The resulting data base contains 772 events with epicenters located worldwide. The relevant parameters of this data base are listed in Appendix A. The event parameters include the date, origin time, epicenter location, bodywave magnitude, and seismic source

TABLE III-1

SEISMIC RESEARCH OBSERVATORY LOCATIONS

Station Number	Station Name	Station Designator	Coordinates	
			Latitude	Longitude
30	Albuquerque, New Mexico *	ANMO	34° 56' 30" N	106° 27' 30" W
31	Ankara, Turkey **	ANTO	40° N	33° E
32	Bogota, Columbia **	BOCO	5° N	74° W
33	Chiang Mai, Thailand **	CHTO	18° 48' N	99° E
35	Guam, Marianas Is. *	GUMO	13° 35' 16" N	144° 51' 58.6" E
36	Mashhad, Iran *	MAIO	36° 18' N	59° 29' 40" E
38	Mundaring, Australia *	NWAO	32° 55' 42" S	117° 14' 9" E
40	Shillong, India **	SHIO	25° 34' N	91° 53' E
41	Taipei, Taiwan **	TATO	25° N	121° 30' E
42	Wellington, New Zealand *	SNZO	41° 18' 37" S	174° 42' 16.7" E

* Evaluated in this report.

** Coordinates approximate.

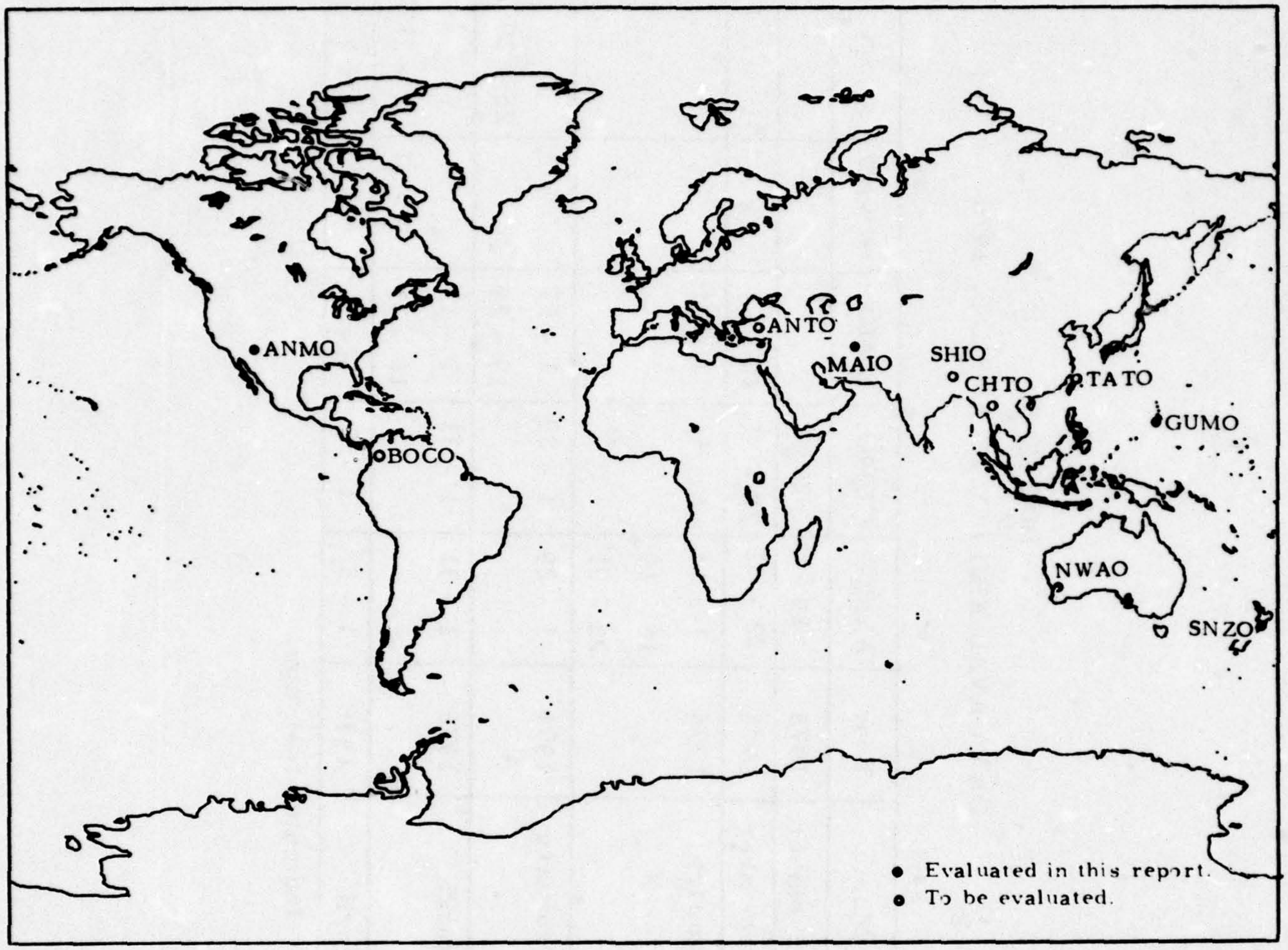

FIGURE III-1

LOCATIONS OF SRO STATIONS

TABLE III-2

DATA AVAILABILITY TO APRIL 5, 1976

Month	Year	ANMO	GUMO	MAIO	NWAO	SNZO
November	1975	29*	29*			
December	1975	22 - 31	22 - 31	28 - 31		
January	1976	1 - 14 16 - 19 22 - 31	1 - 31	1 - 31		
February	1976	1 - 29	1 - 29	1 - 12 19 - 29		25 - 29
March	1976	1 - 31	1 - 31	1 - 13 16 - 31	9 - 31	1 - 31
April	1976	1 - 5	1 - 5	1 - 5	1 - 5	1 - 5

* Indicates test tape.

region. Each event is assigned a unique event number. At the time the data base was formed, no Preliminary Determination of Epicenter lists (PDE lists) were available, so that it was not possible to eliminate deep earthquakes from the list of events to be analyzed.

The ANMO data base consists of events 0001 to 0397 of the appendix. The GUMO data base consists of events 0001 to 0398, the MAIO data base of events 0067 to 0377, the NWAO data base of events 0507 to 0772, and the SNZO data base of events 0399 to 0654.

Near the end of the contract period, some PDE event lists became available, giving us depth information on some of our events. Since these lists were not complete, we have retained in our data base those events which are listed as deep (> 100 km), since to remove them might imply that there are no deep events remaining in the data base. Where applicable, these known deep events will be isolated from the shallow events. An event in the data base is called a presumed explosion when it has an epicenter near a known test site and the depth assigned to it by the PDE lists is zero. (We require it to be near a known test site to eliminate the rockbursts and chemical explosions associated with mining activity which are occasionally reported in seismic event lists.)

The distribution of the data base for each station as a function of epicentral distance is shown in Figures III-2 to III-4. We see from these figures that the great majority of ANMO events have epicentral distances between 65° and 115°. The GUMO events show a wider distribution, with the majority of events having epicentral distances between 25° and 105°. The MAIO events clearly separate into three groups with epicentral distances between 5° and 35°, between 55° and 75°, and between 125° and 135°. The majority of the NWAO events have epicentral distances between 45° and 105°. The SNZO events separate into two groups with epicentral distances between 5° and 25° and between 55° and 135°. We make note of these differing distributions, since they will affect our estimates of detection capability.

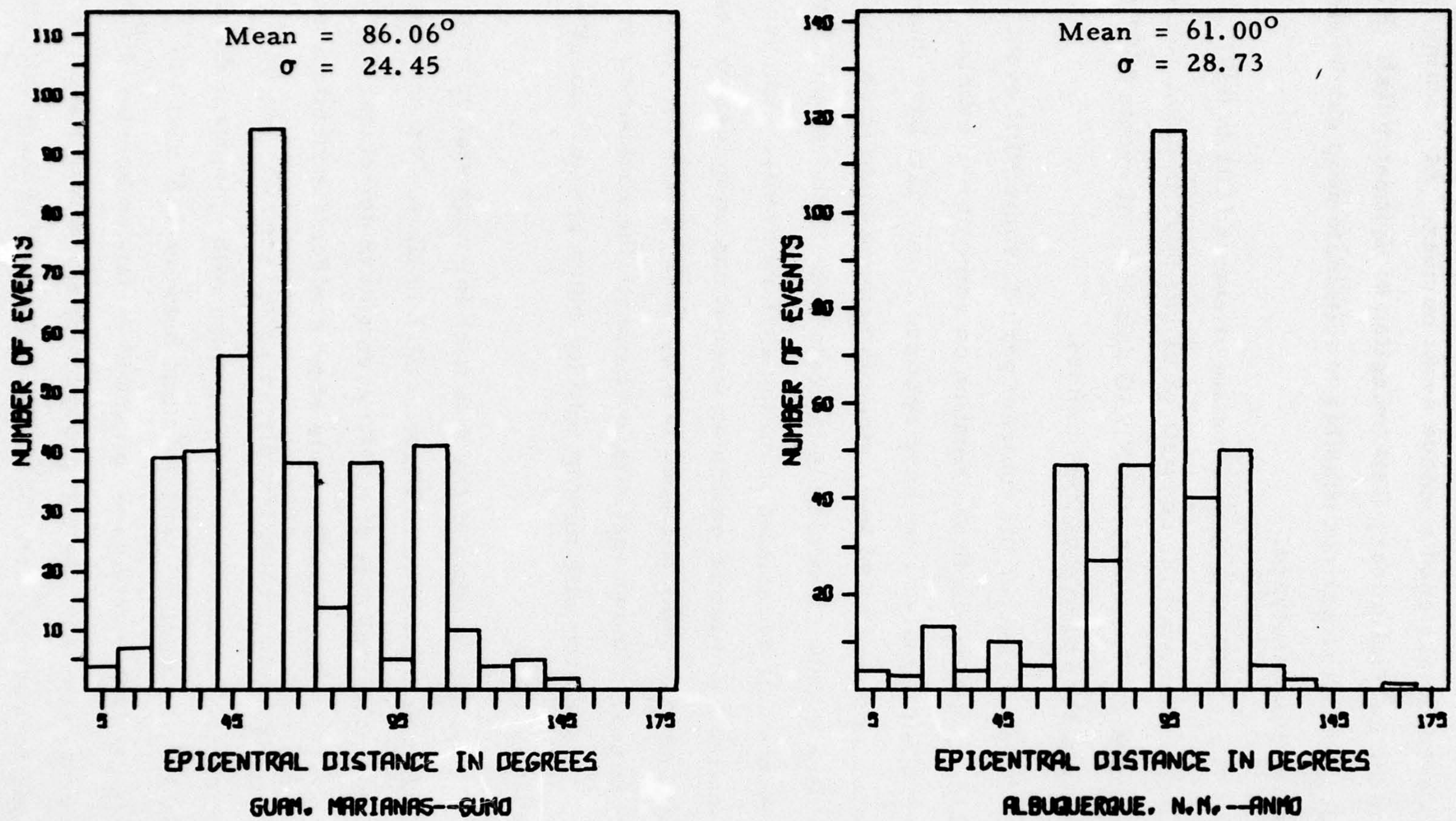

FIGURE III-2

DISTRIBUTION OF EVENTS BY EPICENTRAL DISTANCE: ANMO AND GUMO

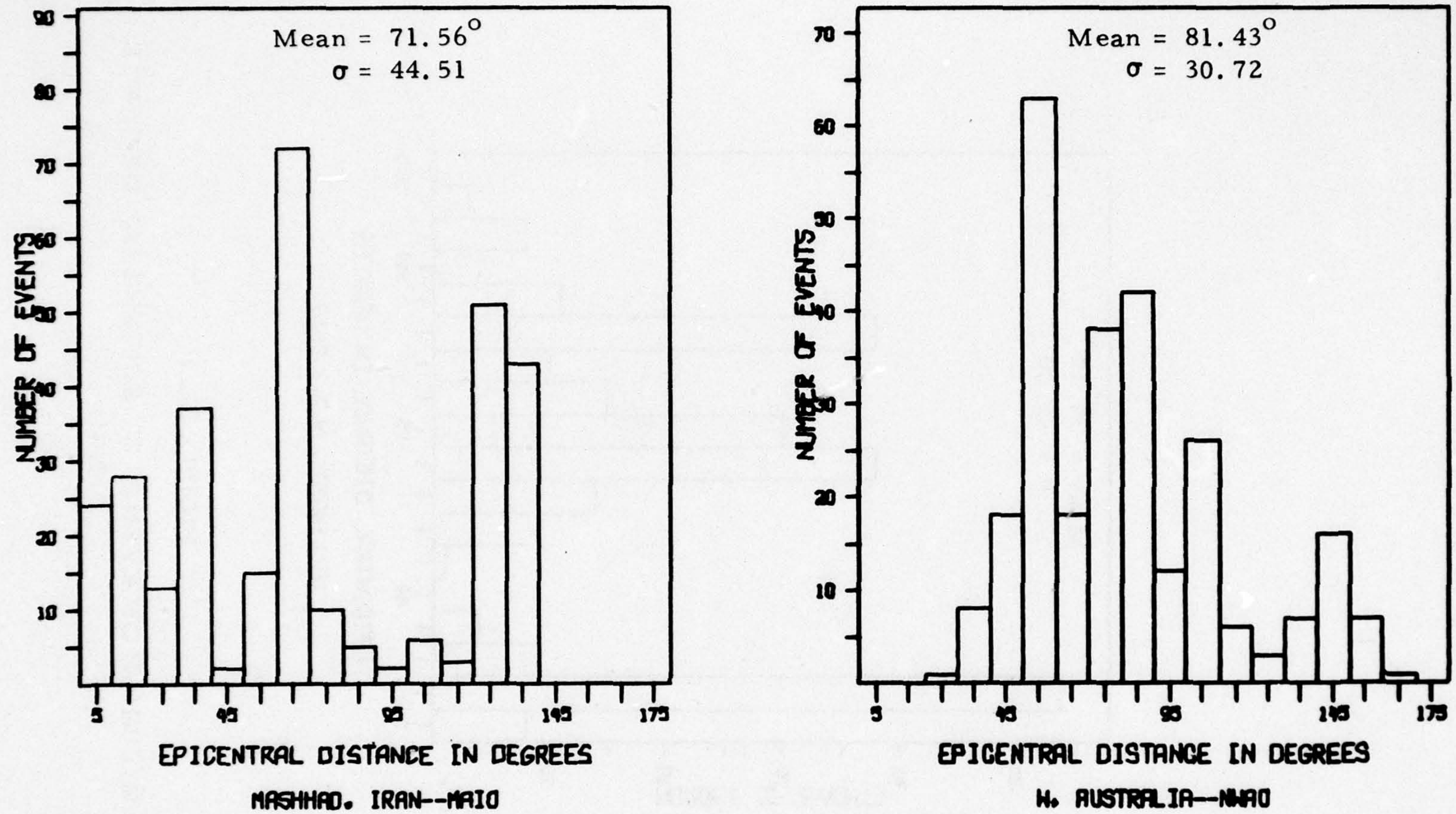

FIGURE III-3

DISTRIBUTION OF EVENTS BY EPICENTRAL DISTANCE: MAIO AND NWAO

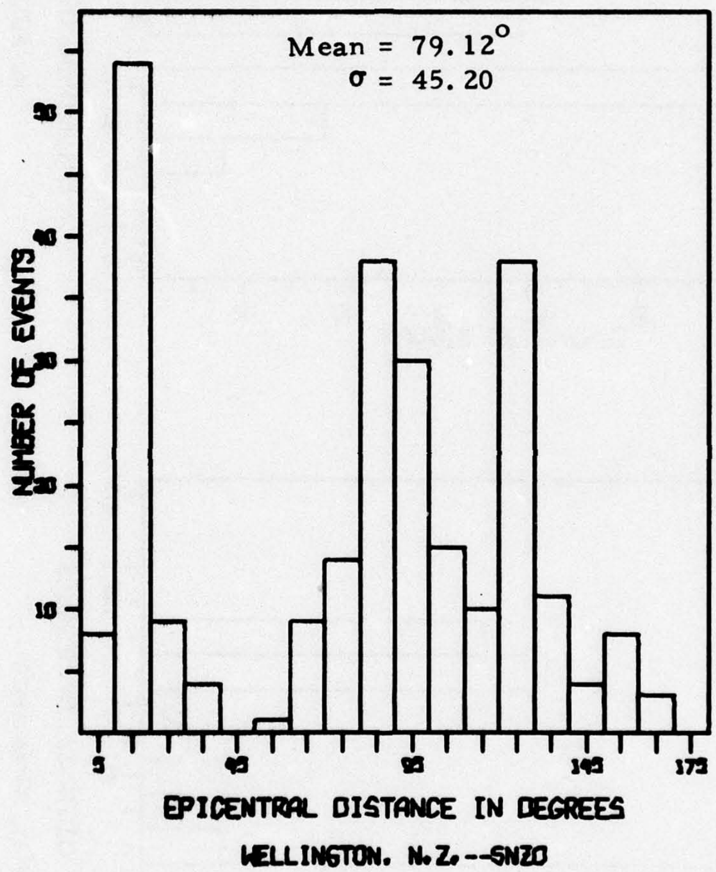

FIGURE III-4

DISTRIBUTION OF EVENTS BY EPICENTRAL DISTANCE: SNZO

B. METHOD OF DATA PROCESSING

Figures III-5 and III-6 illustrate the manner in which the SRO data were processed.

The computer processing of SRO short-period data was carried out on the PDP-15 computer system using the Interactive Seismic Processing System (ISPS) data analysis package (Ringdal, Shaub, and Black, 1975). The data were first copied on the IBM 360/44 from the original tape to a temporary tape, changing the density from 800 BPI to 1600 BPI. The short-period record headers were then listed using the PDP-15 computer. This header list was then compared with a list of P-wave arrival times for the events of the data base. (These P-wave arrival times were computed using the Jeffery-Bullen travel-time tables.) Those events for which the time gate enclosing the expected P-wave arrival time had been recorded were then edited on the PDP-15 from the 1600 BPI tape and stored on the disk. (We note that the P-wave is not observed for epicentral distances greater than 103 degrees. Therefore, only those events in the data base with epicentral distances less than 103 degrees were looked for in the header list.)

Analysis of each edited segment was then carried out, consisting of bandpass filtering (0.5 - 4.0 Hz), computation of RMS noise, computation of noise spectra, checking for P detection, and measurement of peak amplitude and period of the P-wave when detected. Calcomp plots of noise spectra and edited time traces were made to provide a permanent record of all data.

The computer processing of SRO long-period data was carried out on the IBM 360/44 computer system. In order to carry out the data processing, the front-end (edit) program of the Very Long Period Experiment (VLPE) analysis package was modified to read the SRO tape format. In this way, all following programs in the analysis package could be applied to the

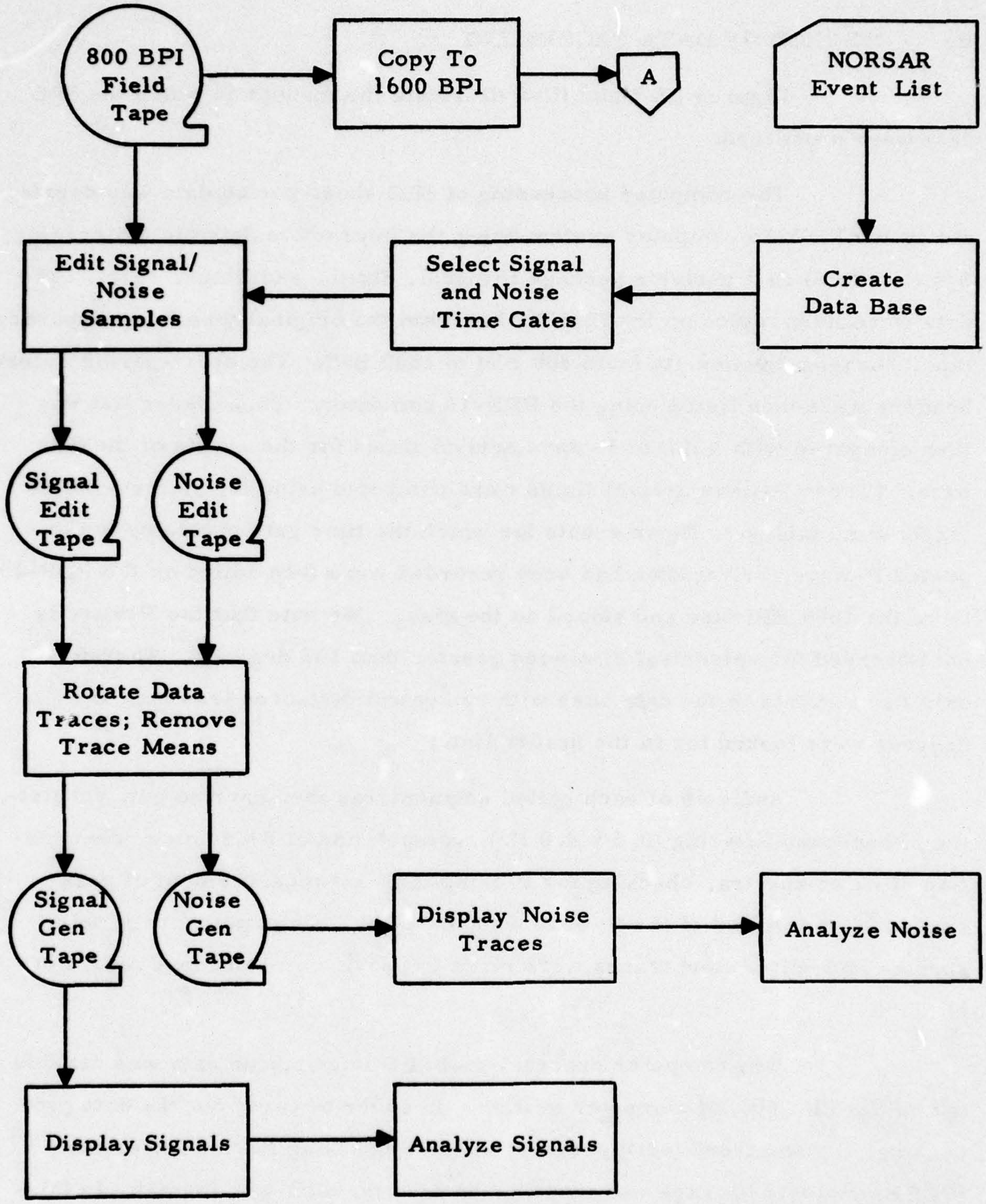

FIGURE III-5

LONG-PERIOD DATA PROCESSING FLOW CHART
(IBM 360/44 DATA PROCESSING)

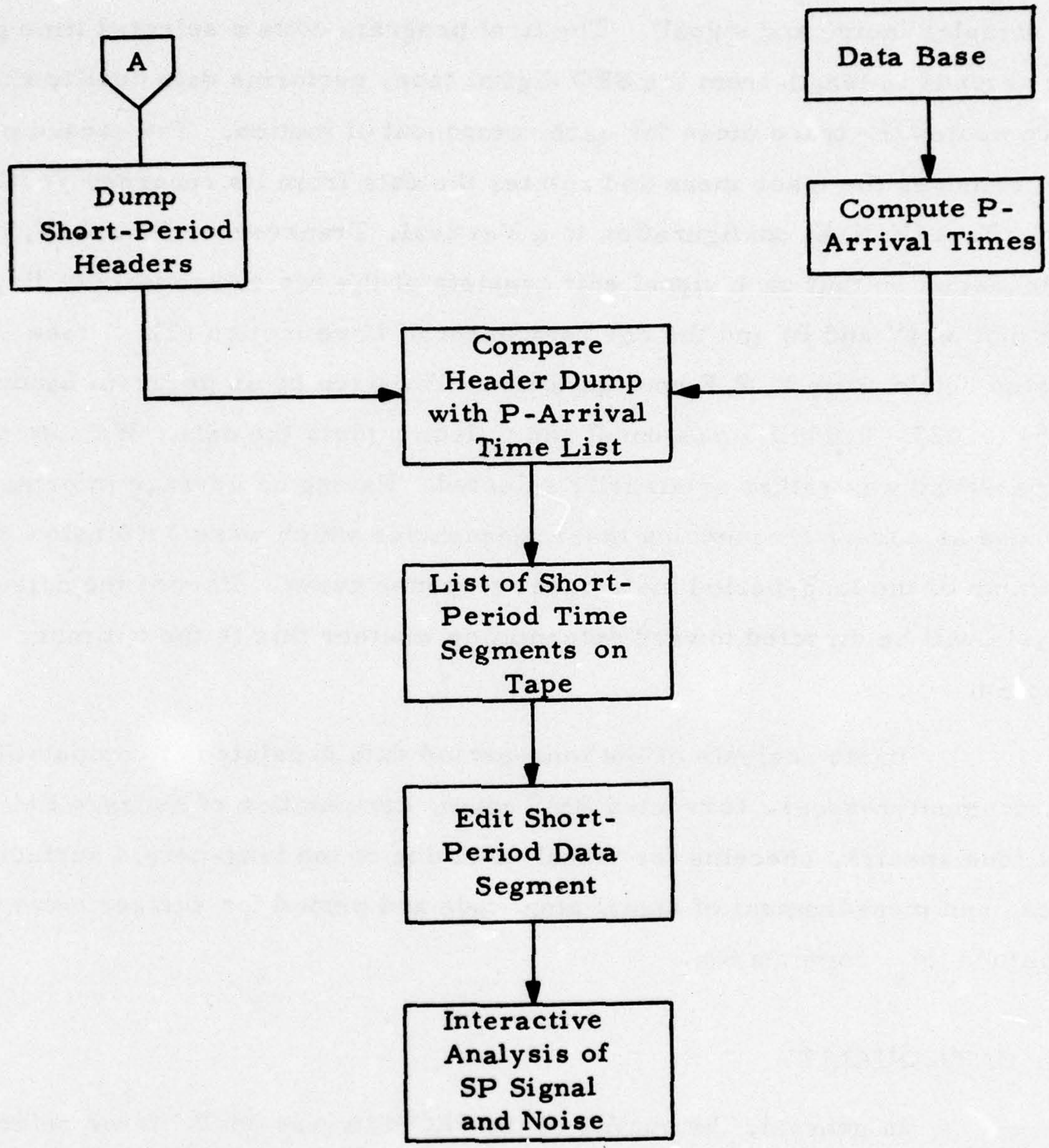

FIGURE III-6

SHORT-PERIOD DATA PROCESSING FLOW CHART (PDP-15 DATA PROCESSING)

SRO data without change. Three basic programs were run on all long-period data samples (noise and signal). The first program edits a selected time gate 4096 seconds in length from the SRO digital tape, performs data quality checks, and computes the trace mean for each component of motion. The second program removes the trace mean and rotates the data from its recorded Vertical, North, East (V, N, E) configuration to a Vertical, Transverse, Radial (V, T, R) configuration so that each signal edit consists of the two components of Rayleigh motion (V and R) and the one component of Love motion (T). Noise samples retain their V, N, E configuration. The third basic program bandpass filters (0.023 - 0.059 Hz passband) and Calcomp plots the data. We note that this passband was rather arbitrarily selected. Having no advance information, we chose as corner frequencies those frequencies which were 3 dB below the maximum of the long-period instrument response curve. Part of the noise analysis will be directed toward determining whether this is the optimum passband.

Basic analysis of the long-period data consisted of computation of instrument-response corrected RMS noise, computation of average RMS amplitude spectra, checking for visual detection of the long-period surface waves, and measurement of signal amplitude and period for surface wave magnitude (M_s) computation.

C. DATA QUALITY

In general, the quality of the SRO data was good. If we refer to Table III-3, we see that the number of malfunctions is in most cases quite low. (In this table, short-period data is denoted by "P", for the P-wave, and long-period data is denoted by "V", "T", and "R", for the three components of long-period motion.) The term "malfunction" is used here to indicate any non-seismic occurrence which, occurring in the signal gate, would mask

TABLE III-3

SUMMARY OF SRO EVENT PROCESSING

Station	Component	Detected	Non-detected	Mixed	No Data Recorded	Malfunctions	$\Delta > 103^o$	Total
ANMO	P	81	57	2	140	0	95	375
	V	97	199	75	2	2	--	
	T	87	161	75	2	50	--	
	R	92	151	75	2	55	--	
GUMO	P	0	18	0	321	0	58	397
	V	100	180	101	0	16	--	
	T	97	181	102	0	17	--	
	R	100	180	102	0	15	--	
MAIO	P	58	25	6	124	0	98	311
	V	105	121	80	3	2	--	
	T	103	125	78	3	2	--	
	R	99	127	80	3	2	--	
NWAO	P	9	15	0	185	0	57	266
	V	71	148	27	4	16	--	
	T	58	163	28	4	13	--	
	R	65	156	28	4	13	--	
SNZO	P	2	24	0	152	3	75	256
	V	54	153	20	4	25	--	
	T	58	147	22	4	25	--	
	R	54	150	22	4	26	--	

the seismic data under analysis. The types of malfunctions commonly observed on the SRO data are glitches, single spikes, multi-spikes, data dropouts, and calibration signals. These are illustrated in Figure III-7.

The worst case we find in Table III-3 is that of the horizontal components of the ANMO station, where approximately 14 percent of the signals were lost (i.e., their detection status could not be determined) to malfunctions. The great majority of these malfunctions were glitches which, when viewed in the recorded V, N, E configuration, occur on the north component. This is illustrated in Figure III-8. Rotation of the data to the V, T, R configuration puts the glitches on both horizontals. It is believed that these glitches are associated with weather changes.

At the GUMO station, the malfunctions were primarily glitches, with some calibration signals and multi-spikes. The malfunctions at MAIO, NWAO, and SNZO were primarily multi-spikes.

One other occurrence which could be considered to be a malfunction is the case where no data are recorded. This can be classed as a malfunction only for long-period data, since the automatic short-period detector determines whether short-period data will be recorded. We note from Table III-3 that, in the worst case, less than 2 percent of our long-period data were lost to this type of malfunction.

We note that the only short-period malfunctions (at SNZO) were short-period calibrations. The short-period data at two of the five stations suffered from a severe problem. At GUMO, the noise level was so high that the amplitudes were too great to be recorded properly. As a result, the data, when displayed, consisted of a continuous series of spikes with constant amplitude. Any P-waves which may have been present were indistinguishable from the noise. At SNZO, the noise levels occasionally became high enough for this to occur. As mentioned in Section II, the quantization rate has been

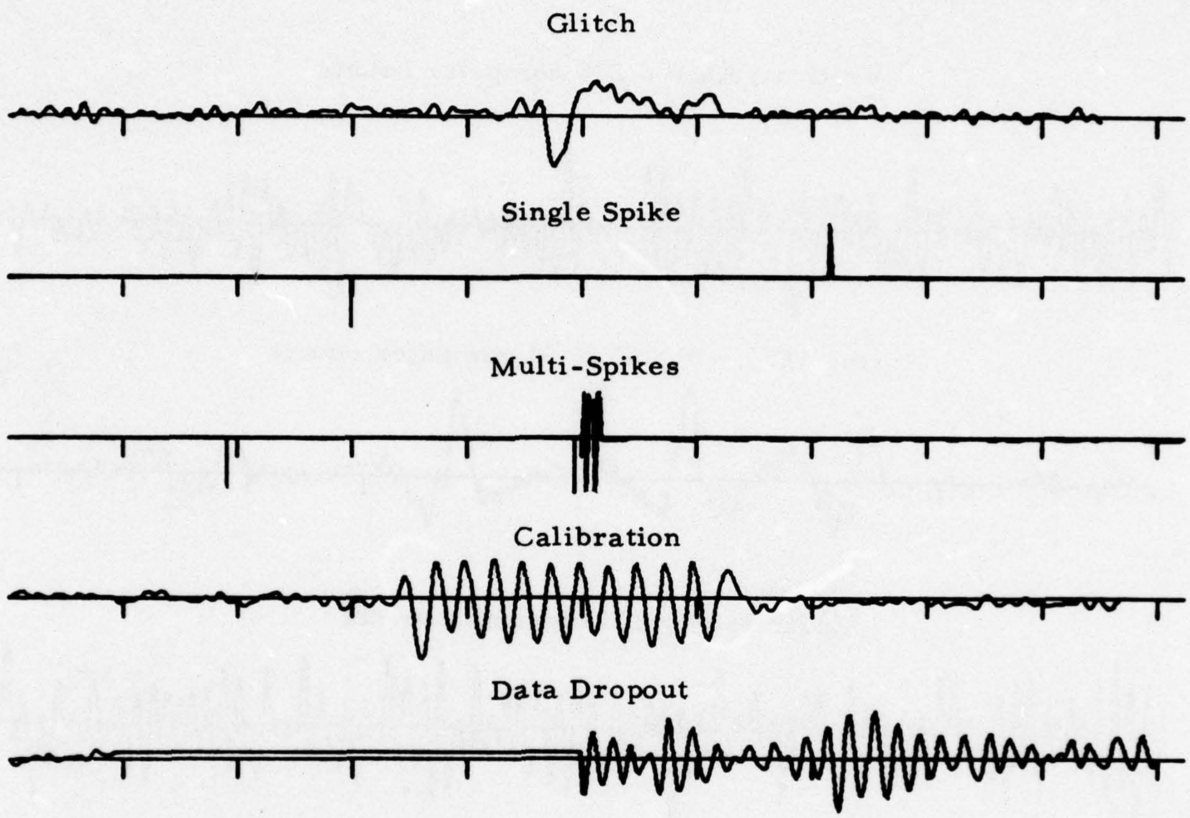

FIGURE III-7

TYPES OF MALFUNCTIONS

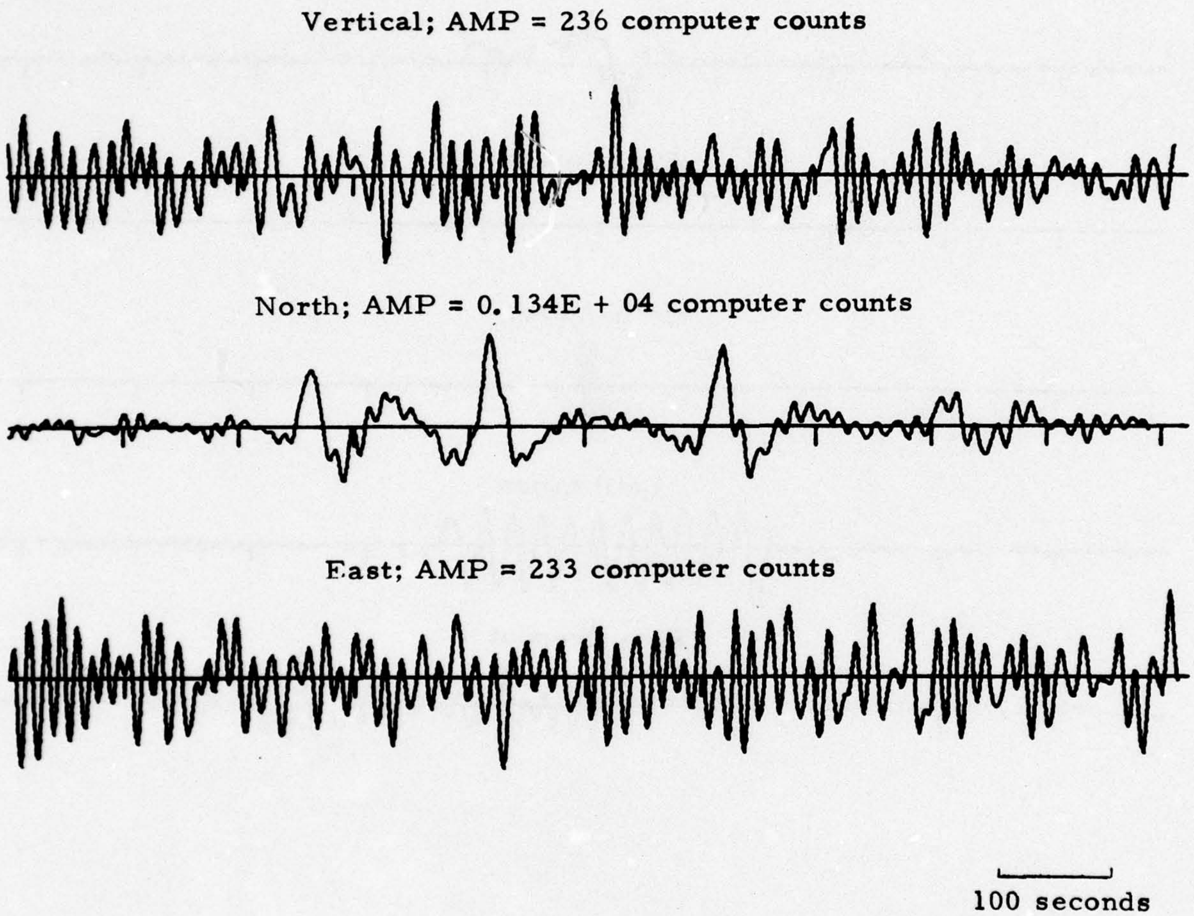

FIGURE III-8

ALBUQUERQUE LONG-PERIOD DATA
SHOWING GLITCH-TYPE MALFUNCTIONS ON THE NORTH COMPONENT

changed at GUMO and SNZO from 2000 computer counts per millimicron (cc/mμ) to 2 computer counts per millimicron (cc/mμ). Visual checks of data recorded after the changeover show that the data now looks like short-period data rather than spikes. This is illustrated in Figure III-9, where the upper trace shows GUMO short-period data recorded before the changeover and the lower trace shows GUMO short-period data recorded after the changeover.

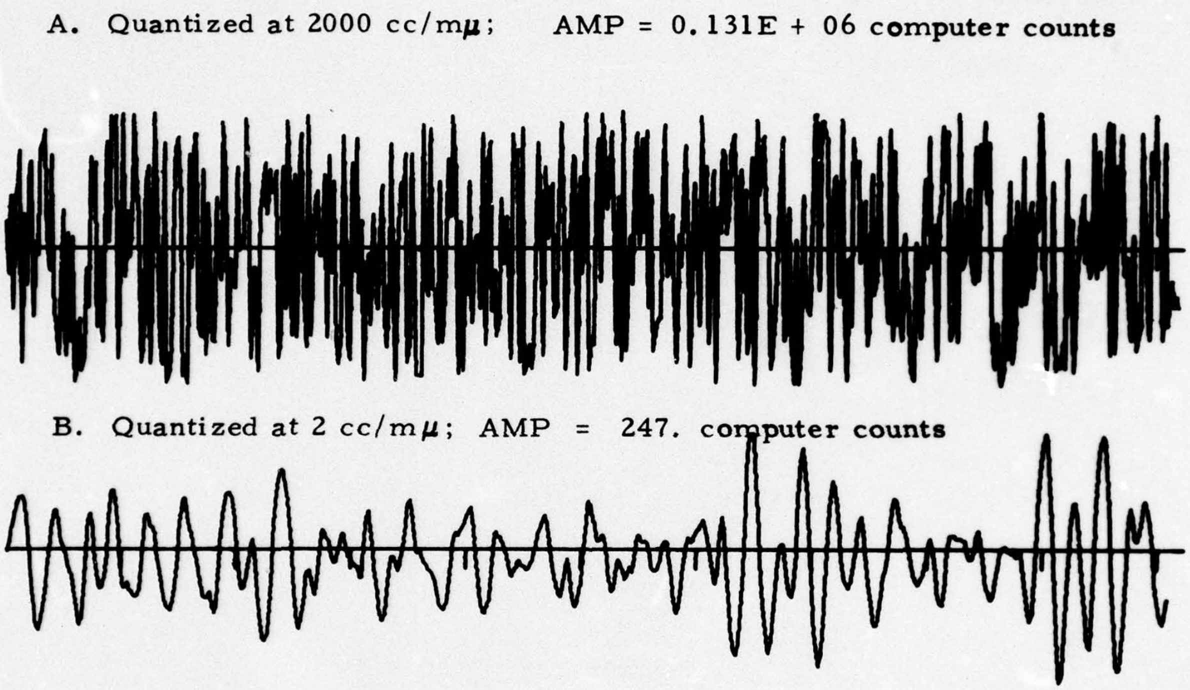

FIGURE III-9

TYPICAL GUMO SHORT-PERIOD DATA

SECTION IV

NOISE CHARACTERISTICS AT THE SEISMIC RESEARCH OBSERVATORIES

A. VERTICAL-COMPONENT SHORT-PERIOD NOISE

The short-period noise analysis was conducted on the PDP-15 computer using the Interactive Seismic Processing System (ISPS) (Ringdal, Shaub, and Black, 1975). Subject to data availability, our goal was a minimum of three noise samples per day from each station. Noise samples were obtained in two ways. First, while processing short-period events, a set of noise samples was collected by selecting the time segment prior to the observed arrival of the P-wave. Next, to reach the desired number of samples, a second set of short-period edits was made, each edit starting at the first time point of a data segment output by the short-period automatic detector. This was done to avoid picking noise samples in the P-coda of an event, which would give falsely high RMS noise values. The segments used to compute RMS noise were from 20 to 50 seconds in length.

After the time gate was selected, each sample was filtered by a 0.5 to 4.0 Hz bandpass filter. The RMS noise was then computed in the time domain by the formula:

$$RMS = \left[\frac{\sum_{i=1}^{n} (x_i)^2}{n} \right]^{1/2}$$

where n = number of data points,

x_i = the i^{th} data point.

No instrument response correction was applied, since capability to perform this operation has not yet been built into the ISPS package. The individual RMS noise values for each day were then averaged to provide a more stable daily RMS noise estimate and converted to millimicrons. The results are plotted in Figures IV-1 to IV-3. Of the five stations evaluated, the short-period noise field is lowest at station 30 (ANMO), averaging 0.36 millimicrons with little deviation from the mean. The next lowest values of RMS noise are found at station 36 (MAIO), where the RMS noise values average 0.51 millimicrons. We note that deviations from the mean are somewhat greater here than at station 30. Next in order of increasing RMS noise is station 38 (NWAO), where the RMS noise values average 6.42 millimicrons. At station 42 (SNZO), the RMS noise values average 19.42 millimicrons, with large deviations from the mean. The largest values of short-period RMS noise are found at station 35 (GUMO), averaging 31.01 millimicrons with small deviations from the mean.

Figures IV-4 and IV-5 show the long-term trend in the short-period RMS noise for stations 30 (ANMO), 35 (GUMO), and 36 (MAIO). (No corresponding plots for stations 38 (NWAO) or 42 (SNZO) were prepared due to insufficient data.) The station 30 data shows a low for the month of February, followed by a gradual rise during March and April. No observable trend can be found in the RMS noise levels for station 35. The data for station 36 shows the opposite trend from that of station 30, with the RMS noise dropping off in the months of March and April. Comparison of Figures IV-4 and IV-5 with the corresponding plots of Figures IV-1 and IV-2 suggests that trends in the data might be better revealed if they were computed on a ten-day basis rather than a monthly basis.

In order of increasing short-period RMS noise, the stations are ANMO, MAIO, NWAO, SNZO, and GUMO. We note that ANMO and MAIO are

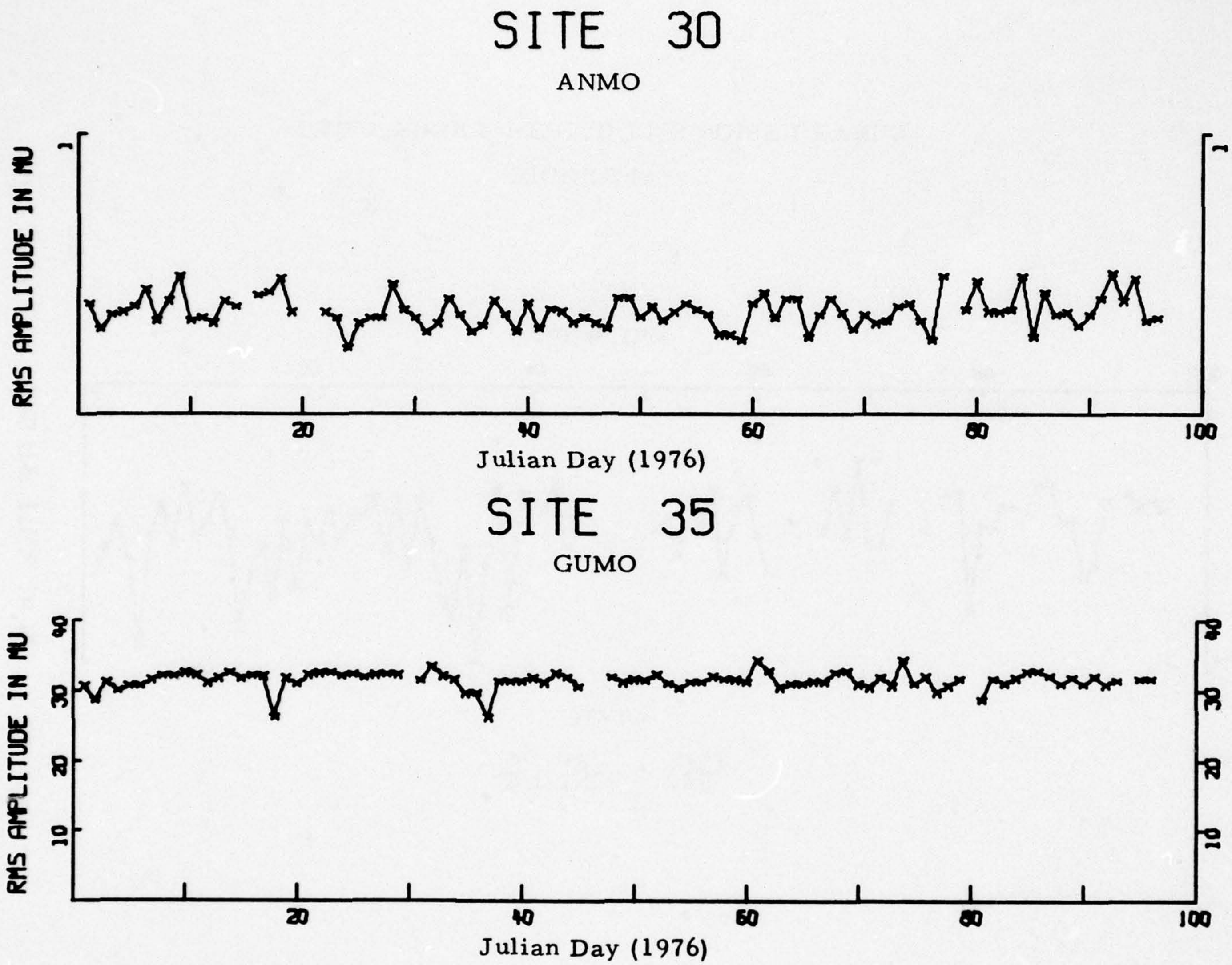

FIGURE IV-1

DAILY SHORT-PERIOD RMS NOISE LEVELS

SITE 36

MAIO

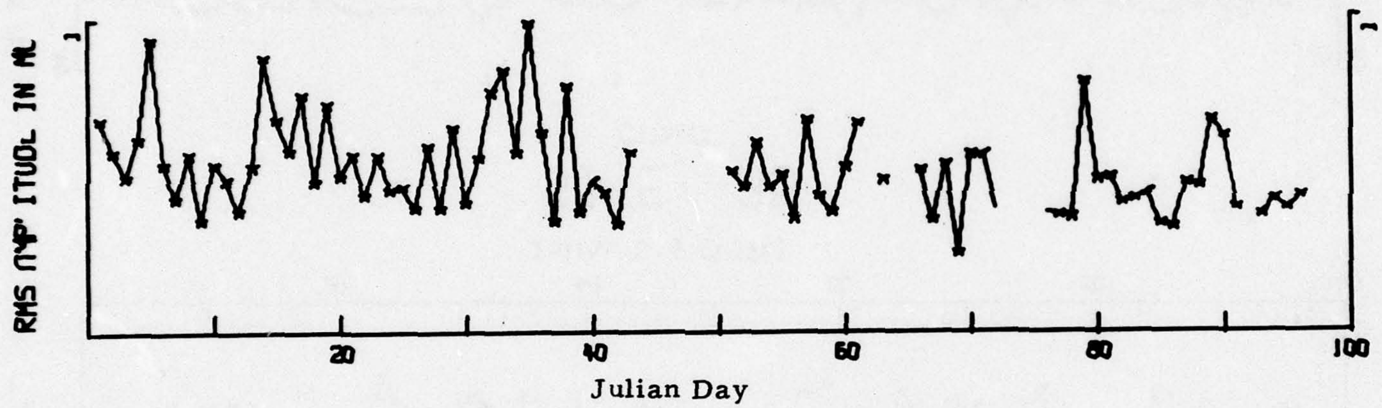

FIGURE IV-2

DAILY SHORT-PERIOD RMS NOISE LEVELS

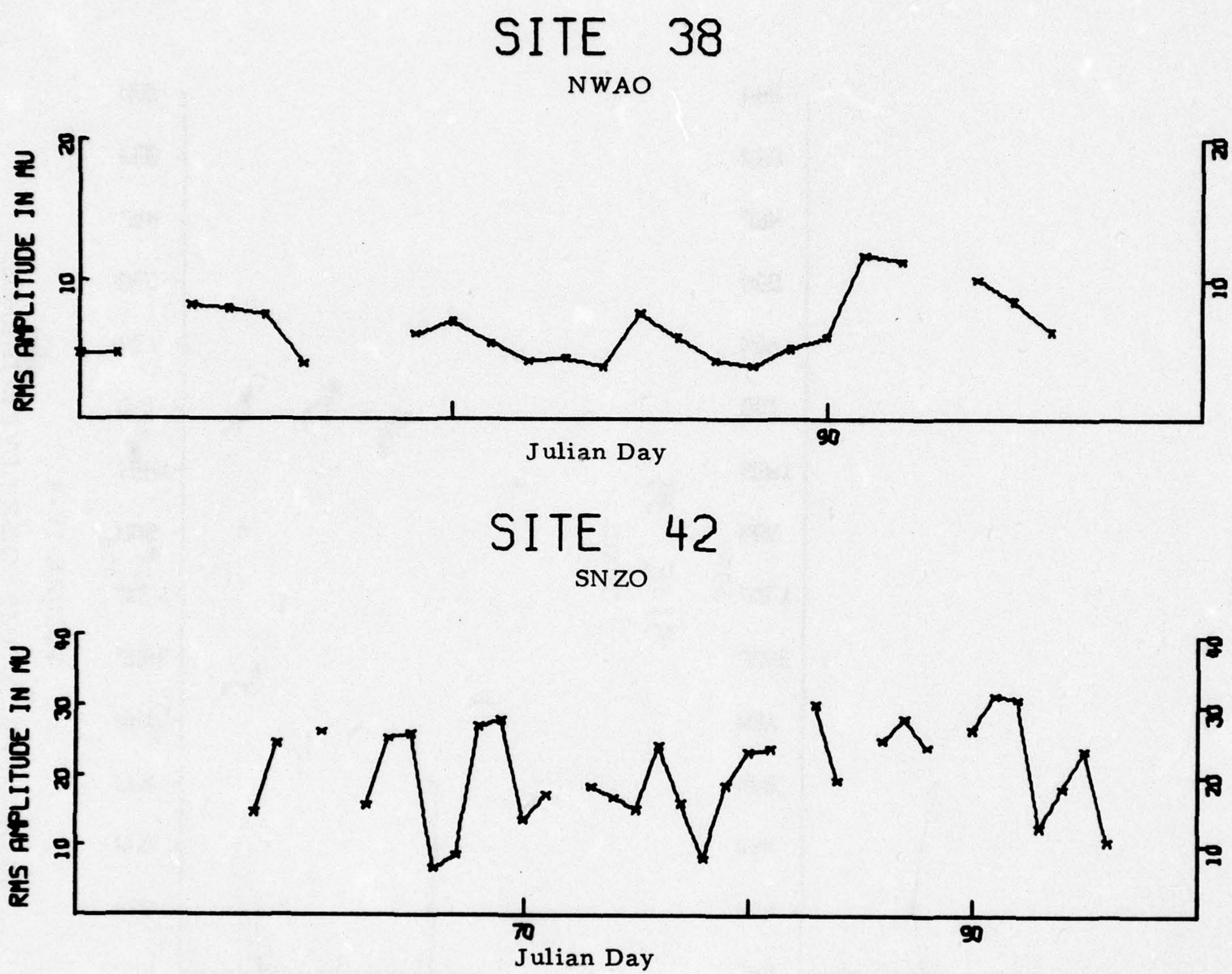

FIGURE IV-3

DAILY SHORT-PERIOD RMS NOISE LEVELS

SITE 30

ANMO

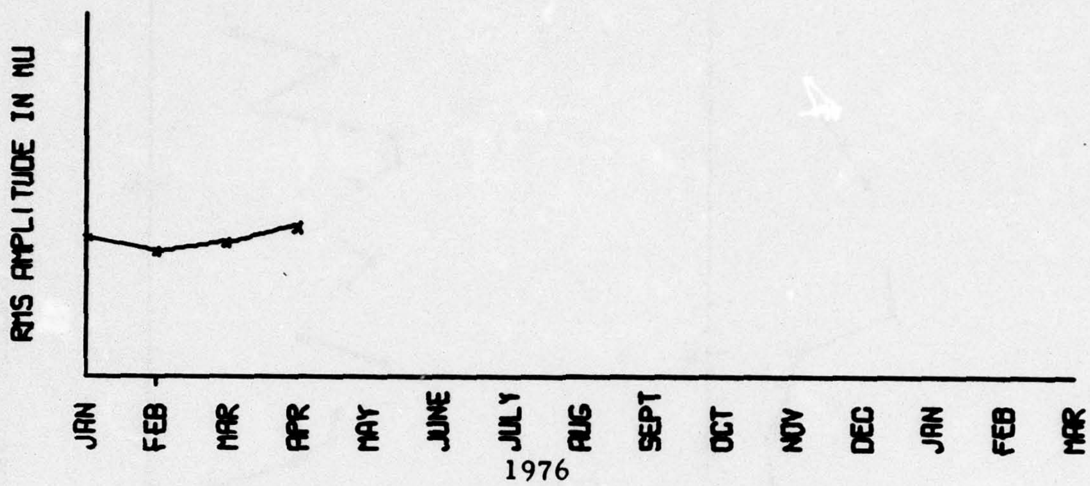

SITE 35

GUMO

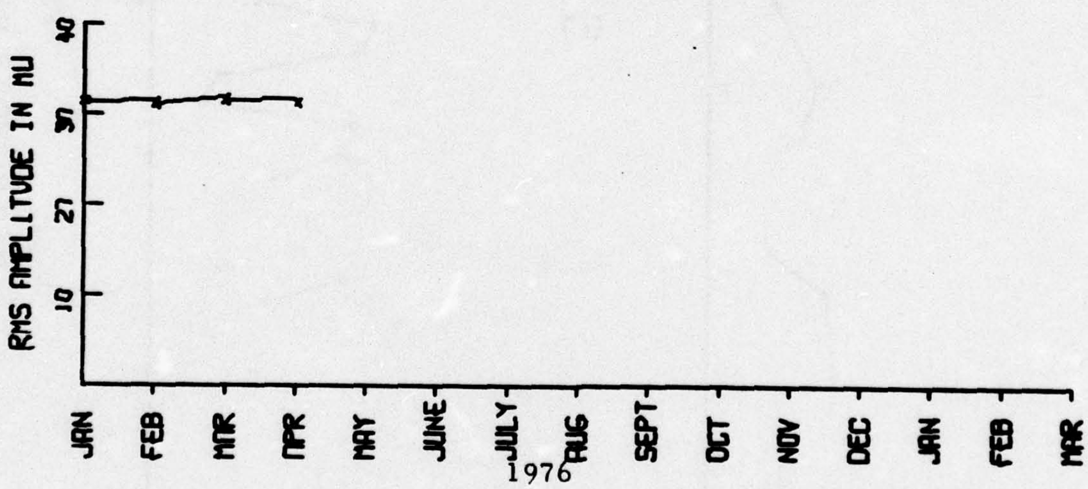

FIGURE IV-4

SHORT-PERIOD RMS NOISE LEVEL TRENDS: ANMO AND GUMO

SITE 36

MAIO

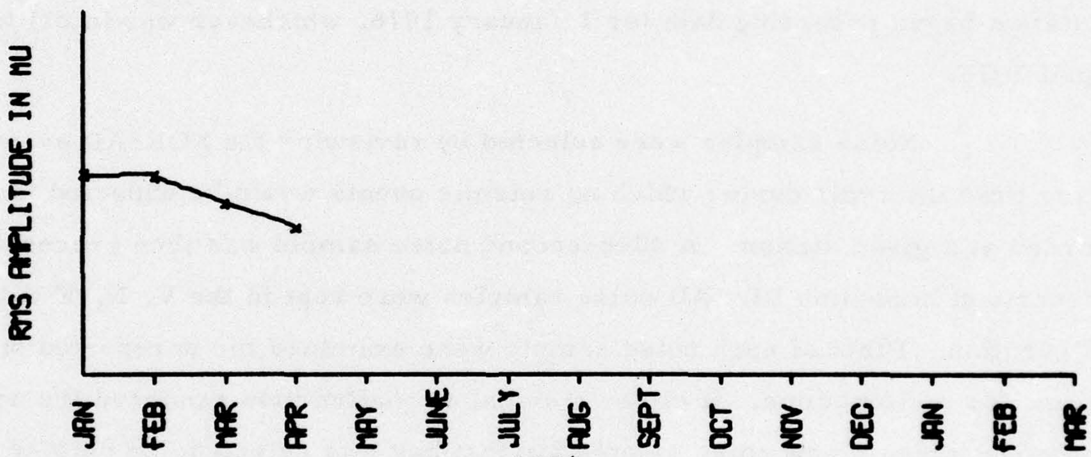

FIGURE IV-5

SHORT-PERIOD RMS NOISE LEVEL TRENDS:
MAIO

located approximately 1100 km inland from the nearest coastline, NWAO is located approximately 150 km from the nearest coastline, SNZO is located essentially at the coastline, and GUMO is on an island. This would suggest that RMS noise levels above a base level of approximately 0.5 millimicrons are closely related to wave energy injected into the land at the coastline.

B. THREE-COMPONENT LONG-PERIOD NOISE

The goal of the long-period noise analysis was to estimate the long-period RMS noise levels and spectral content of the noise field for each of the three components of motion (V, N, and E) at each station under evaluation. For each station, the evaluation time frame was from the date at which the station began recording data (or 1 January 1976, whichever was later) to 5 April 1976.

Noise samples were selected by reviewing the NORSAR event list for time intervals during which no seismic events would be expected to be recorded at a given station. A 4096-second noise sample was then processed as described in Section III. All noise samples were kept in the V, N, E trace configuration. Plots of each noise sample were examined for unreported signals and for malfunctions. If either a signal or malfunction rendered the noise sample unusable, a new noise sample for that day was selected. If neither signals nor malfunctions were observed, the entire 4096-second sample was included in the noise data base. Occasionally, only part of the noise sample was usable, the remainder containing either a signal or a malfunction. In this case, 2048 seconds of the sample were used.

After this visual check, the data were processed in the following steps:

- Each sample was Fourier transformed in order to compute a power spectrum smoothed to 64 frequencies ($\Delta f = 0.003906$ Hz).

- RMS noise levels corrected for instrument response were computed from the power spectra using Parseval's formula.
- Average RMS amplitude spectra corrected for instrument response were computed from the power spectra.

The instrument-response corrected spectral power density estimates of each component of motion were integrated over the 17.0 - 43.5 second passband to yield RMS ground motion using the equation:

$$RMS_a^b = \sqrt{\Delta f \sum_{i=a}^{b} |A(f_i)|^2 \; C(f_i)^2}$$

where Δf = the elemental frequency interval (Δf = 0.003906 Hz),

$|A(f_i)|^2$ = the discrete Fourier transform spectral density estimate at frequency f_i,

$C(f_i)$ = the instrument response correction at frequency f_i,

a = the initial frequency index, and

b = the final frequency index.

The normalized instrument response curves are shown in Figure IV-6.

Figures IV-7 to IV-11 show the calculated values of RMS noise in millimicrons (mμ) for the Vertical, North, and East components of motion plotted versus Julian day of 1976. These values were measured in the 0.023 to 0.059 Hz (17.0 - 13.5 second) passband. Consecutive days of data are connected by lines. The mean values and standard deviations of the RMS noise amplitudes are listed in Table IV-1.

Figures IV-7, IV-8, and IV-9 for ANMO, GUMO, and MAIO cover a common time period. For each of these stations, the largest excursions from the mean occur during January between days 16 and 18. Smaller

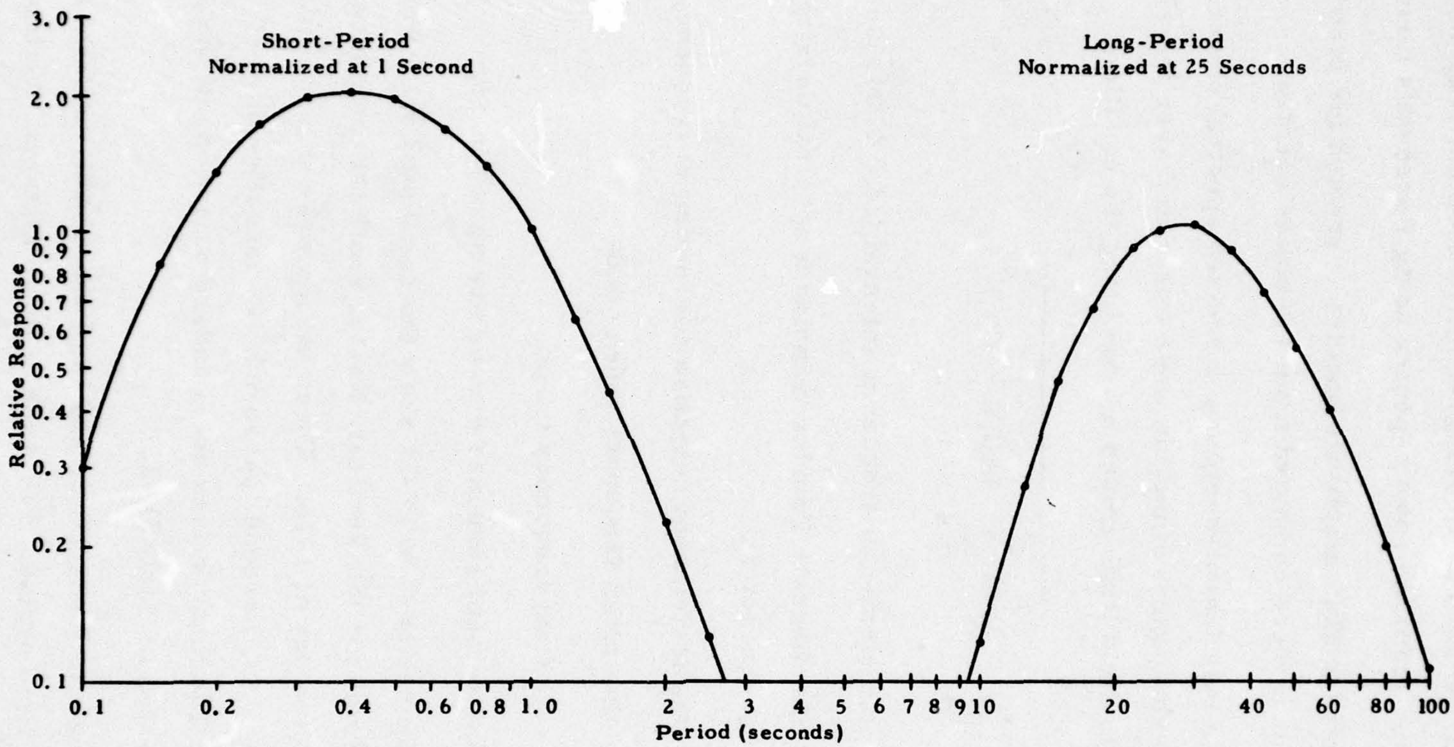

FIGURE IV-6

NORMALIZED INSTRUMENT RESPONSE CURVES

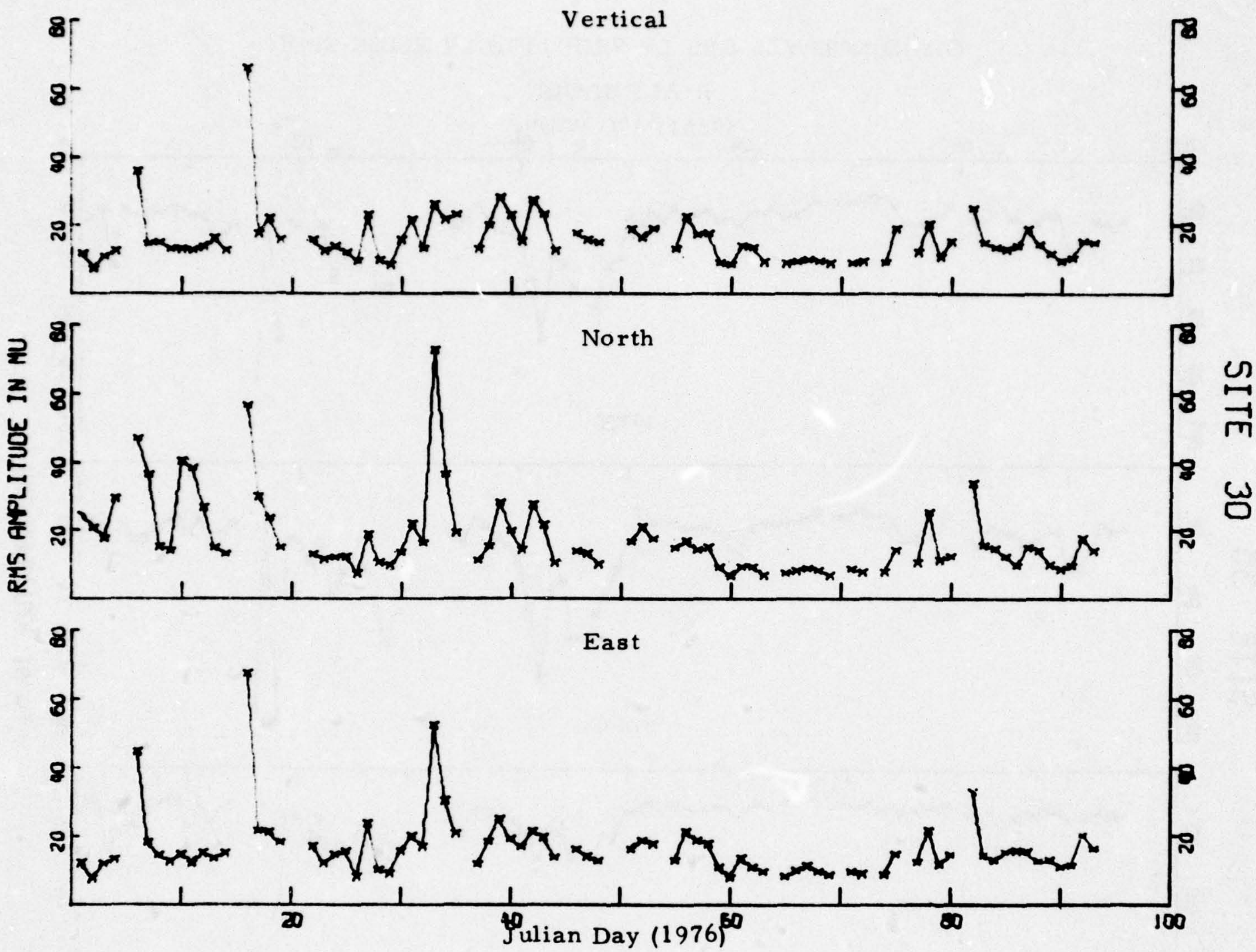

FIGURE IV-7

RMS NOISE AMPLITUDES AT SRO STATION ANMO

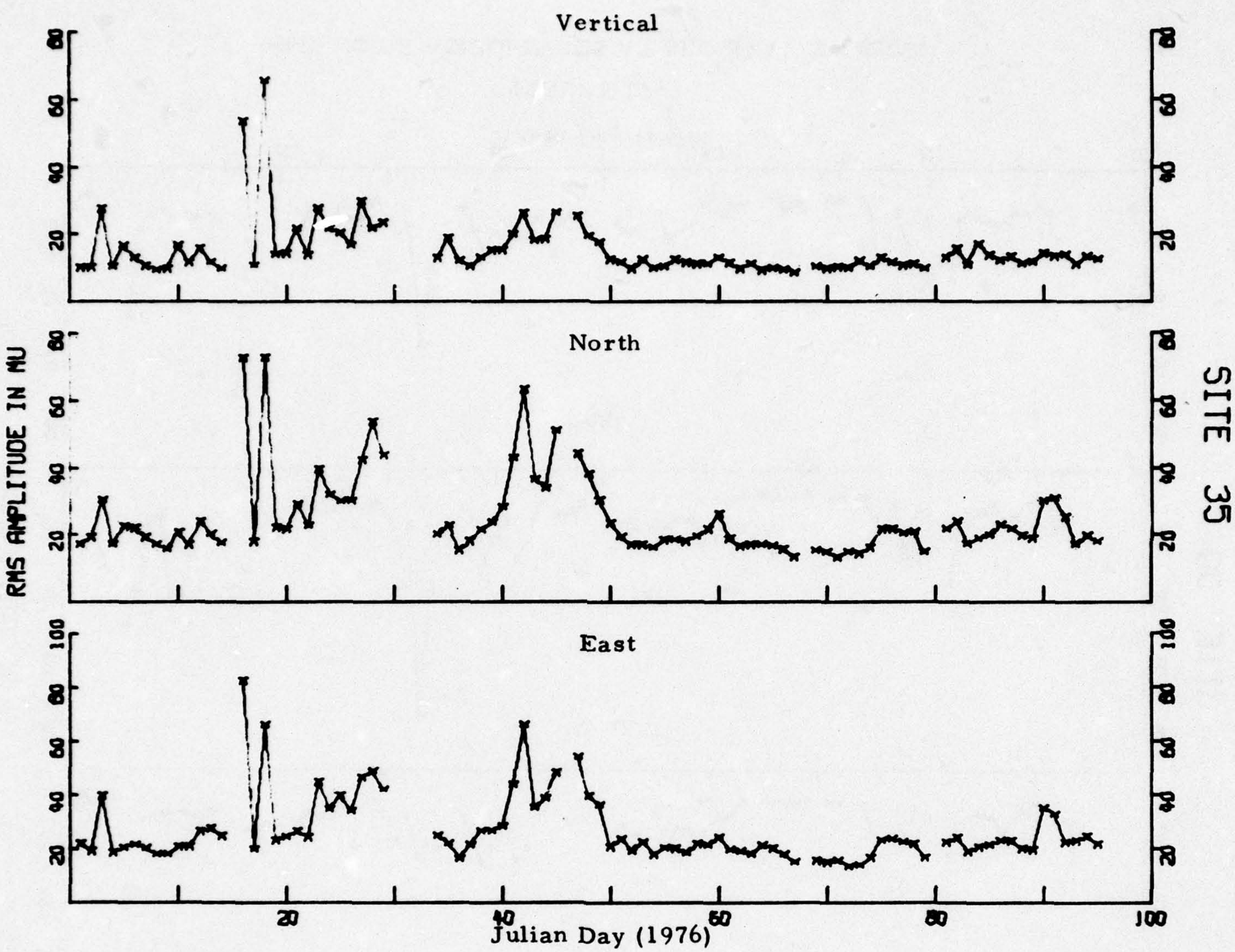

FIGURE IV-8

RMS NOISE AMPLITUDES AT SRO STATION GUMO

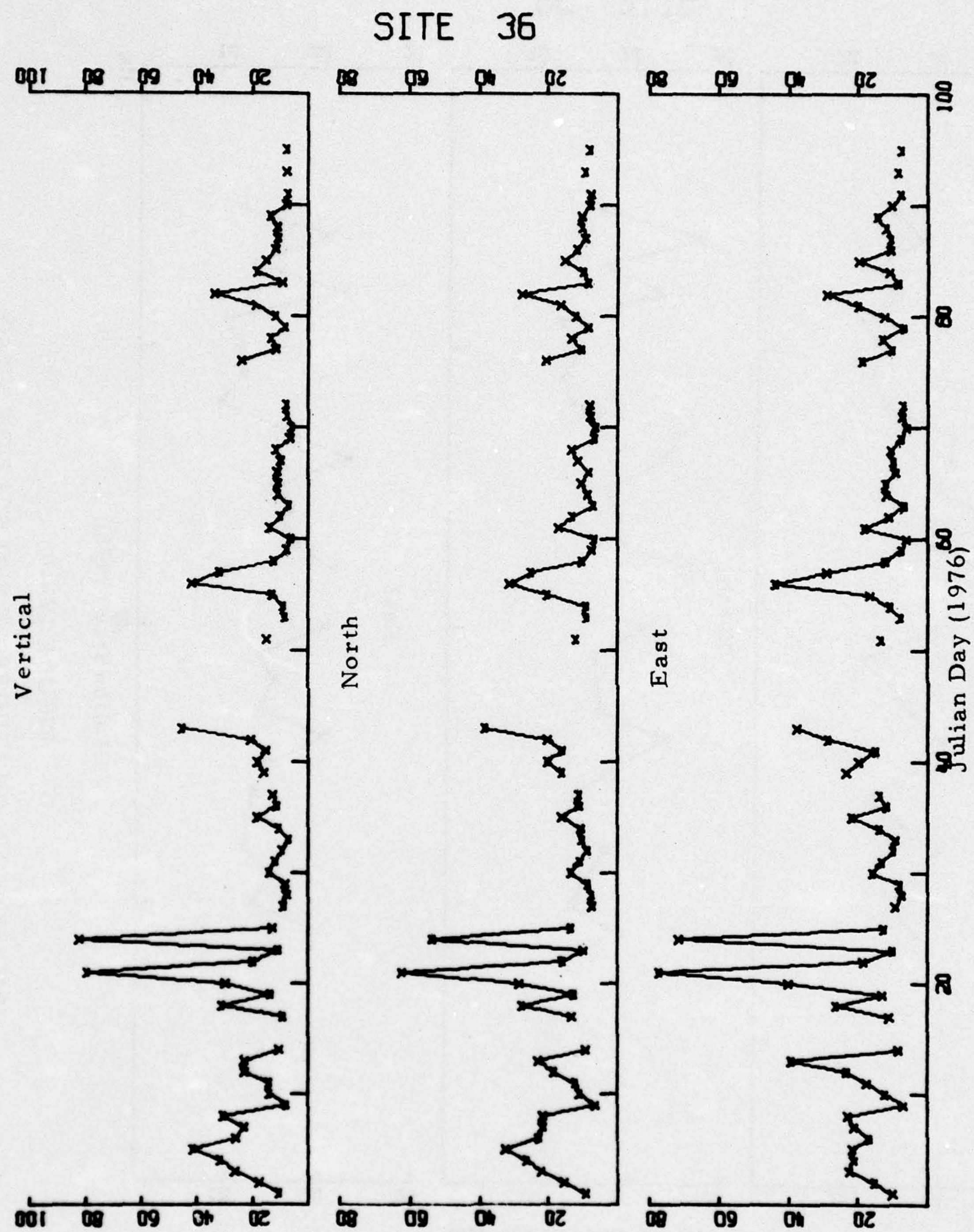

FIGURE IV-9

RMS NOISE AMPLITUDES AT SRO STATION MAIO

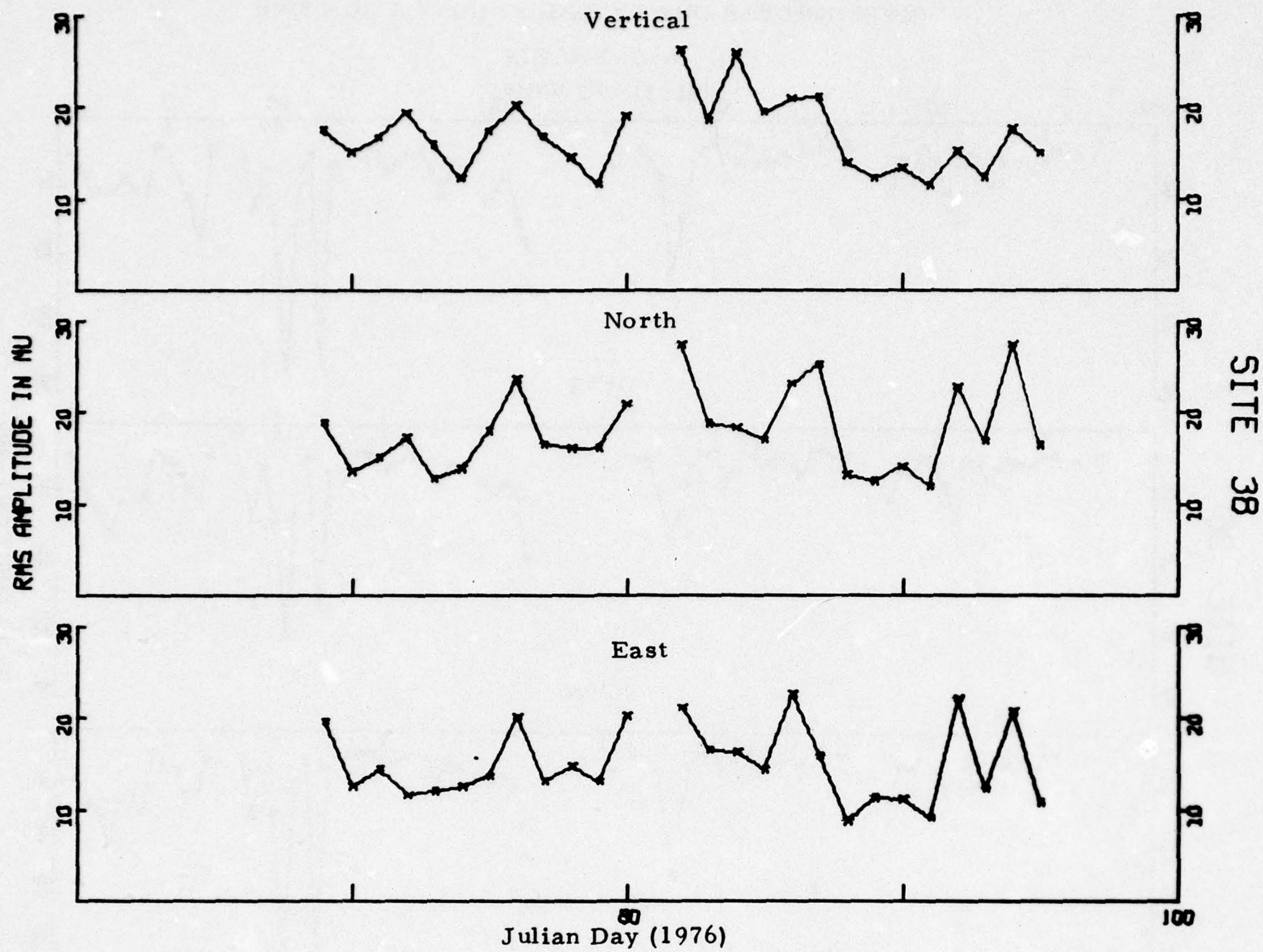

FIGURE IV-10

RMS NOISE AMPLITUDES AT SRO STATION NWAO

SITE 42

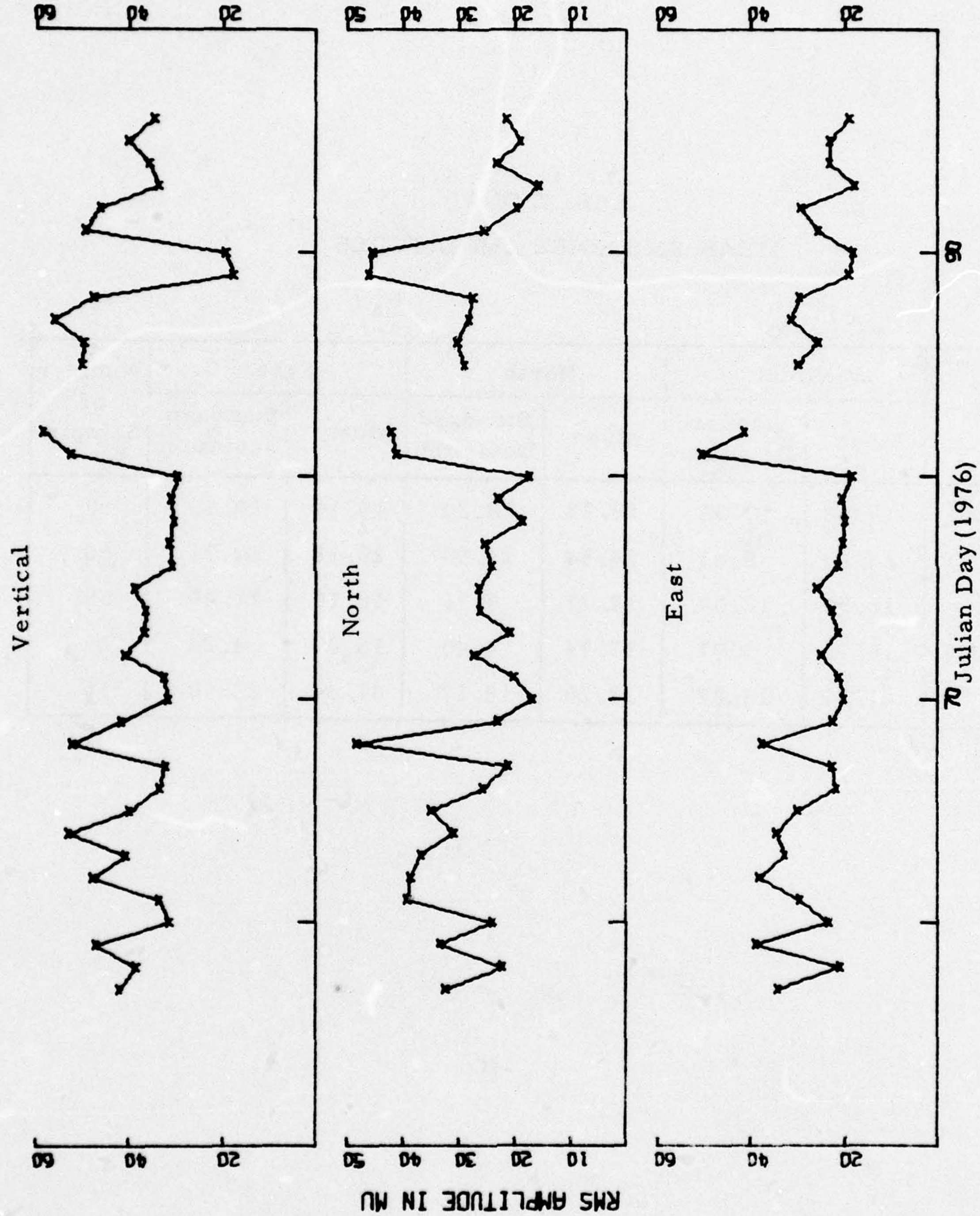

FIGURE IV-11

RMS NOISE AMPLITUDES AT SRO STATION SNZO

TABLE IV-1

MEAN RMS NOISE AMPLITUDES

Station	Vertical		North		East		Number of Samples
	Mean	Standard Deviation	Mean	Standard Deviation	Mean	Standard Deviation	
ANMO	18.18	17.09	19.78	18.29	19.19	20.53	80
GUMO	14.84	8.93	24.54	12.90	26.18	12.71	68
MAIO	16.50	12.09	14.77	9.31	16.16	11.45	66
NWAO	16.76	3.97	17.74	4.40	15.00	4.24	25
SNZO	41.14	13.27	32.26	18.17	31.34	23.52	35

deviations occur during February at each of the three stations. The RMS noise shows little variation during March. The RMS noise data for NWAO and SNZO is too sparse to make any observations about the noise trends. In contrast to the short-period RMS noise, GUMO shows relatively low average RMS noise values, having the lowest vertical-component RMS noise of the five stations and the second-lowest (after MAIO) North- and East-component RMS noise. The highest average RMS noise values were recorded at SNZO.

The long-term noise level trends for ANMO, GUMO, and MAIO are shown in Figures IV-12 to IV-14. (The data for NWAO and SNZO are too limited at this time to compute any long-term trends.) At ANMO and GUMO, the RMS noise drops to a minimum during March and starts to increase again in April. In contrast to this, the MAIO RMS noise shows a decline from January to April.

Figures IV-15 to IV-19 present the results of averaging all available instrument-response corrected noise spectra at each station. All three components of motion are shown. This averaging removes minor variations in the spectra. We will first discuss several unusual features of these plots. Considering the ANMO data, we see that the North component shows much higher RMS amplitudes than the other two components at periods above 28 seconds. This is solely due to the glitches discussed in Section III, which are so prevalent that for many days it was not possible to obtain a glitch-free noise sample.

A very interesting feature of the GUMO data is the local maximum occurring at 26 seconds, just where one might expect a minimum. (A somewhat similar feature can be found on the North component of MAIO and NWAO.) There are two possible causes for this phenomenon. First, it is possible that the instrument response for this station differs from the one shown in Figure IV-6, this difference being most pronounced at periods

SITE 30

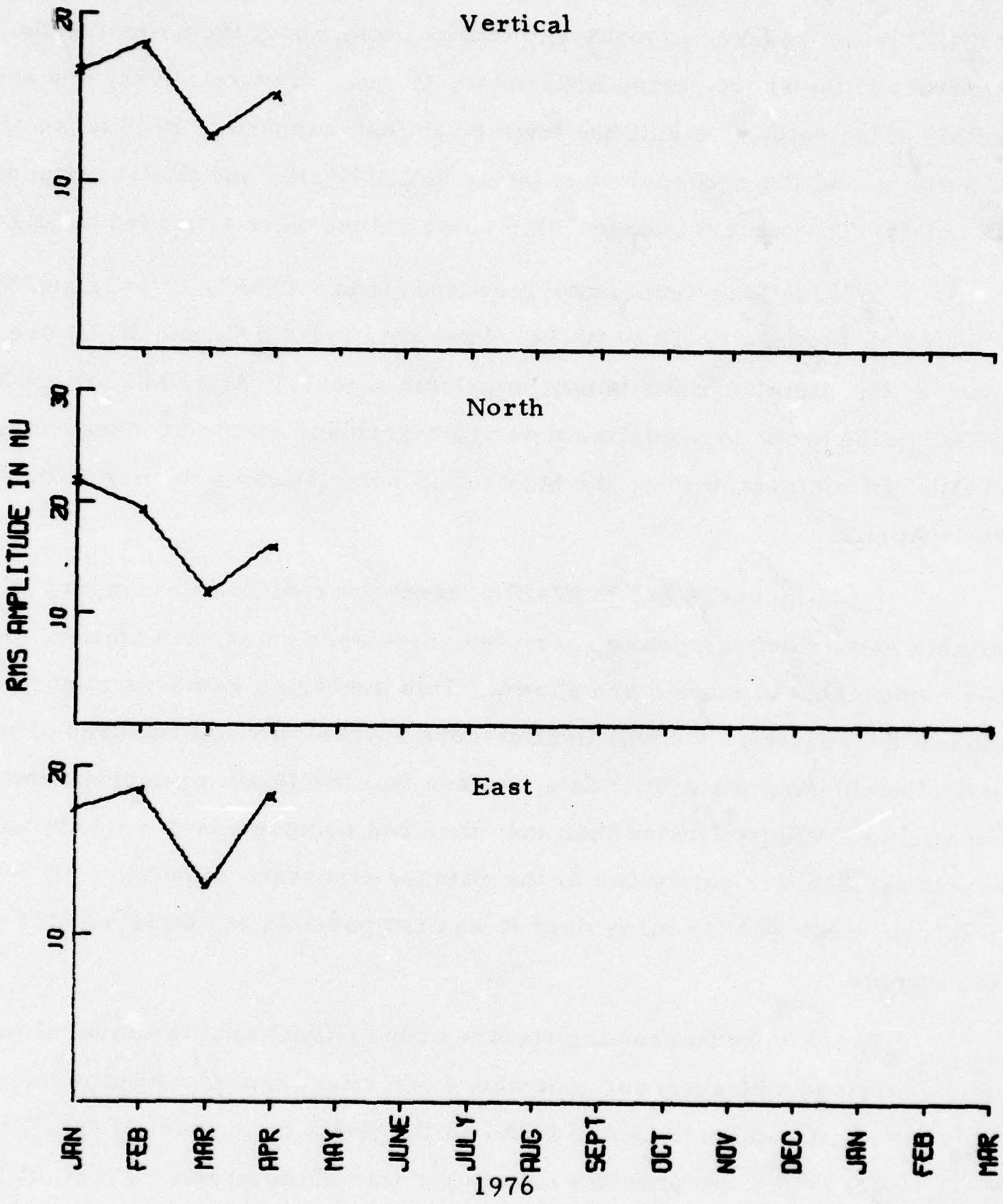

FIGURE IV-12

AVERAGE MONTHLY RMS NOISE AMPLITUDES
AT SRO STATION ANMO

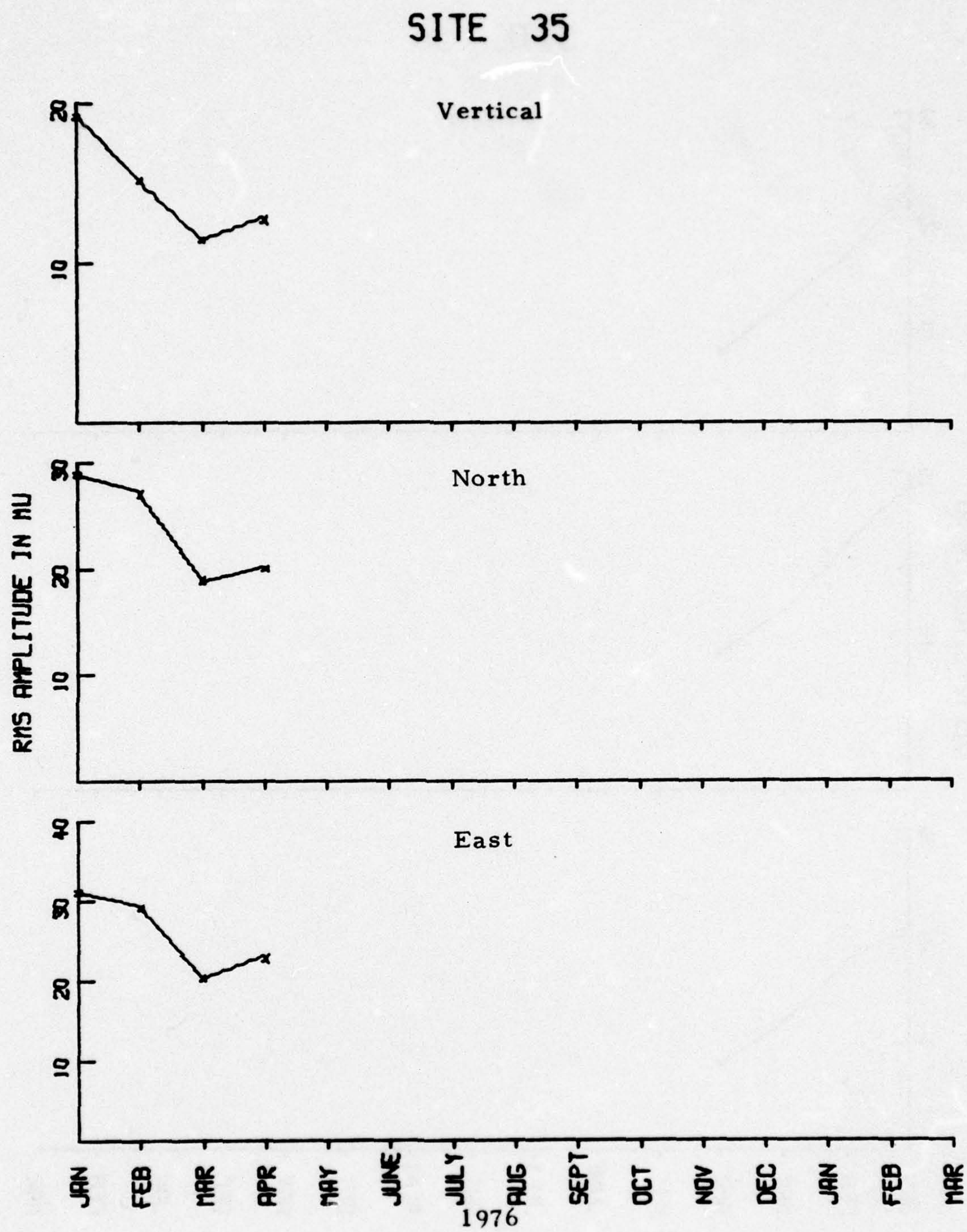

FIGURE IV-13

AVERAGE MONTHLY RMS NOISE AMPLITUDES
AT SRO STATION GUMO

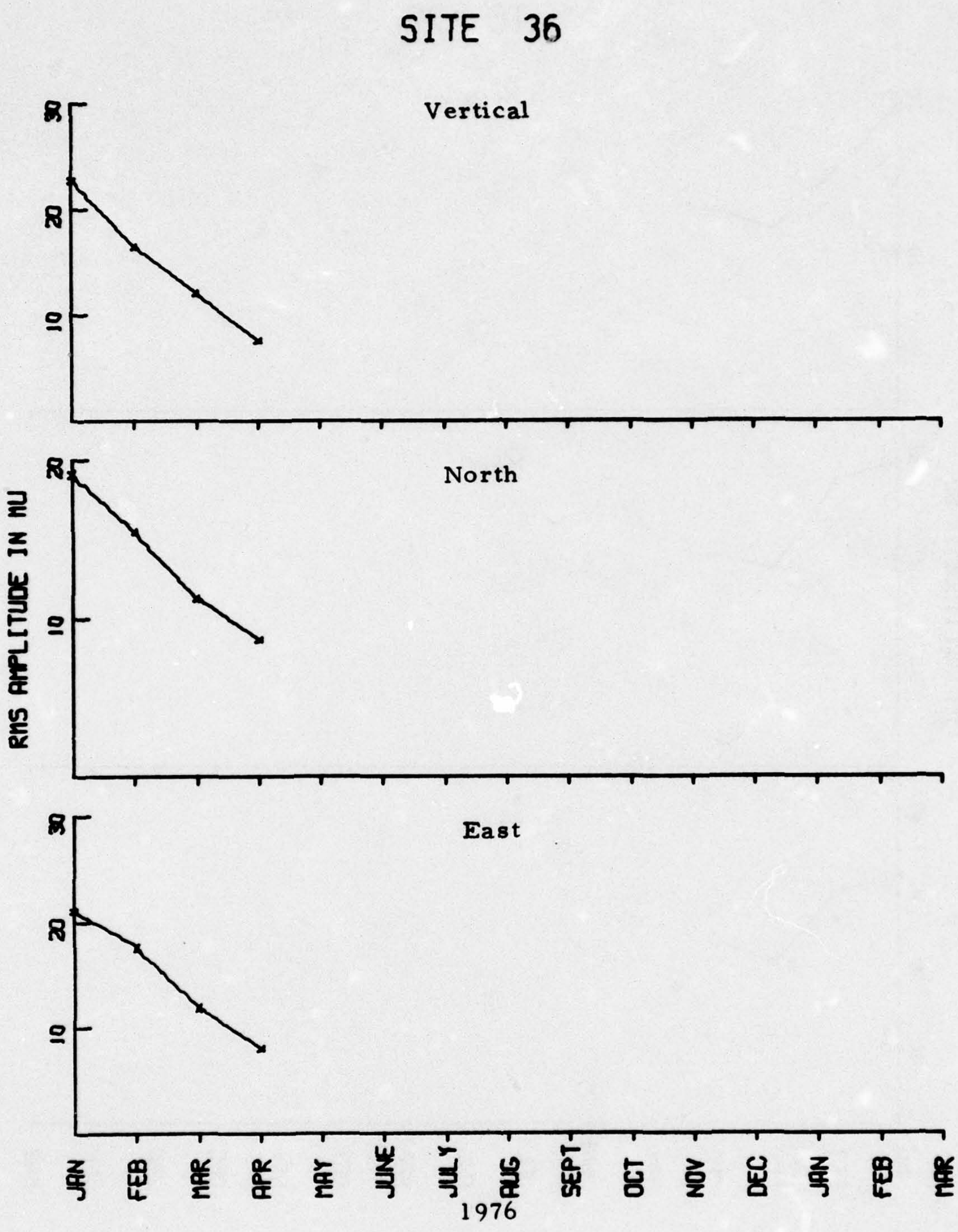

FIGURE IV-14

AVERAGE MONTHLY RMS NOISE AMPLITUDES AT SRO STATION MAIO

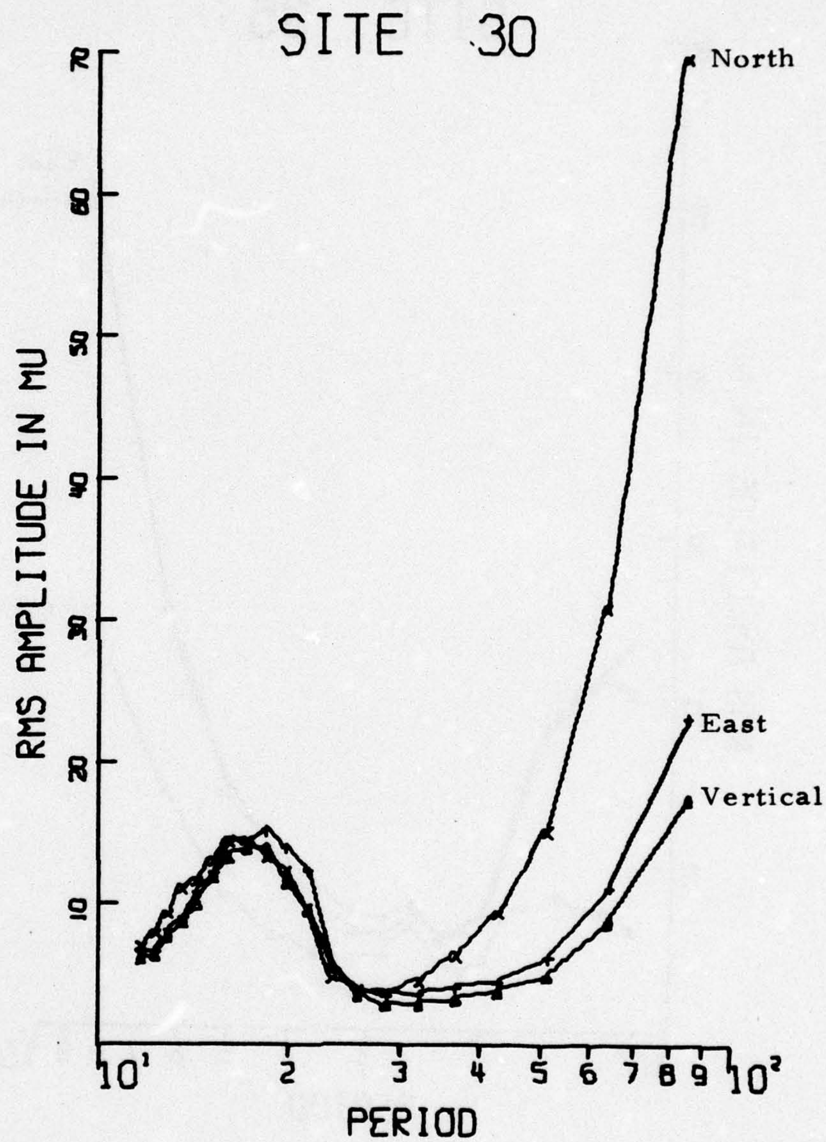

FIGURE IV-15

AVERAGE RMS AMPLITUDE SPECTRA
ANMO LONG-PERIOD NOISE

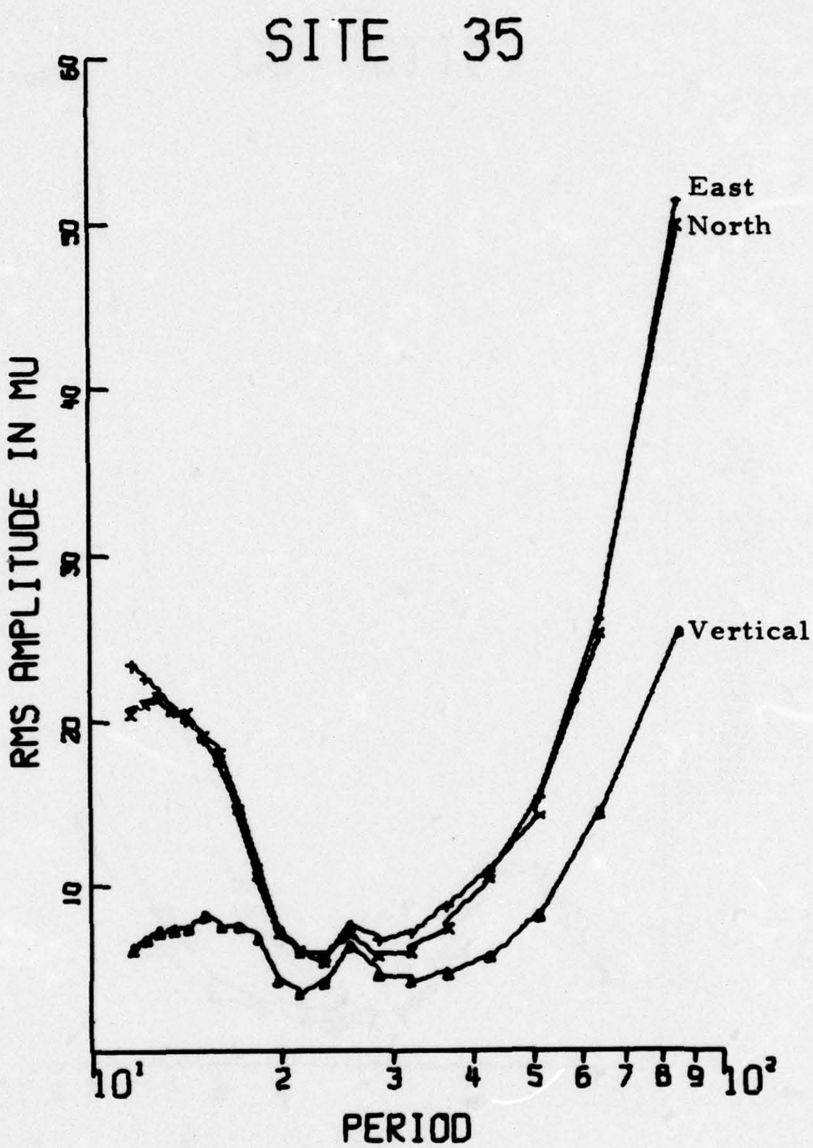

FIGURE IV-16

AVERAGE RMS AMPLITUDE SPECTRA
GUMO LONG-PERIOD NOISE

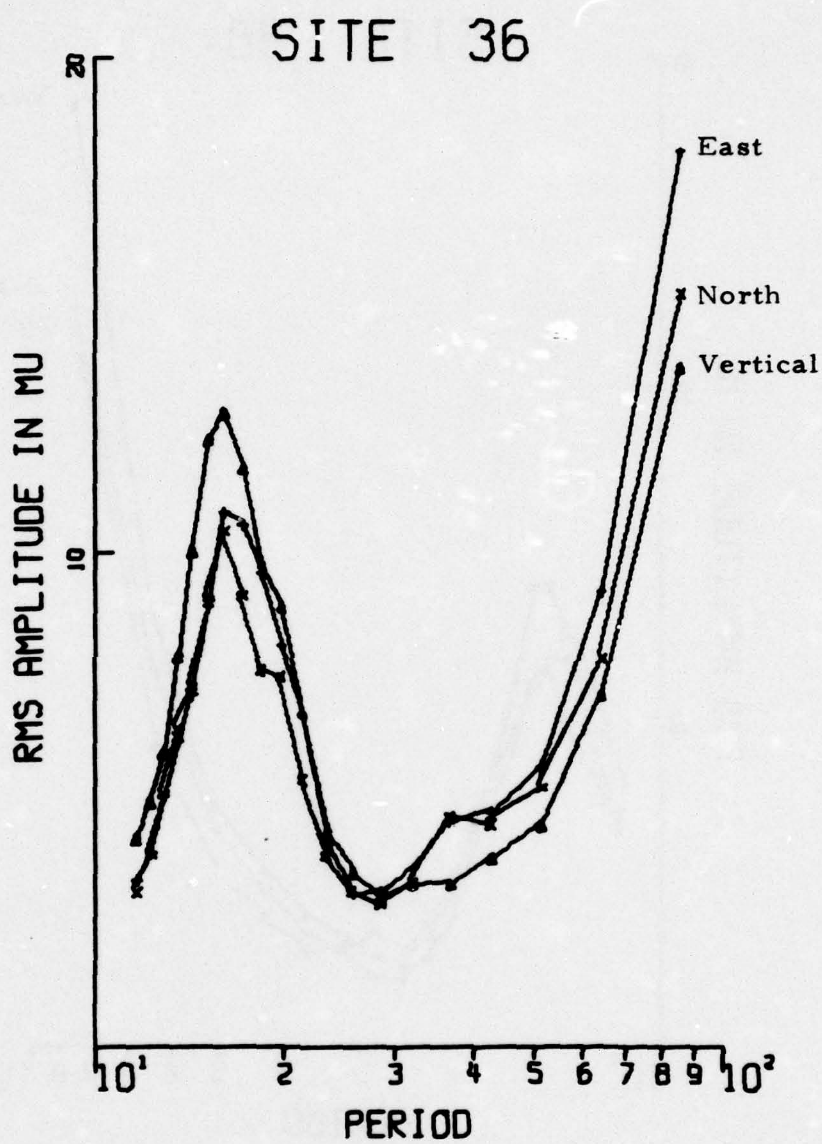

FIGURE IV-17

AVERAGE RMS AMPLITUDE SPECTRA
MAIO LONG-PERIOD NOISE

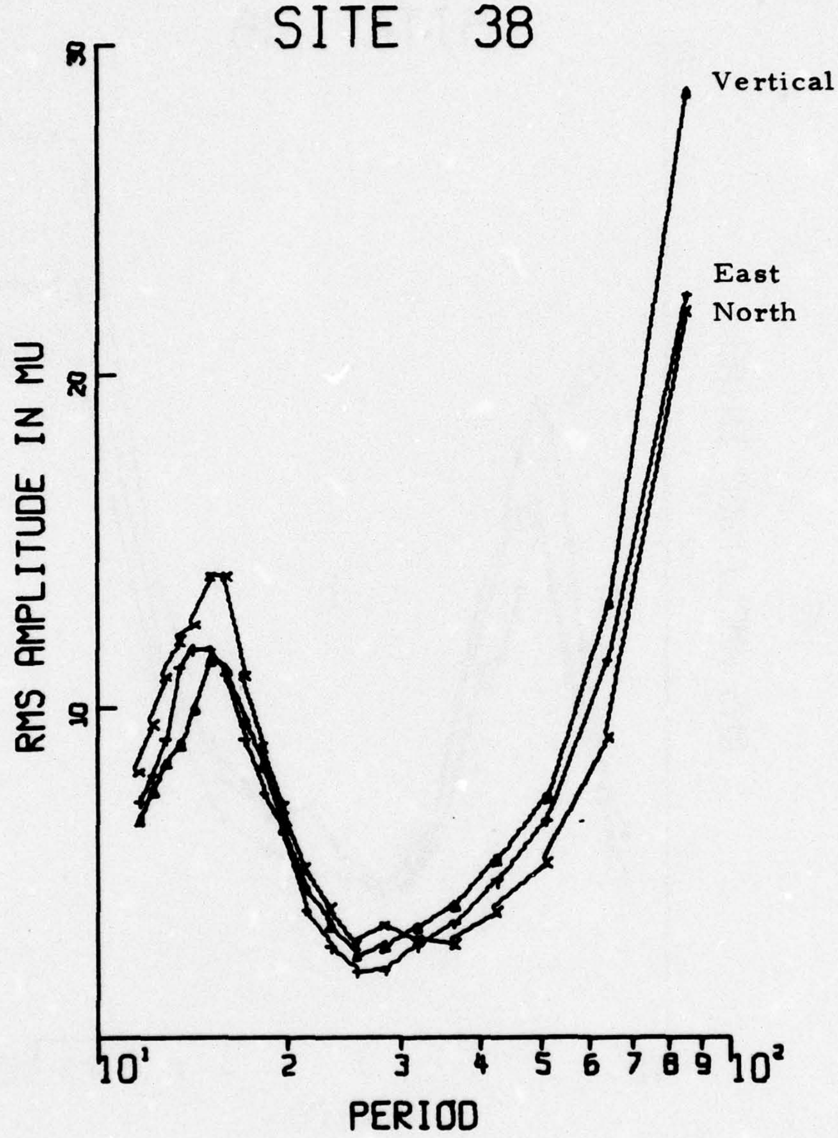

FIGURE IV-18

AVERAGE RMS AMPLITUDE SPECTRA
NWAO LONG-PERIOD NOISE

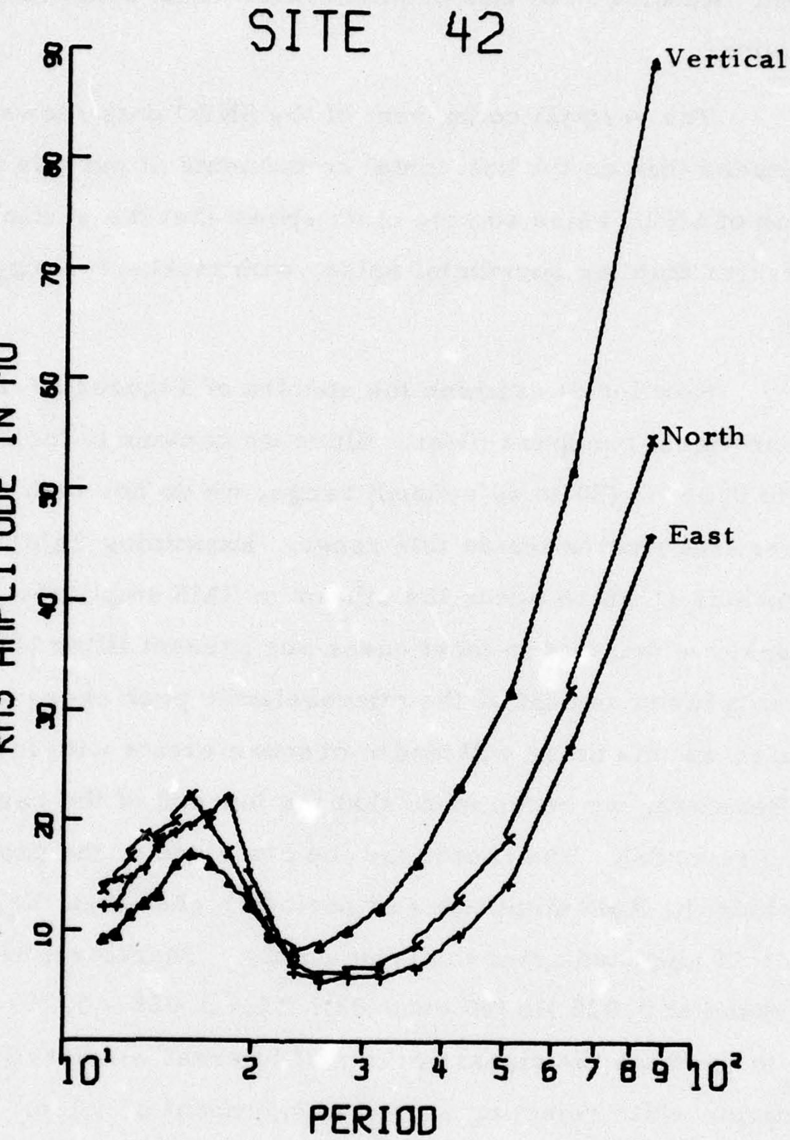

FIGURE IV-19

AVERAGE RMS AMPLITUDE SPECTRA
SNZO LONG-PERIOD NOISE

between 23 and 30 seconds. Second, the noise at 26 seconds may indeed be higher than at periods just above and below 26 seconds for some reason as yet unknown. Resolution of this problem must await detailed calibration data for this station.

The vertical component of the SNZO data shows much greater RMS amplitudes than do the horizontal components at periods above 23 seconds. Examination of SNZO noise sample plots shows that the vertical noise is indeed different than the horizontal noise, with markedly longer periods predominating.

Now let us examine the spectra of Figures IV-15 and IV-16 in terms of our signal bandpass filter. Since we commonly look for signals in the 0.025 to 0.05 Hz (20 to 40 second) range, we do not wish to place our filter corner frequencies inside this range. Examining Table IV-2, which lists the periods at which occur the minimum RMS amplitude and the microseismic peak, we see that in most cases our present filter (17.0 - 43.5 seconds) lets in a large amount of the microseismic peak energy. This is clearly unacceptable, as this noise will tend to obscure events with low signal-to-noise ratios. Therefore, we recommend that the low end of the passband be set at 0.05 Hz (20 seconds). The choice for the other end of the passband is not obvious, since the RMS amplitudes at periods higher than the period of the minimum RMS amplitude rise fairly smoothly. Therefore, let us set this end of the passband at 0.025 Hz (40 seconds). This 0.025 - 0.050 Hz passband will permit us to examine the signal periods of interest without filter-induced signal degradation while rejecting a maximum amount of noise.

TABLE IV-2

PERIODS OF MICROSEISMIC PEAKS AND SPECTRAL MINIMA

Station	Period at which Min. Occurs			Period of Microseismic Peak		
	V	N	E	V	N	E
ANMO	28	28	32	17	16	18
GUMO	21	23	23	15	12	13
MAIO	28	28	26	16	16	16
NWAO	26	26	26	15	15	15
SNZO	23	26	26	16	16	18

SECTION V

SRO DETECTION CAPABILITY

The goal of this phase of the SRO evaluation was to determine estimates of the detection capability of each SRO station for both short-period and long-period data. Due to the limited size of the data base for each station, these estimates were made on a worldwide basis only. Regionalization of detection capability will have to await an enlarged data base.

A. DIRECT ESTIMATES OF SHORT-PERIOD DETECTION CAPABILITY

The criteria determining whether an event was detected on the recorded vertical short-period component are as follows:

- Waveform under analysis is at least 12 dB above the preceding noise.
- Waveform is impulsive, not emergent.
- Waveform begins within ± 20 seconds of predicted arrival time.

The requirement that the amplitude of the waveform under analysis be at least 12 dB above the preceding noise amplitudes is set high because the amplitude change is of overriding importance when searching for P-waves on a single component of motion. It must be remembered that we do not have available the information which three components of short-period motion provide, i.e., the approximate arrival azimuth provided by the direction (up or down) of the first arrival and the approximate epicentral distance provided by the P-S arrival time separation. (S is rarely observed on the vertical component.) Therefore, to help insure that the waveform we are analyzing is a P-wave, we must have a large increase in amplitude over the noise.

We require the waveform to be impulsive in order that we may determine the P-wave arrival time. Without this, we cannot be sure of fulfilling the third requirement. By allowing an arrival gate of $\pm$ 20 seconds, we recognize that the origin time and/or epicenter coordinates may be in error, causing deviation from the predicted arrival time. Also, we must bear in mind that we had at the time of analysis no depth information and that the predicted arrival time is based on the assumption that the event occurred at normal (33 km) depth. Differences in depth will also cause changes in arrival time.

The third criterion is not absolute. It is possible that origin time and epicenter coordinates may be in error (perhaps due to great epicentral depth) such that the P-wave may arrive outside the time gate. In cases where this happened and no other event in the NORSAR event list could be found which could have arrived at that time, a detection was declared. This was, however, a rare occurrence.

The results of this first look at the detection capability of the short-period component of motion are illustrated by Figures V-1 to V-4 and are summarized in Table V-1. The upper portion of each figure shows an m_b histogram of the available data broken down into number of detections and non-detections. The lower portion of each figure shows the maximum likelihood curve fitted to the data. In each figure, "MB50" denotes the 50 percent detection threshold, "MB90" denotes the 90 percent detection threshold, "SIGMA" is related to the slope of the maximum likelihood curve, and "RHO" denotes the quality of the results (Ringdal, 1974). There is no figure for the GUMO short-period data, since no events were detected on the short-period component at this station due to the abnormally high RMS noise level.

We must emphasize that these results are determined from only those events for which data was recorded. The events which failed to trigger the automatic detector or which had epicenters greater than 103°

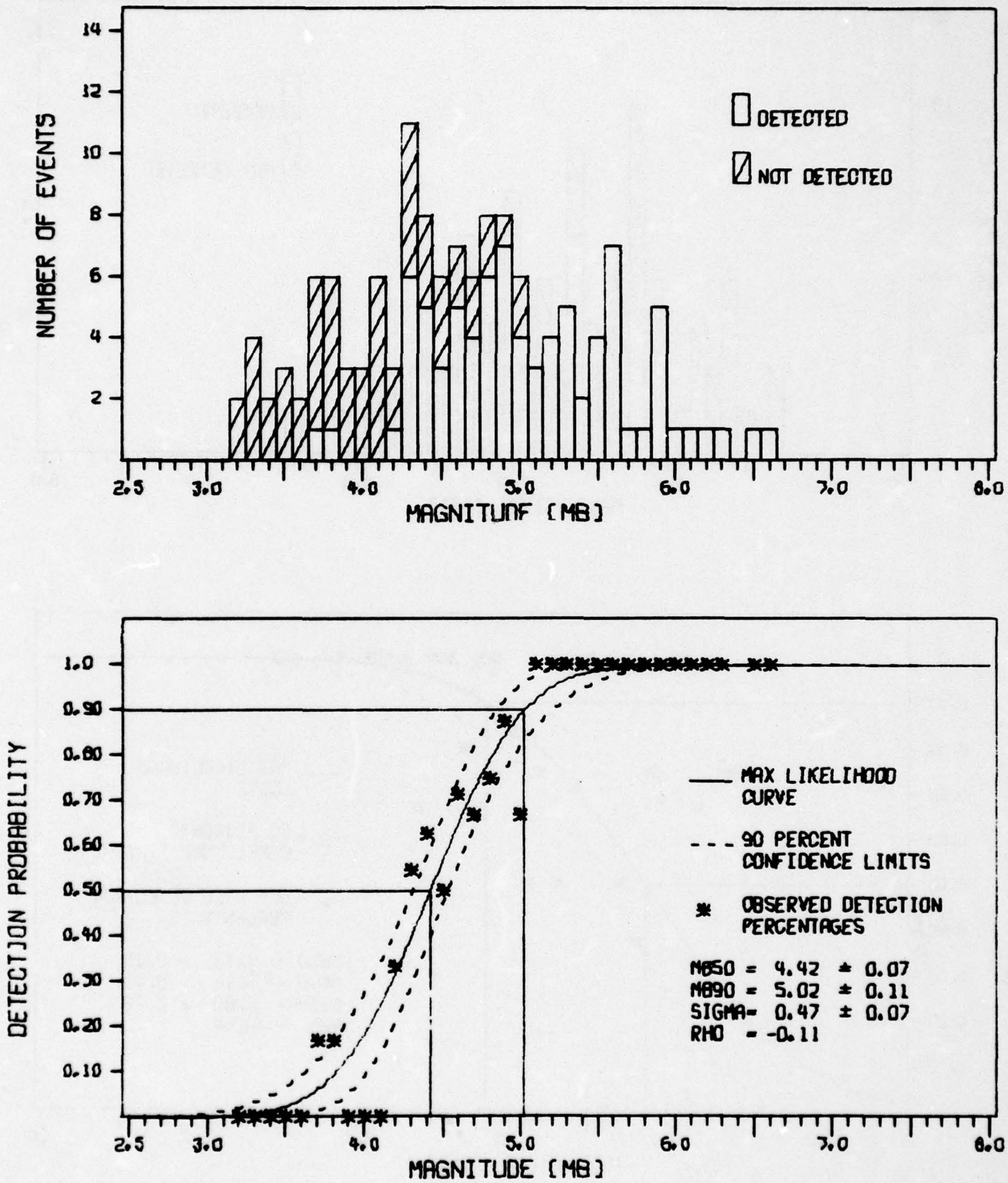

FIGURE V-1

ANMO SHORT-PERIOD DETECTION STATISTICS

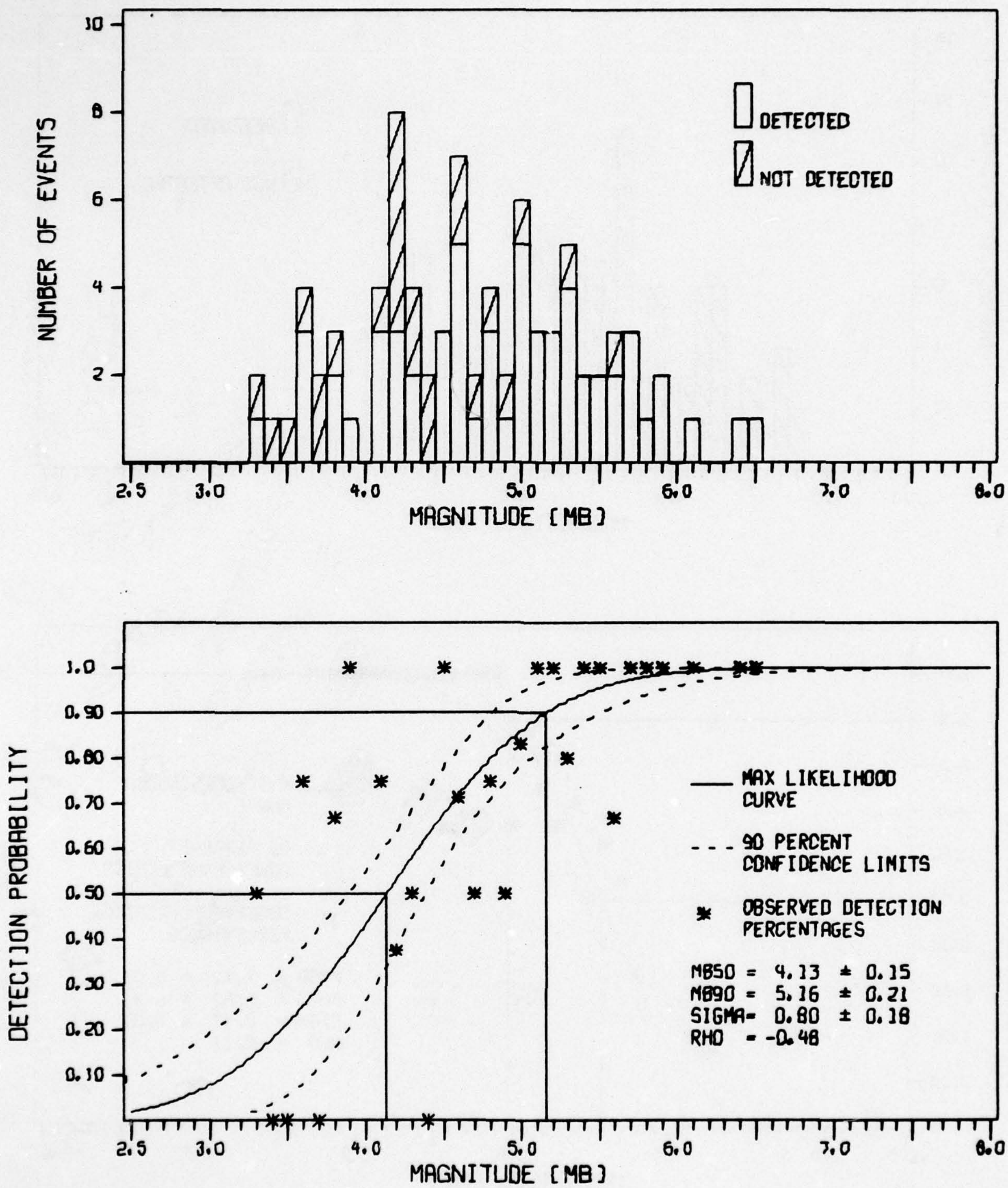

FIGURE V-2

MAIO SHORT-PERIOD DETECTION STATISTICS

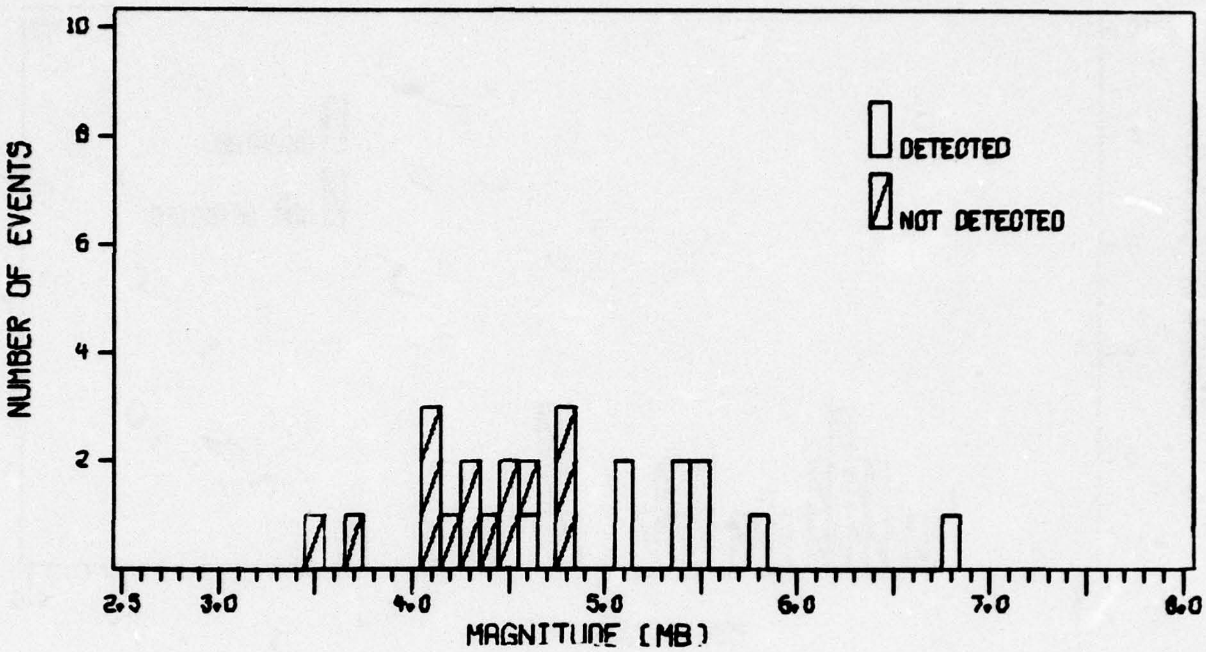

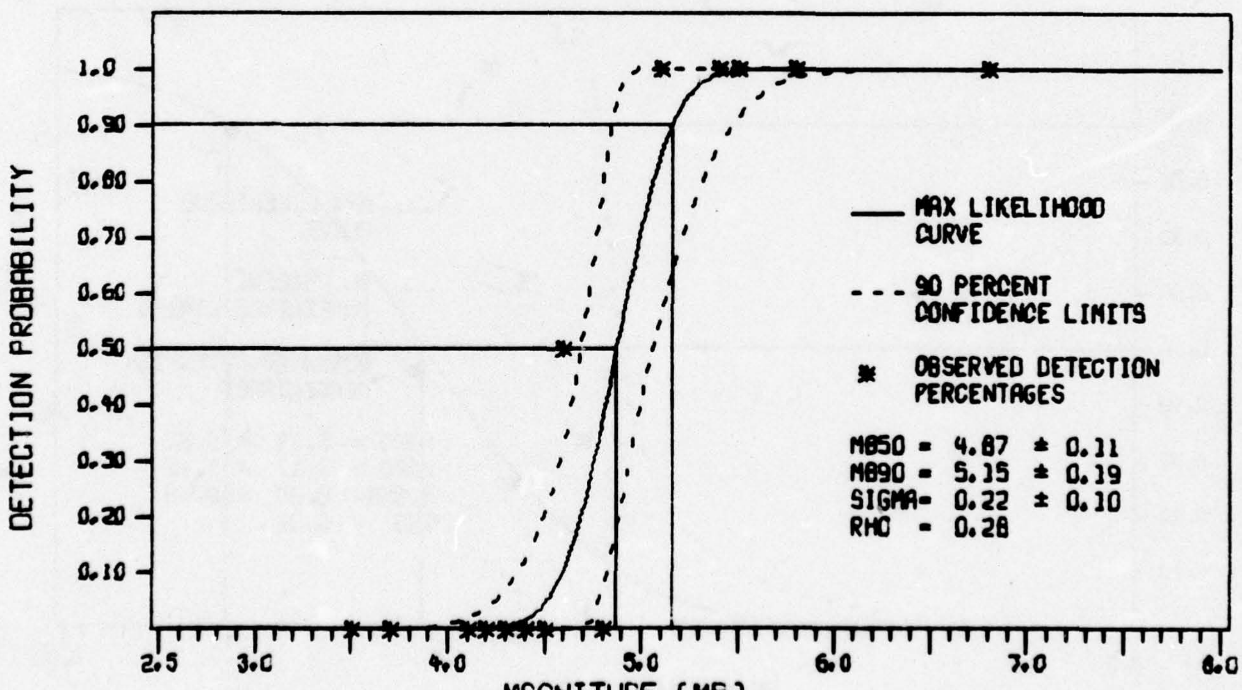

FIGURE V-3

NWAO SHORT-PERIOD DETECTION STATISTICS

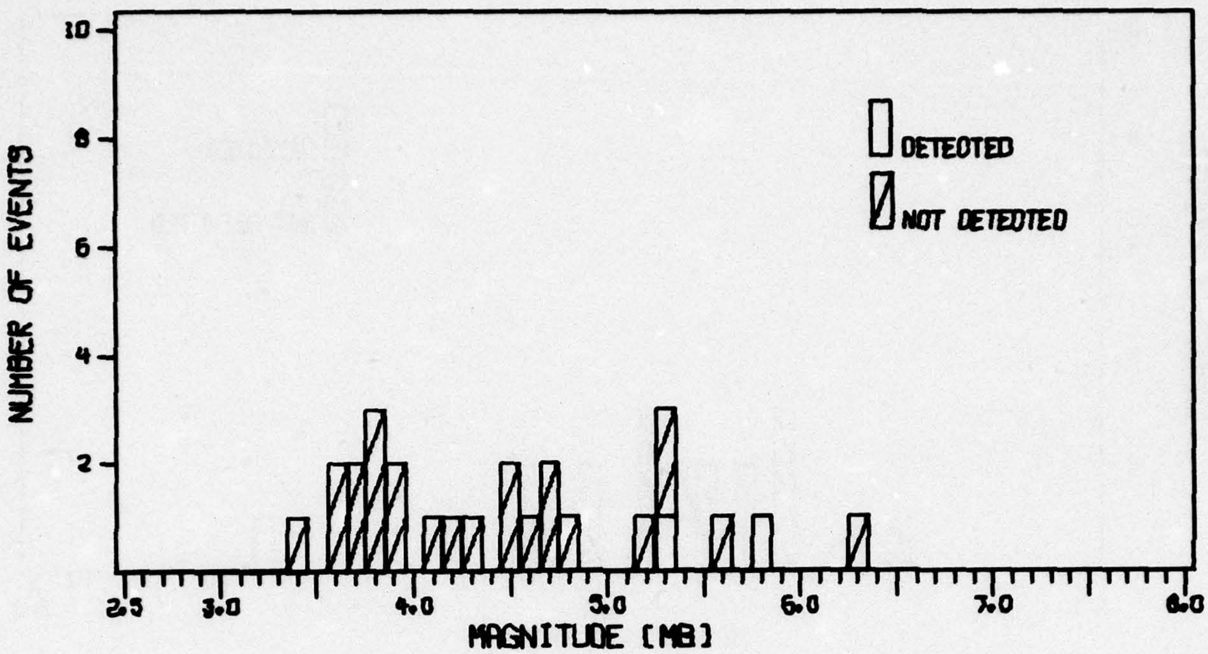

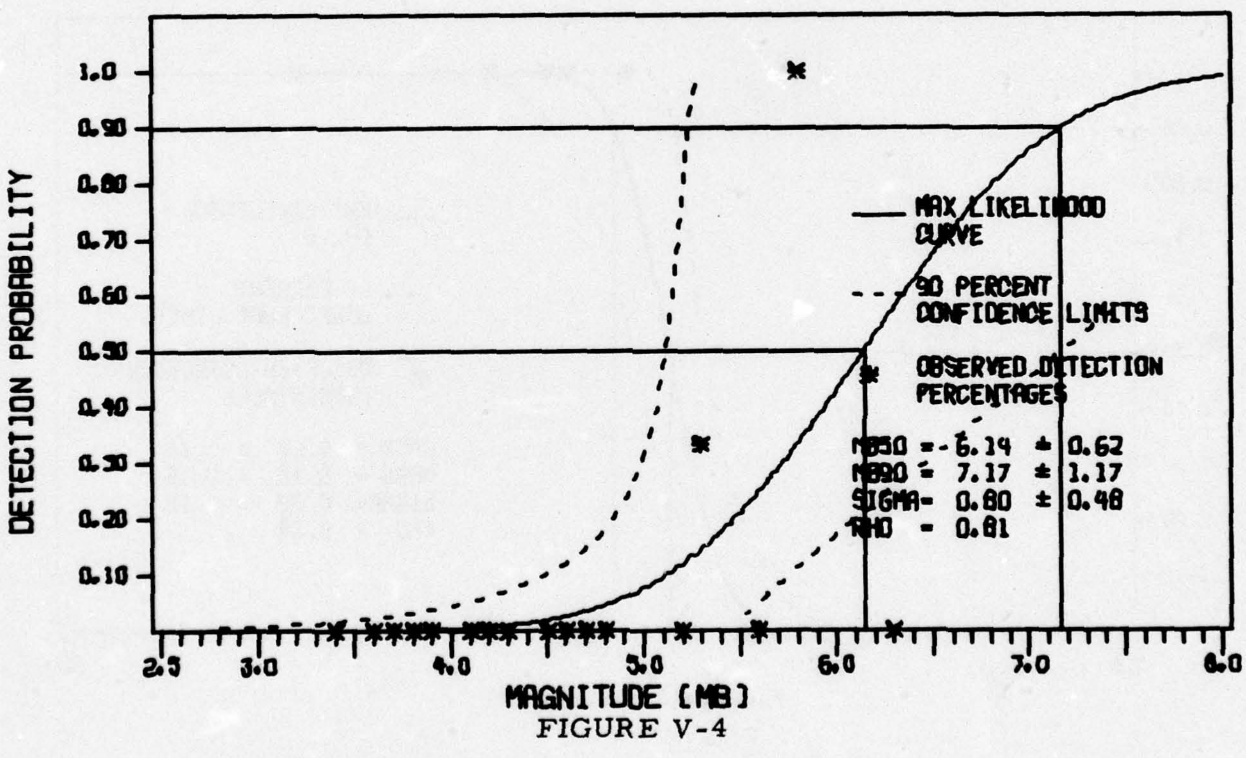

FIGURE V-4

SNZO SHORT-PERIOD DETECTION STATISTICS

TABLE V-1

SUMMARY OF BODYWAVE MAGNITUDE (m_b) DETECTION THRESHOLDS

Station	50% m_b Detection Threshold	90% m_b Detection Threshold
All Events		
ANMO	4.42 $\pm$ 0.07	5.02 $\pm$ 0.11
MAIO	4.13 $\pm$ 0.15	5.16 $\pm$ 0.21
NWAO	4.87 $\pm$ 0.11	5.15 $\pm$ 0.19
SNZO	6.14 $\pm$ 0.62	7.17 $\pm$ 1.17
Shallow (depth < 100 km) Earthquakes		
ANMO	4.47 $\pm$ 0.07	5.06 $\pm$ 0.11
MAIO	4.14 $\pm$ 0.15	5.17 $\pm$ 0.22
NWAO	4.87 $\pm$ 0.19	5.15 $\pm$ 0.19
SNZO	6.14 $\pm$ 0.62	7.17 $\pm$ 1.17

away from the station have been excluded from the detection statistics. Therefore, we may consider these results to be representative of the case where short-period data is continually recorded, assuming that the short-period noise levels discussed in Section IV remain constant.

Figures V-1 to V-4 show that we can trust only the detection threshold for ANMO. Due to the number of detected events at low m_b values, the variance of the detection threshold for the MAIO data is high. The available number of detections and non-detections for NWAO and SNZO is simply too small to produce reliable detection threshold estimates. This problem will be resolved in future work when we expand the data base.

The short-period detection results presented here include all available events, including deep events and presumed explosions. The detection probability curves of Figures V-1 to V-4 were recomputed with all deep events and presumed explosions removed. The results of this recomputation are summarized in Table V-1. We see from this table that the inclusion of these deep events and presumed explosions makes essentially no difference in the short-period detection thresholds of these stations.

B. INDIRECT ESTIMATES OF LONG-PERIOD DETECTION CAPABILITY

It is possible to derive detection threshold magnitudes from ambient noise levels, since detection of a seismic event depends on the signal-to-noise ratio at the recording station. Unger (Unger, 1974) developed the theoretical background for this method and tested it on Very Long Period Experiment data. In this method, it is assumed that an event can be detected when its maximum amplitude exceeds that of the surrounding noise by a certain margin. We may then assign a magnitude to the maximum noise amplitude A occurring in a certain time gate, using some period T and some epicentral distance Δ. For surface waves, this magnitude is:

$$M_{s\,NOI} = \log_{10}(A/T) + \log_{10}\Delta + 1.12$$

where $\log\Delta + 1.12$ represents the distance correction. The probability of detecting an event of given magnitude $M_{s\,SIG} = x$ is:

$$P(\text{DET } M_{s\,SIG} = x) = P(M_{s\,NOI} \leq x) .$$

As described by Unger (Unger, 1974), the 50 percent detection threshold is determined from the average of the random variable M_s where M_s is the noise magnitude plus the station magnitude difference due to period minus the station bias. Thus, in our computations, we use the logarithm of the geometric mean of the noise amplitude, the signal period T, and the epicentral distance Δ. The final detection capability estimation algorithm which Unger develops is:

$$M_{s\,50} = \text{MEAN LOG AMP} - \log_{10} T_o * G(T_o) + \log_{10} \Delta_o + d(T_o) - \bar{b} + C$$

where

MEAN LOG AMP	=	the mean of the logarithm of the maximum peak-to-peak seismometer output noise amplitudes,
$\log_{10} T_o$	=	the logarithm of the geometric mean of the period of the maximum signal amplitude,
$G(T_o)$	=	the instrument response correction at T_o,
$\log_{10}\Delta_o$	=	the logarithm of the geometric mean of the signal epicentral distances,
$d(T_o)$	=	the station magnitude difference due to T_o,
$\bar{b}$	=	the mean station bias, and
C	=	$1.12 + \log_{10}$ of the detection criterion margin.

In this case, 30 consecutive noise samples from each station were used to compute MEAN LOG AMP. The parameter T_o was selected to be 20 seconds, since this period was more often observed in detected signals than either 30 seconds or 40 seconds. $G(T_o)$ was then the instrument response correction at 20 seconds picked from the long-period instrument response curve of Figure IV-6. The parameter Δ_o was varied from 10^o to 100^o in 10^o increments to give us a table of M_{s50} versus epicentral distance. The parameter $d(T_o)$ was picked from the plot of magnitude difference versus period found in Unger's report (Unger, 1974). A continental path was assumed for ANMO and MAIO and an oceanic path for GUMO, NWAO, and SNZO. Since we had no previous knowledge of the mean station bias, $\bar{b}$ was assumed to be zero. The detection criterion margin was set at a factor of 2, making $C = 1.12 + \log_{10}(2) = 1.42$. This choice means that, in order to be detected, the peak amplitude of a signal must be twice the peak noise amplitude. This is a somewhat conservative choice, since it is sometimes possible to detect a signal whose peak amplitude is less than twice the peak noise amplitude. The results of these computations are listed in Table V-2.

C. DIRECT ESTIMATES OF LONG-PERIOD DETECTION CAPABILITY

Direct estimates of long-period SRO detection capability were made for each of the five stations evaluated in this report. The criteria for determining whether detection was achieved for a given event are:

- The presence of dispersion in the signal gate.
- A peak in the dispersed wave train 3 dB or more above any peak outside the dispersed wave train and inside a 20 minute time gate centered at the expected peak occurrence time.
- The onset of the signal occurs within ± 180 seconds of the expected signal onset time.

TABLE V-2

INDIRECT ESTIMATES OF 50 PERCENT DETECTION THRESHOLD

Δ	ANMO		GUMO		MAIO		NWAO		SNZO	
	M_{s50}	m_{b50}	M_{s50}	m_{b50}	M_{s50}	m_{b50}	M_{s50}	m_{b50}	M_{s50}	m_{b50}
10^o	2.91	3.97	2.84	4.13	2.94	4.12	2.93	4.04	3.30	4.08
20^o	3.21	4.16	3.15	4.31	3.24	4.27	3.23	4.22	3.60	4.28
30^o	3.39	4.28	3.32	4.41	3.41	4.36	3.41	4.33	3.77	4.40
40^o	3.51	4.35	3.45	4.49	3.54	4.43	3.53	4.40	3.90	4.48
50^o	3.61	4.42	3.54	4.54	3.64	4.48	3.63	4.46	4.00	4.55
60^o	3.69	4.47	3.62	4.59	3.72	4.53	3.71	4.51	4.08	4.60
70^o	3.75	4.51	3.69	4.63	3.78	4.56	3.78	4.55	4.14	4.64
80^o	3.81	4.55	3.75	4.66	3.84	4.59	3.84	4.59	4.20	4.68
90^o	3.86	4.58	3.80	4.69	3.89	4.62	3.89	4.62	4.25	4.72
100^o	3.91	4.61	3.84	4.72	3.94	4.64	3.93	4.64	4.30	4.75

ANMO: m_{b50} computed from $M_s = 1.55\ m_b - 3.24$

GUMO: m_{b50} computed from $M_s = 1.72\ m_b - 4.27$

MAIO: m_{b50} computed from $M_s = 1.90\ m_b - 4.88$

NWAO: m_{b50} computed from $M_s = 1.66\ m_b - 3.78$

SNZO: m_{b50} computed from $M_s = 1.49\ m_b - 2.78$

These M_s-m_b relationships are taken from Table VI-1 on page VI-8.

In practice, these criteria are not absolute. Occasionally, an event was considered to be detected which did not meet all of these criteria. Signal peaks could be less than 3 dB above noise peaks and still be recognized as signals from their dispersion characteristics. Also, some signals arrived later than the third criterion allows but were still recognized as detections. The most interesting case of this is the case of signals originating in the Kurile Islands-Kamchatka area as recorded at MAIO. An example of this is shown in Figure V-5. We see in this figure that the visible signal of each event arrives later than would be expected and that the dispersion is weaker than would be expected. In the $m_b = 4.8$ event, dispersion cannot be seen, while in the $m_b = 5.5$ event, the dispersion is weak. The most prominent feature of each signal is the 20-second energy arriving late in the signal gate. During the course of examining signals from this region as recorded at MAIO, it was found that this 20-second energy is so consistent in appearance and arrival time that it could serve as a detection criterion; i.e., if this energy is present, the event is detected. On low signal-to-noise ratio events, this feature was visible even though dispersion was weak or not visible and the observed arrival was later than expected. Thus, it is sometimes possible to find specific features of a seismic waveform from a given region as recorded at a given station which enable us to detect these events even though all detection criteria may not be satisfied.

The results of this detection study are shown in Figures V-6 to V-10. As in the case of the short-period data, the histograms in the upper portion of each of these figures show the m_b distribution and number of detections and non-detections for the available data. Only events for which a detection/non-detection decision could be made are included. Those events which were mixed or contained malfunctions have been removed. The lower portion of each figure shows a maximum likelihood fit to the data points derived from the relative number of detections and non-detections. We show in

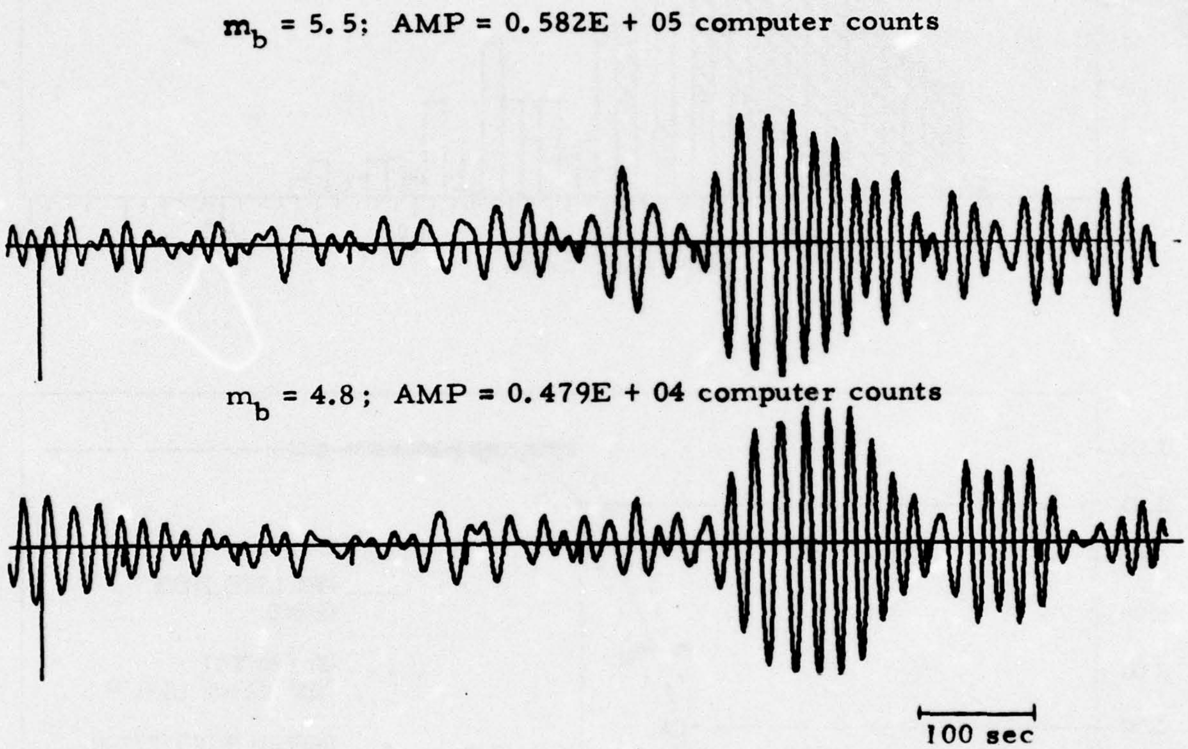

FIGURE V-5

LR-V FROM TWO KAMCHATKA AREA EARTHQUAKES
AS RECORDED AT MAIO

Filter Passband = 0.023 - 0.059 Hz

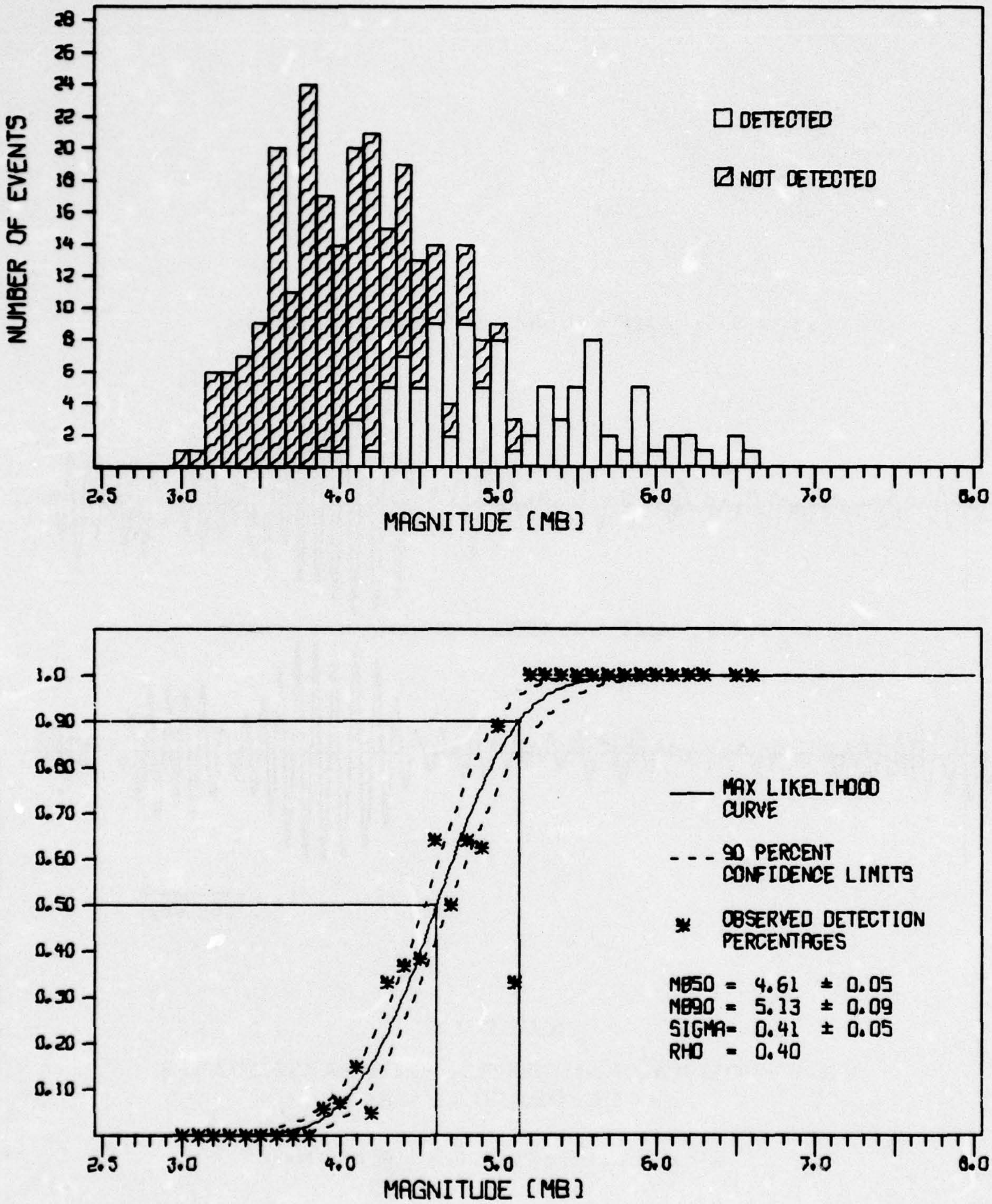

FIGURE V-6

ANMO LONG-PERIOD VERTICAL COMPONENT DETECTION STATISTICS

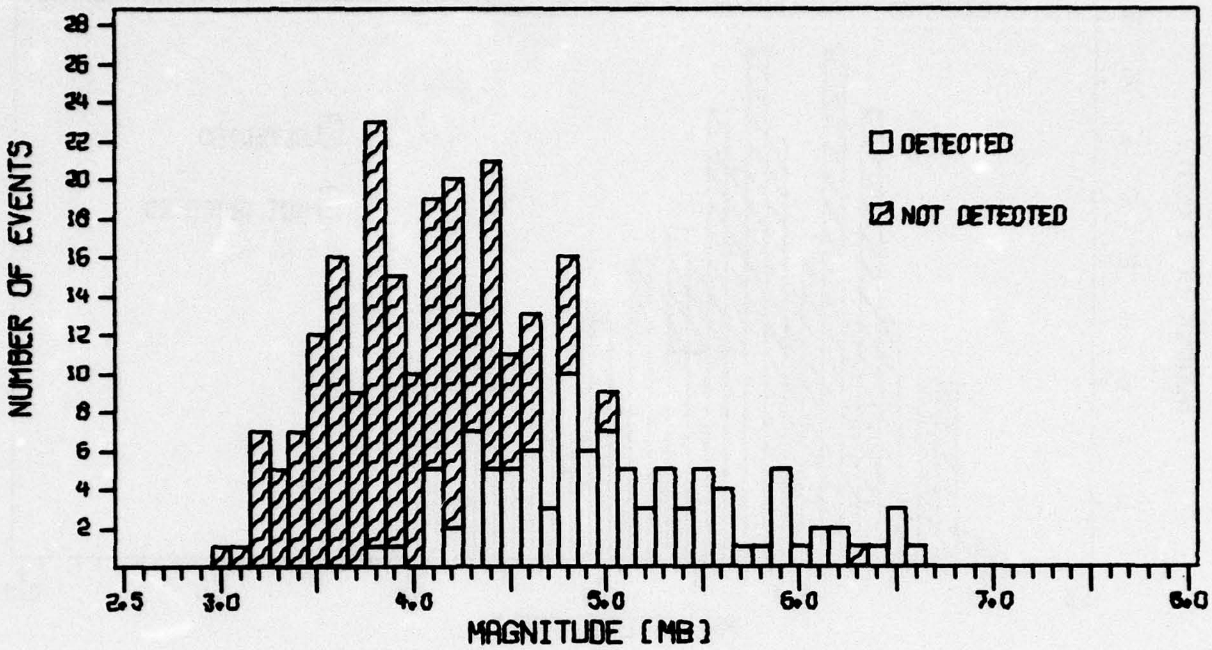

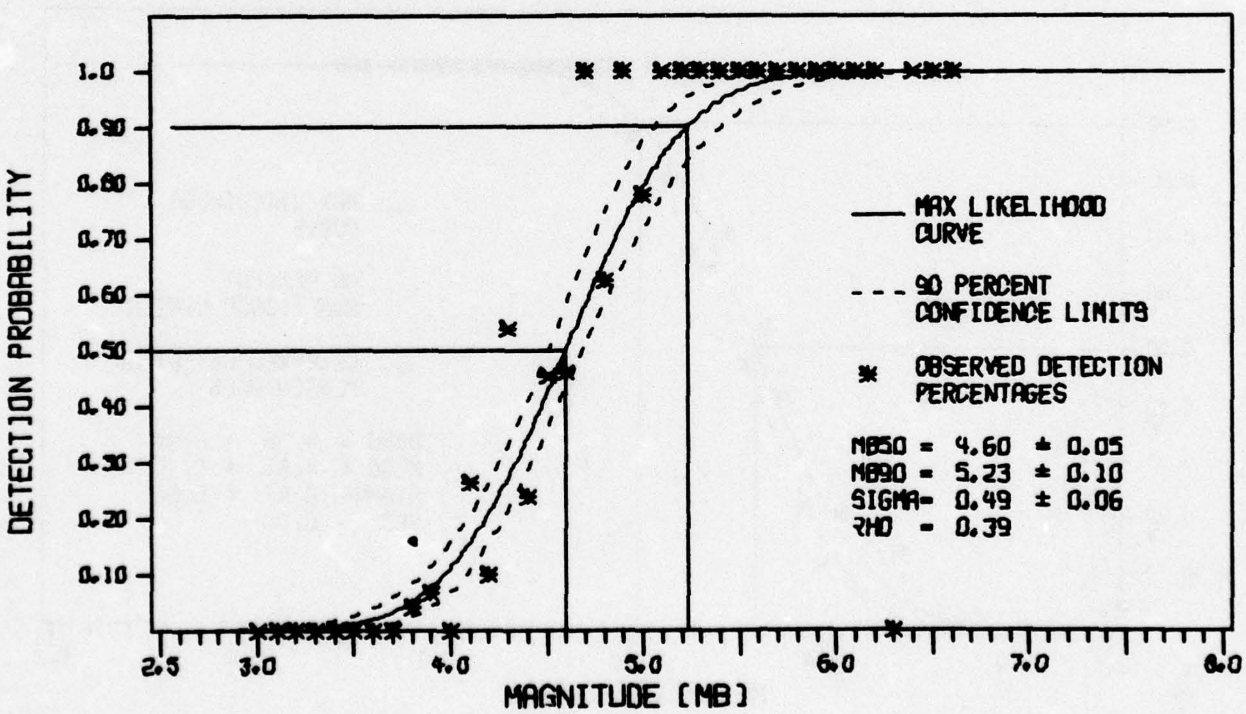

FIGURE V-7

GUMO LONG-PERIOD VERTICAL COMPONENT DETECTION STATISTICS

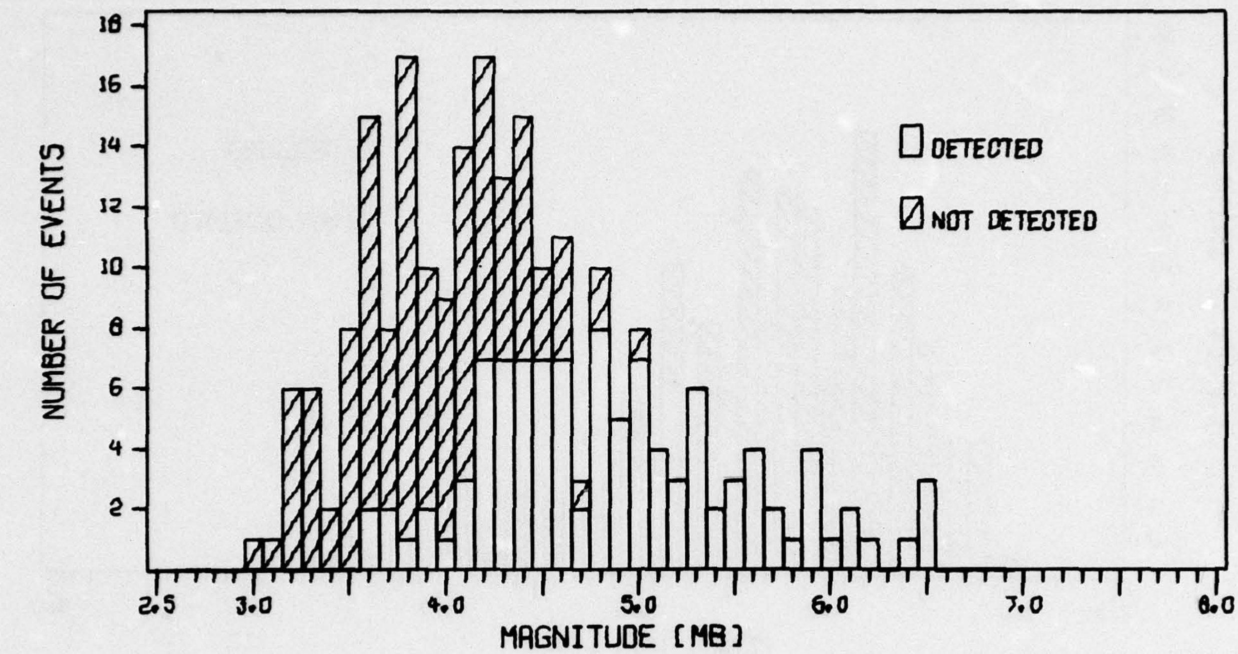

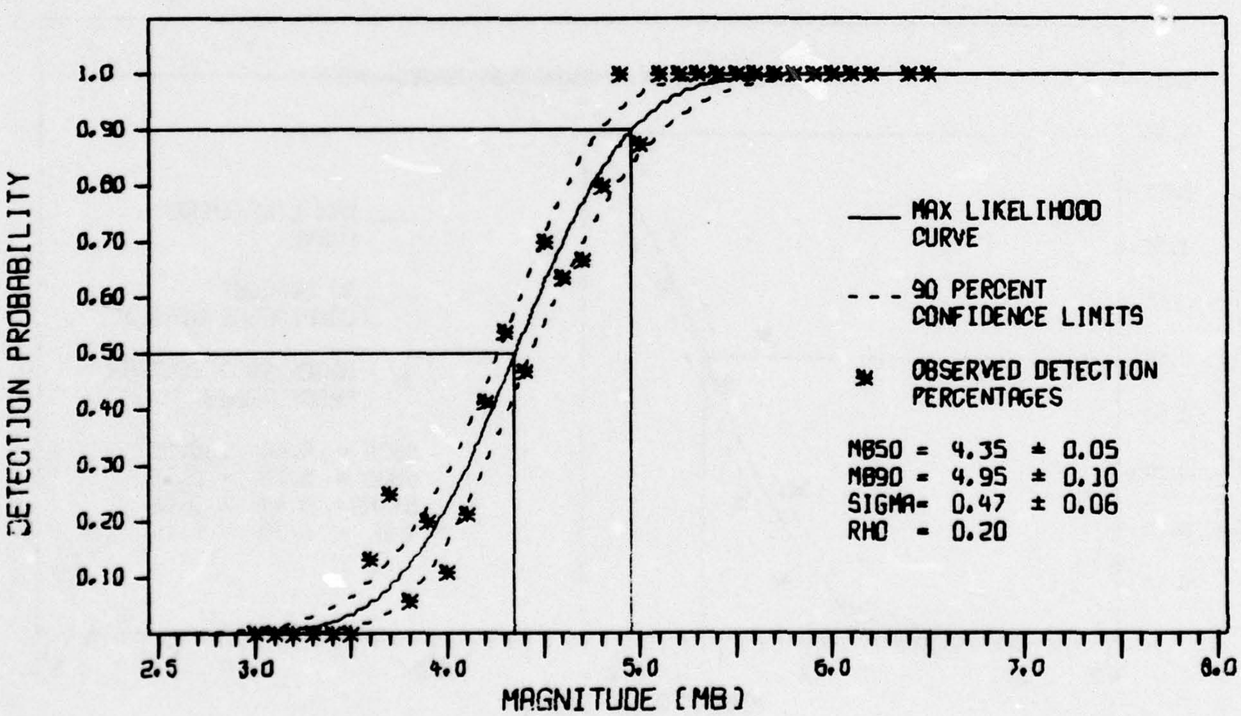

FIGURE V-8

MAIO LONG-PERIOD VERTICAL COMPONENT DETECTION STATISTICS

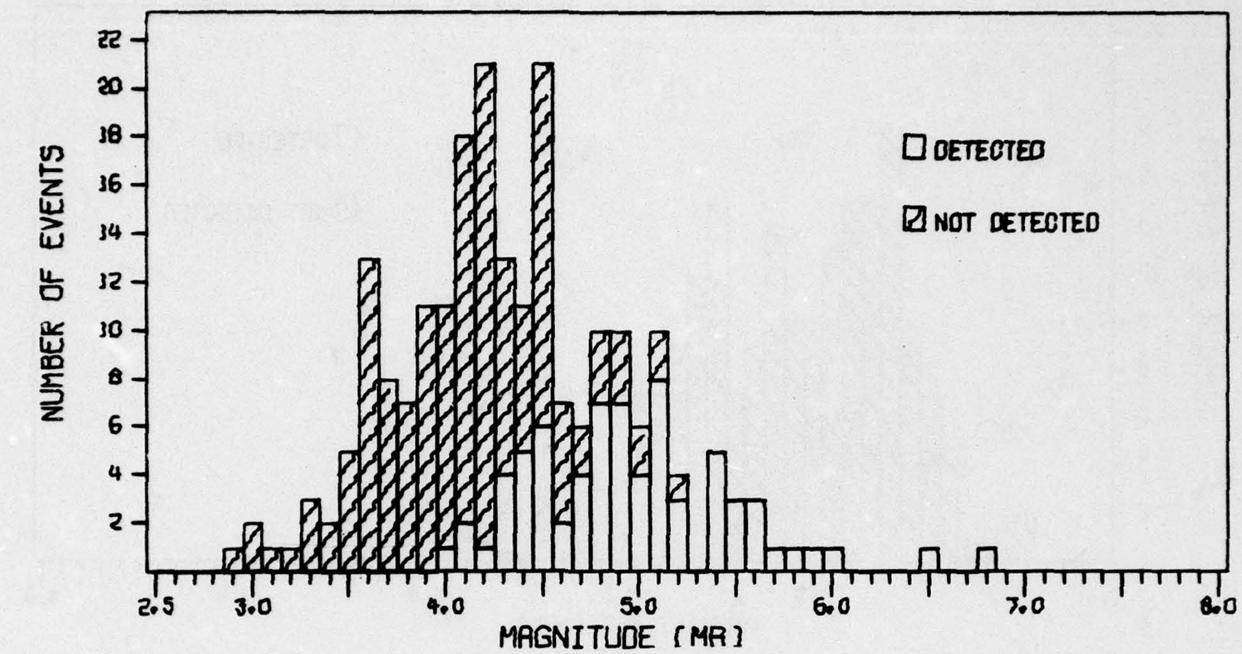

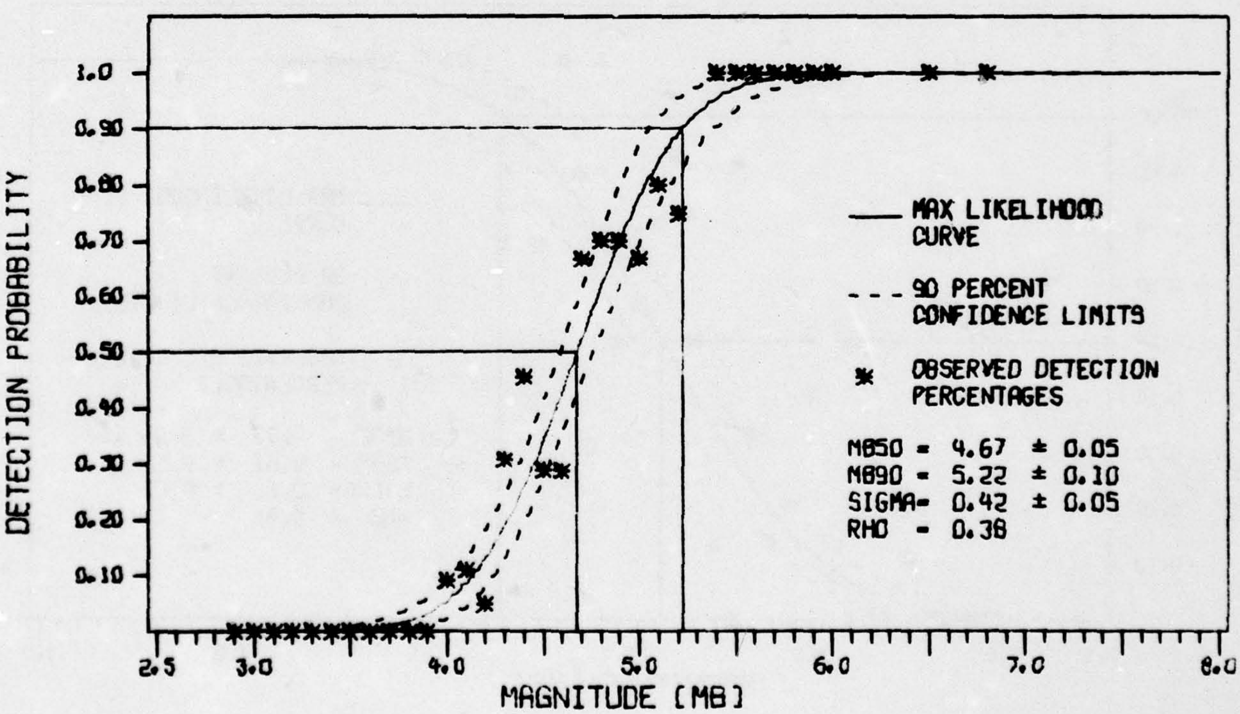

FIGURE V-9

NWAO LONG-PERIOD VERTICAL COMPONENT DETECTION STATISTICS

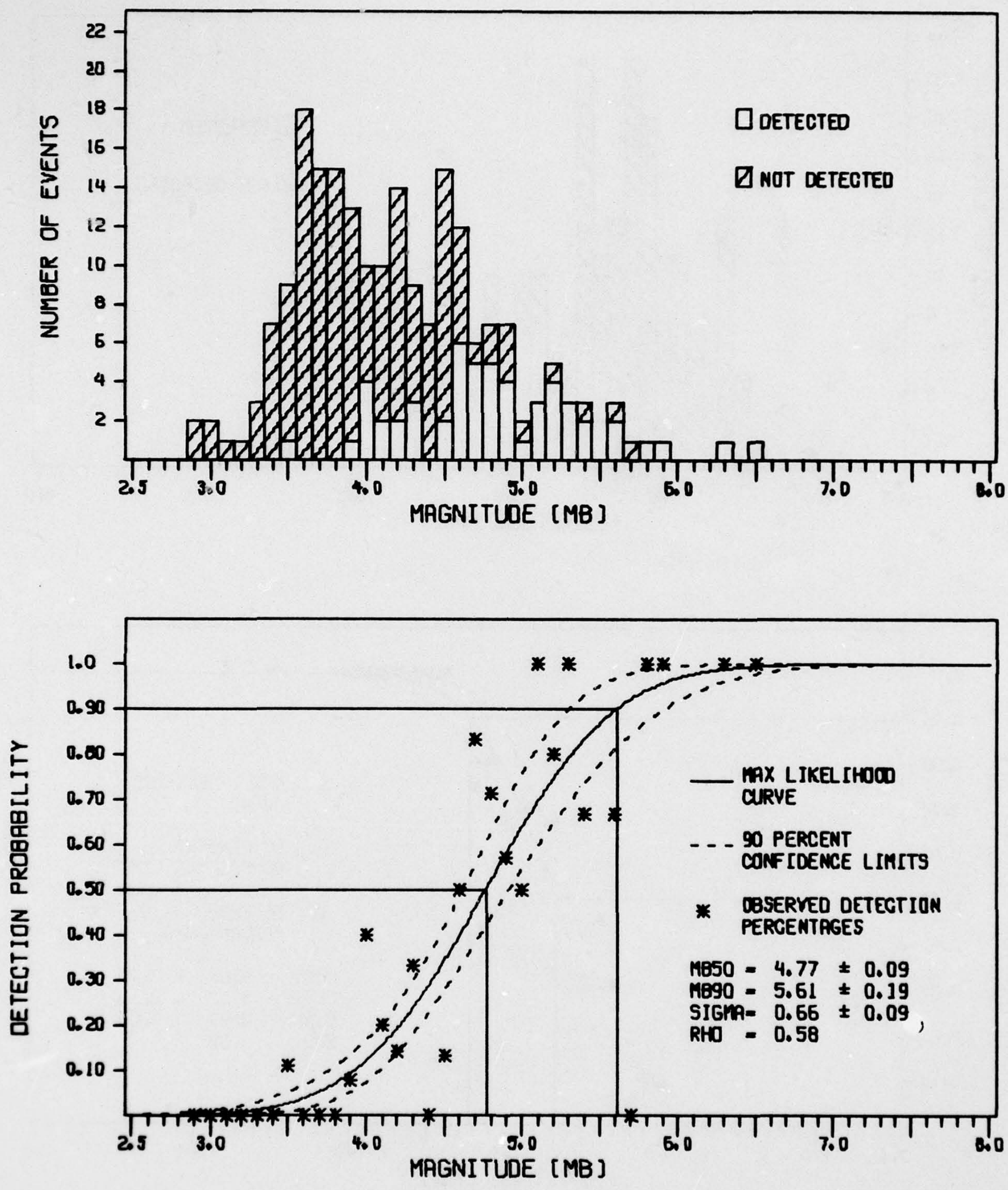

FIGURE V-10

SNZO LONG-PERIOD VERTICAL COMPONENT DETECTION STATISTICS these figures only the results for the vertical component at each station, since the results for the other two components are essentially the same. The detection capability results are summarized in Table V-3.

We recognize that to some extent the direct estimates of detection capability may be analyst-dependent. However, we do not believe that this is a serious problem, since we had occasion to test this by having two analysts check the SNZO and GUMO data. We found that, with very few exceptions, the analysts agreed on which events were detected and which were not detected. Although lacking a quantitative figure, we believe that the false alarm rate associated with our detection data is very low (< 1 percent).

TABLE V-3

SUMMARY OF LONG-PERIOD BODYWAVE MAGNITUDE (m_b) DETECTION RESULTS

Data Base Used	Station	50% m_b Detection Thresholds		
		V	T	R
Ail events except those containing mixed signals or malfunctions.	ANMO	4.61 ± 0.05	4.64 ± 0.05	4.60 ± 0.05
	GUMO	4.60 ± 0.05	4.57 ± 0.04	4.60 ± 0.05
	MAIO	4.35 ± 0.05	4.39 ± 0.06	4.42 ± 0.06
	NWAO	4.67 ± 0.05	4.85 ± 0.06	4.78 ± 0.06
	SNZO	4.77 ± 0.09	4.72 ± 0.09	4.76 ± 0.09
The above data set minus all presumed explosions and known deep events.	ANMO	4.57 ± 0.05	4.57 ± 0.05	4.51 ± 0.05
	GUMO	4.51 ± 0.05	4.53 ± 0.05	4.51 ± 0.05
	MAIO	4.34 ± 0.05	4.38 ± 0.06	4.41 ± 0.06
	NWAO	4.66 ± 0.05	4.79 ± 0.06	4.76 ± 0.07
	SNZO	4.60 ± 0.07	4.56 ± 0.07	4.60 ± 0.07

SECTION VI
LONG-PERIOD SRO DISCRIMINATION CAPABILITY

A. MEASUREMENT OF M_s

Surface wave magnitudes (M_s) were computed for all events listed in Appendix A which were detected. Whenever possible, the surface wave magnitude was computed on all components at periods of 20, 30, and 40 seconds. The surface wave magnitude was computed by the following formula:

$$M_s = \text{Log}_{10}\left(\frac{A * SF}{T * Q * G}\right) + \text{Log}_{10}\Delta + 1.12 ,$$

where

- A = peak-to-peak amplitude measured in inches on the Calcomp plot,
- SF = scale factor in computer counts per inch,
- T = period in seconds on the measured peak-to-peak amplitude,
- Q = quantization factor (= 5 computer counts per millimicron),
- G = instrument response correction factor, and
- Δ = epicentral distance in degrees.

All measurements were made on traces rotated into the vertical-transverse-radial configuration and bandpass filtered (0.023 - 0.059 Hz pass-band). The instrument response correction factors were derived from the long-period instrument response curve shown in Figure IV-6.

B. SRO DISCRIMINATION CAPABILITY

Whenever possible, the surface wave magnitude was measured at periods of 20, 30, and 40 seconds. In Figures VI-1 to VI-5 we show the $M_s - m_b$ plots for the 20-second data. This period was selected because 20-second energy was available for measurement more often than 30-second or 40-second energy. Known deep (> 100 km) earthquakes are indicated by solid circles, presumed explosions by crosses, and all other events by open circles. The solid line in each figure shows the best fit to the data with neither variable treated as dependent, minimizing the perpendicular distance from the fit to the data points.

It appears from these figures that, based on presently available data, we have a problem discriminating between earthquakes and presumed explosions. However, we note that the majority of the presumed explosions are from southern Nevada and can be separated from the earthquake population on the basis of location. The one detected presumed explosion from Eurasia, event 30, shows good separation from the earthquake population recorded at ANMO. Clearly, in future work on the discrimination part of the SRO evaluation, we will have to obtain more presumed explosions with epicenters in Eurasia.

In Tables VI-1, VI-2, and VI-3 we list the slopes and intercepts for the linear $M_s - m_b$ fits for 20, 30, and 40 second data, respectively. In Figure VI-6 we have plotted the LR-V $M_s - m_b$ fits for these three periods at each of the five stations. At ANMO, MAIO, and NWAO, these plots show that the fit to the 40-second M_s data runs parallel to and below the fit to the 20-second M_s data. It is not clear whether the fit to the 30-second M_s data lies between the fits to the 20-second M_s and 40-second M_s data. At GUMO, the fits to the 20-second M_s, 30-second M_s, and 40-second M_s data appear to be the same. At SNZO, the fit to the 30-second M_s data is parallel to and

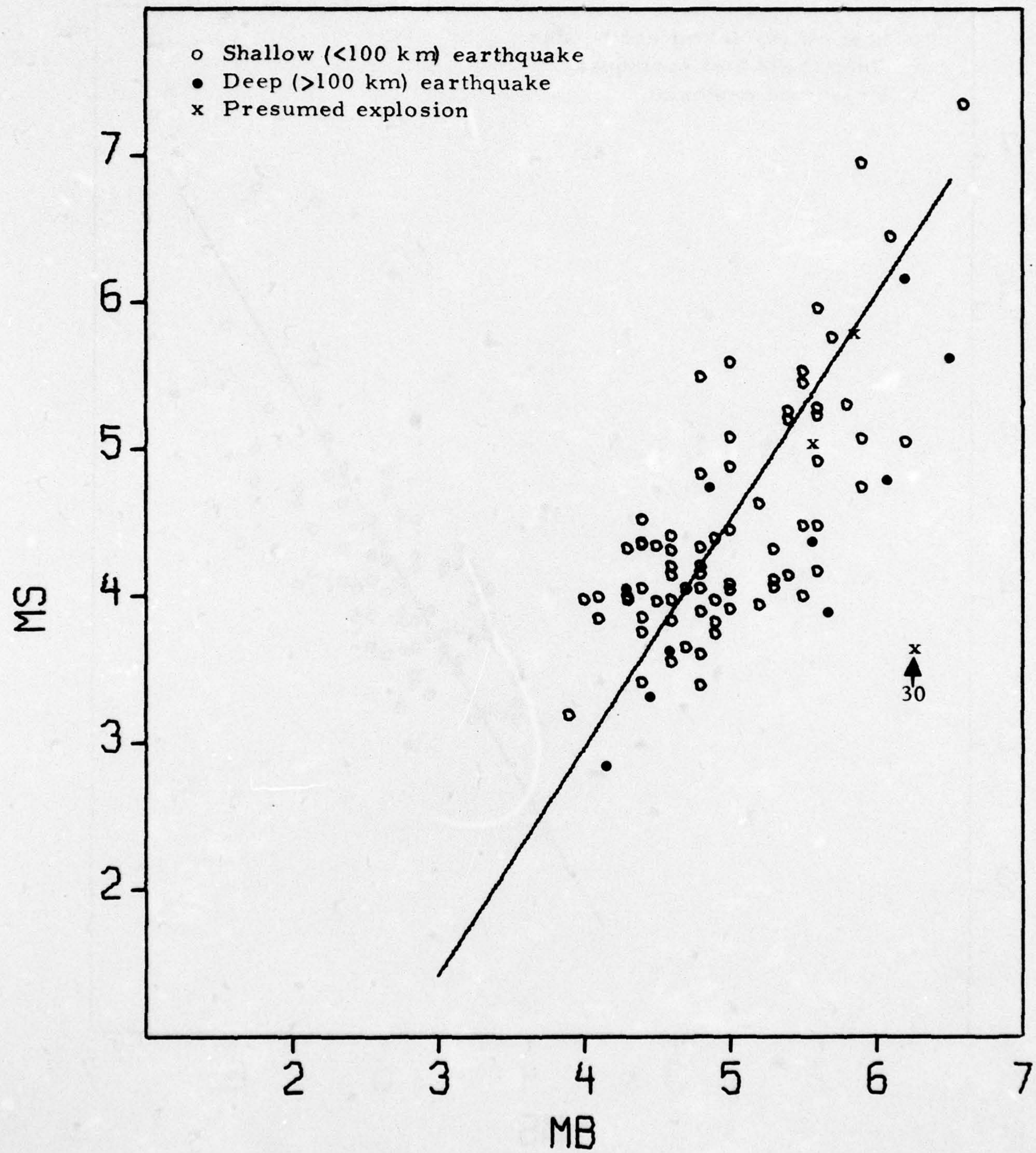

FIGURE VI-1

ANMO 20-SECOND M_s-m_b DATA FOR VERTICAL COMPONENT

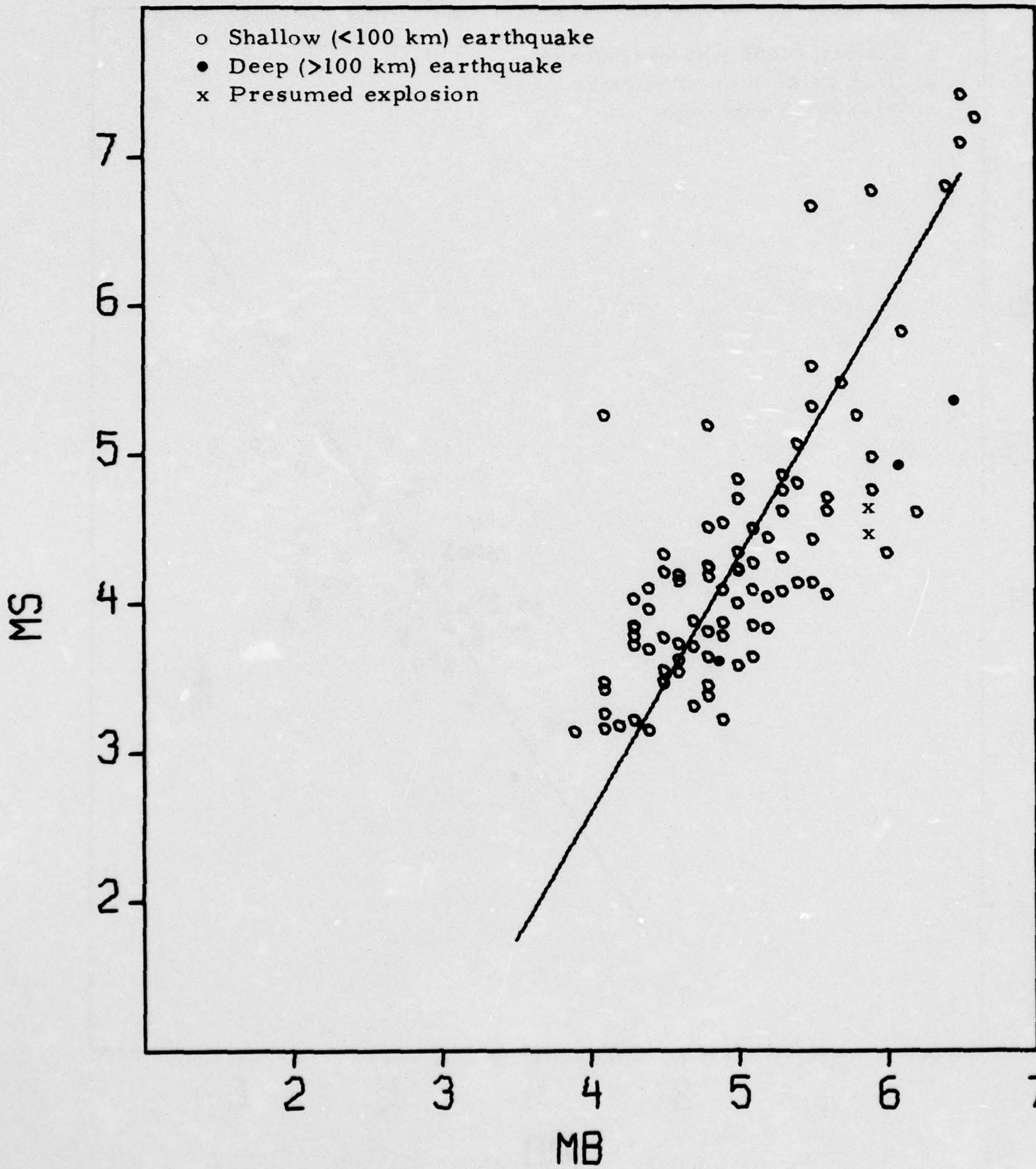

FIGURE VI-2

GUMO 20-SECOND M_s-m_b DATA FOR VERTICAL COMPONENT

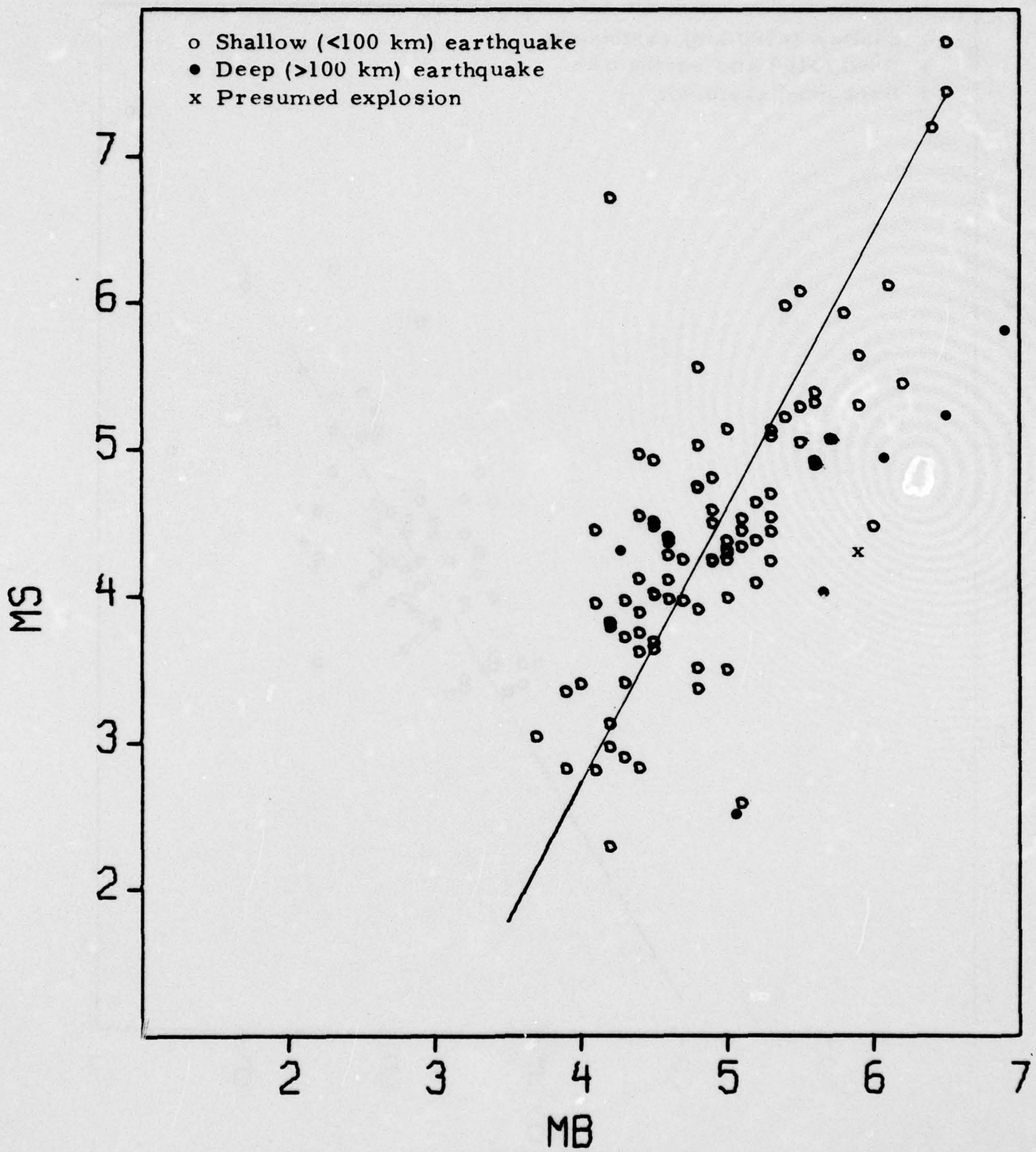

FIGURE VI-3

MAIO 20-SECOND M_s-m_b DATA FOR VERTICAL COMPONENT

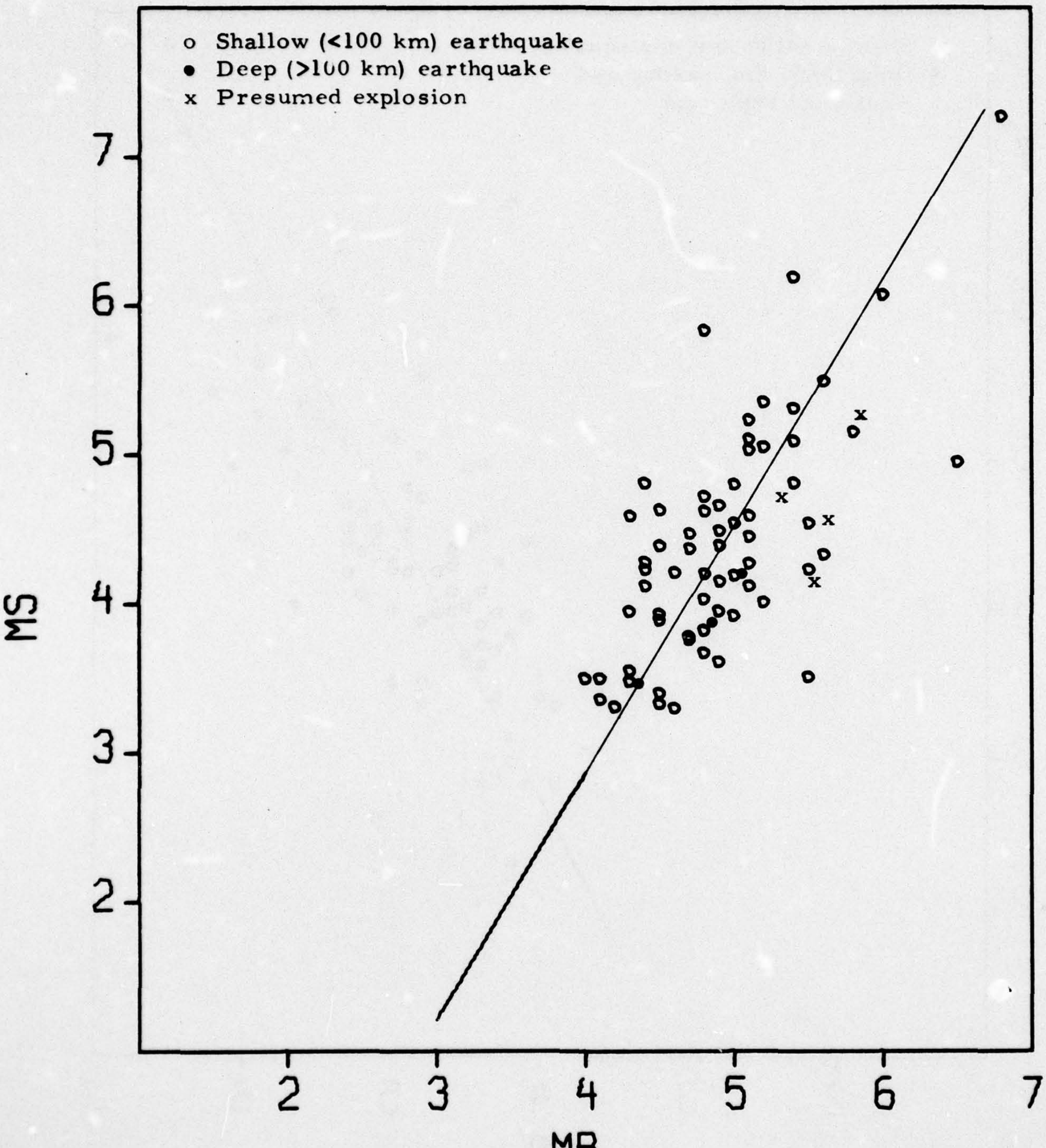

FIGURE VI-4

NWAO 20-SECOND M_s-m_b DATA FOR VERTICAL COMPONENT

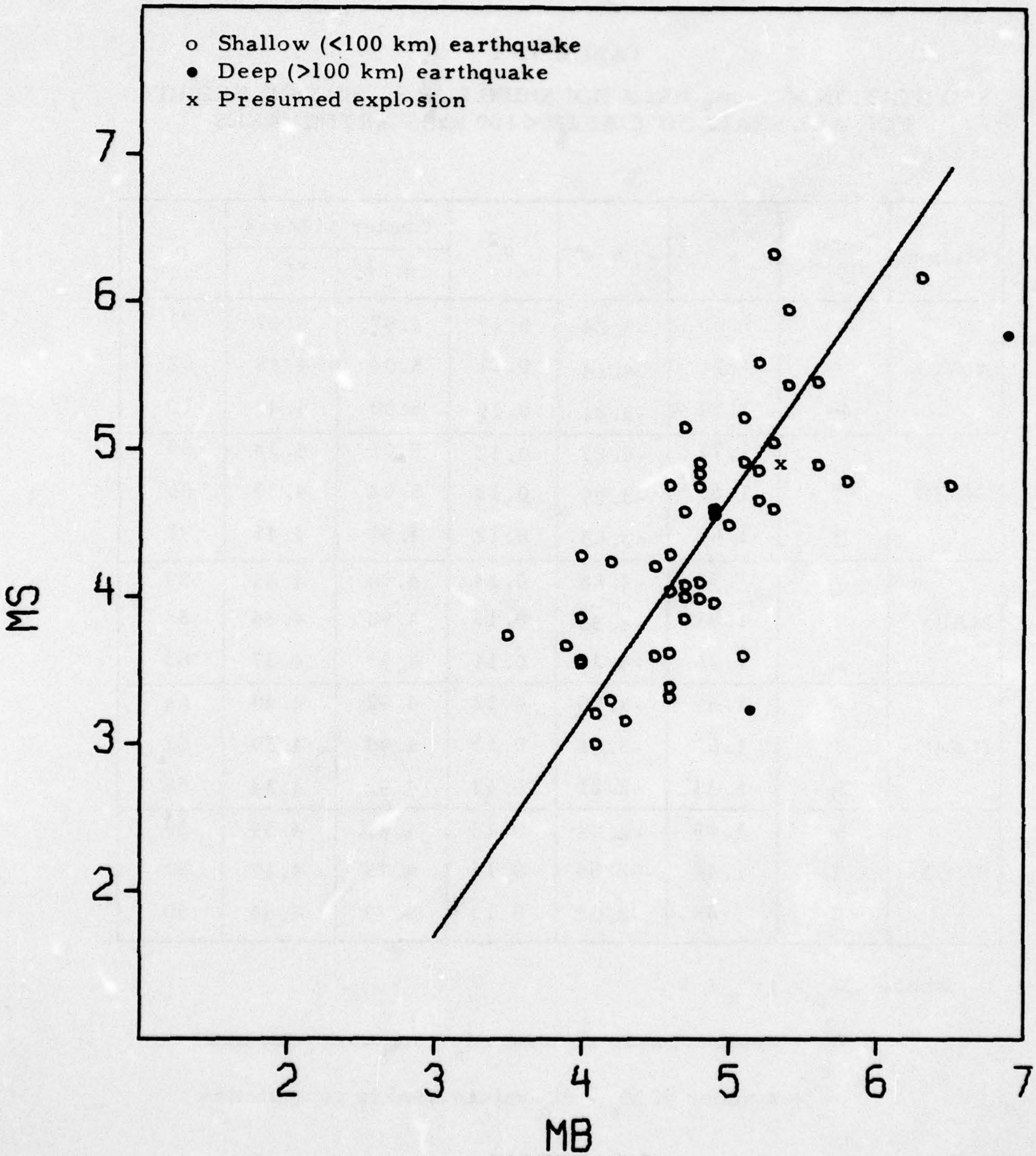

FIGURE VI-5

SNZO 20-SECOND M_s-m_b DATA FOR VERTICAL COMPONENT

TABLE VI-1

SRO STATION M_s - m_b RELATIONSHIPS FOR 20-SECOND ENERGY FOR ALL SHALLOW (DEPTH < 100 km) EARTHQUAKES

Station	Component	a	b	σ^2	Center of Mass		n
					m_b	M_s	
ANMO	V	1.55	-3.24	0.12	4.97	4.47	73
	T	1.71	-4.14	0.11	5.04	4.48	62
	R	1.54	-3.21	0.12	5.00	4.47	72
GUMO	V	1.72	-4.27	0.12	5.01	4.33	89
	T	1.66	-3.99	0.12	5.04	4.39	86
	R	1.62	-3.63	0.12	4.99	4.45	91
MAIO	V	1.90	-4.88	0.14	4.90	4.45	89
	T	1.81	-4.55	0.15	4.90	4.34	83
	R	1.76	-4.29	0.11	4.93	4.37	83
NWAO	V	1.66	-3.78	0.12	4.92	4.40	64
	T	1.65	-3.96	0.15	4.99	4.30	52
	R	1.33	-2.21	0.17	4.92	4.34	58
SNZO	V	1.49	-2.78	0.13	4.81	4.39	50
	T	1.44	-2.64	0.15	4.75	4.17	50
	R	1.45	-2.62	0.13	4.79	4.33	50

where: $M_s = am_b + b$,

σ^2 = variance normal to the M_s - m_b estimate, and

n = number of M_s - m_b values used in computation.

TABLE VI-2

SRO STATION M_s - m_b RELATIONSHIPS FOR 30-SECOND ENERGY FOR ALL SHALLOW (DEPTH < 100 km) EARTHQUAKES

Station	Component	a	b	σ^2	Center of Mass		n
					m_b	M_s	
ANMO	V	1.74	-4.53	0.13	5.00	4.19	74
	T	1.78	-4.65	0.14	5.06	4.33	69
	R	1.91	-5.40	0.14	5.04	4.23	72
GUMO	V	1.90	-5.14	0.17	5.00	4.34	82
	T	1.76	-4.46	0.11	5.07	4.44	74
	R	1.79	-4.48	0.16	5.01	4.47	83
MAIO	V	1.73	-4.37	0.15	4.88	4.08	87
	T	1.64	-3.89	0.14	4.90	4.12	85
	R	1.57	-3.62	0.12	4.94	4.11	78
NWAO	V	1.73	-4.34	0.13	4.92	4.19	61
	T	1.57	-3.67	0.13	4.99	4.14	54
	R	1.61	-3.79	0.13	4.94	4.18	56
SNZO	V	1.54	-3.23	0.13	4.84	4.22	38
	T	1.58	-3.44	0.14	4.76	4.07	52
	R	1.71	-4.30	0.10	4.97	4.21	35

where: $M_s = am_b + b$,

σ^2 = variance normal to the M_s - m_b estimate, and

n = number of M_s - m_b values used in computation.

TABLE VI-3

SRO STATION M_s - m_b RELATIONSHIPS FOR 40-SECOND ENERGY FOR ALL SHALLOW (DEPTH <100 km) EARTHQUAKES

Station	Component	a	b	σ^2	Center of Mass		n
					m_b	M_s	
ANMO	V	1.52	-3.80	0.11	5.05	3.88	55
	T	1.68	-4.48	0.15	5.04	3.99	65
	R	1.41	-3.11	0.11	4.93	3.86	41
GUMO	V	1.94	-5.54	0.17	5.04	4.25	29
	T	1.80	-5.03	0.14	5.25	4.42	27
	R	1.94	-5.44	0.18	5.04	4.35	29
MAIO	V	1.82	-5.25	0.13	5.00	3.86	54
	T	1.98	-6.11	0.10	5.00	3.81	51
	R	1.86	-5.45	0.13	5.02	3.90	49
NWAO	V	1.59	-4.05	0.13	4.98	3.86	29
	T	1.35	-2.84	0.14	4.98	3.96	34
	R	1.63	-4.19	0.11	4.96	3.89	32
SNZO	V	1.01	-1.25	0.03	4.80	3.58	13
	T	1.56	-3.89	0.18	5.01	3.93	18
	R	1.32	-2.71	0.06	4.95	3.83	10

where: $M_s = am_b + b$,

σ^2 = variance normal to the M_s - m_b estimate, and

n = number of M_s - m_b values used in computation.

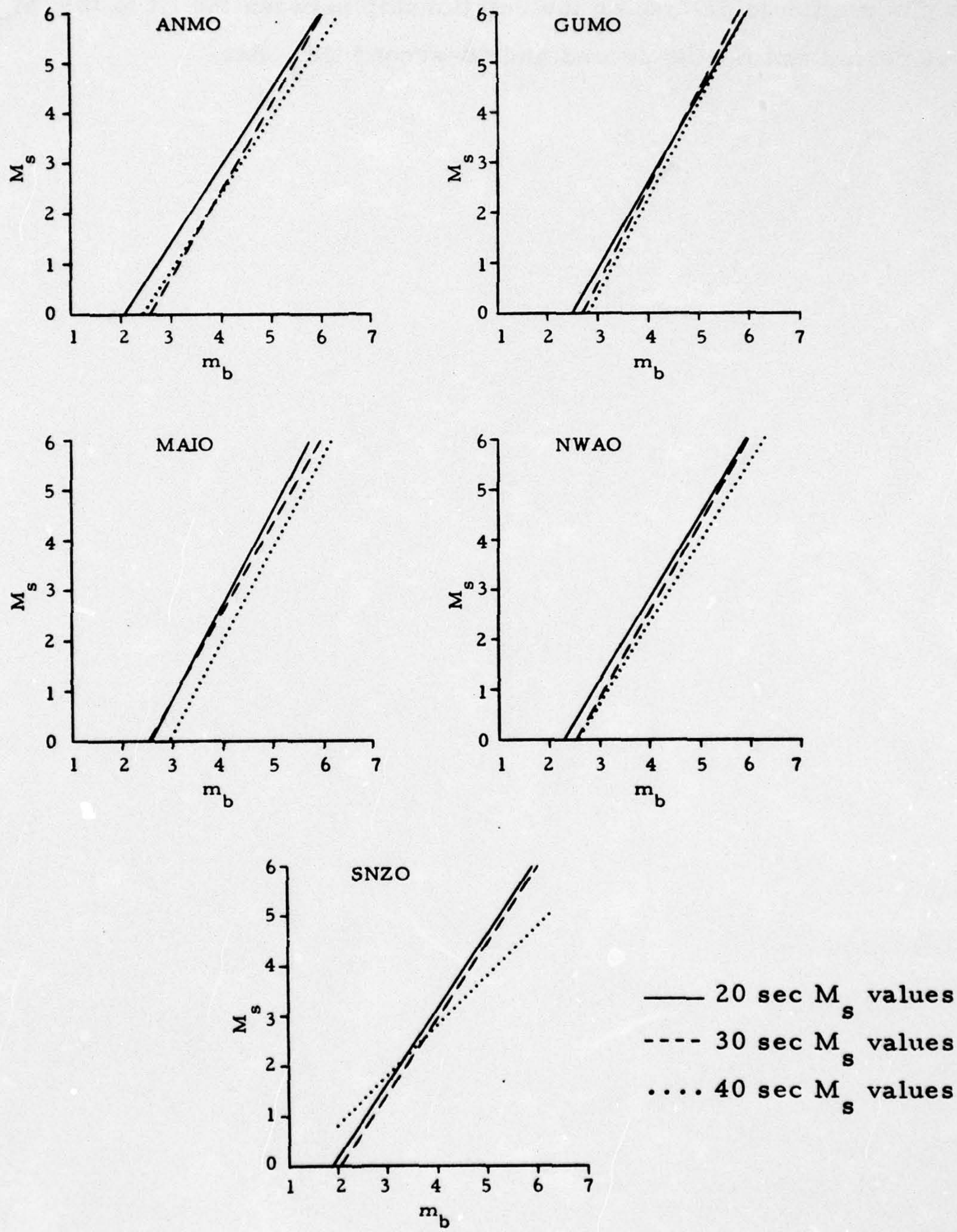

FIGURE VI-6

VERTICAL COMPONENT M_s-m_b RELATIONSHIPS below the fit to the 20-second M_s data. There is too little data at 40 seconds at this station to determine the relationship between the fit to the M_s data for this period and the 20-second and 30-second M_s fits.

SECTION VII
CONCLUSIONS

In this section we will summarize the results of this first evaluation of five of the SRO stations. The major results are:

- In general, the quality of the SRO data is good. In the worst case for long-period data, that of the horizontal components of ANMO, the detection status of 14 percent of the signals analyzed could not be determined due to malfunctions. At the other stations, approximately 10 percent or less of the signals analyzed were lost due to malfunctions.

  The only short-period malfunctions were calibrations at SNZO, where 1 percent of the data could not be analyzed.

- In order of increasing magnitude, the mean short-period RMS noise values were as follows: 0.36 mμ at ANMO, 0.51 mμ at MAIO, 6.42 mμ at NWAO, 19.42 mμ at SNZO, and 31.01 mμ at GUMO. These values are uncorrected for instrument response.

- Short-period noise for all GUMO noise samples and some SNZO noise samples exceeded the system recording capability. When this happened, the noise appeared as a continuous series of spikes. This problem has been corrected by changing the quantization rate at these stations from 2000 computer counts per millimicron to 2 computer counts per millimicron.

- The lowest values of instrument-response corrected long-period RMS noise were recorded at GUMO and MAIO. The values at ANMO and NWAO were slightly higher. The values for SNZO long-period RMS noise were approximately twice the size of the other stations.

- The average instrument-response corrected RMS amplitude spectrum for GUMO noise shows a local maximum near 25 seconds period. The cause of this will have to be investigated in future work.

- Based on the average RMS amplitude spectra for the five stations, the optimum bandpass filter for the SRO data has corner frequencies at 0.025 and 0.050 Hz.

- The short-period 50 percent detection threshold for events with epicentral distances ranging between 0^o and 103^o is 4.42 m_b units for ANMO, 4.13 m_b units for MAIO, 4.87 m_b units for NWAO, and 6.14 m_b units for SNZO. No events were detected on the GUMO short-period component. The variances on the MAIO, NWAO, and SNZO 50 percent detection thresholds were large, suggesting that more data are required at these stations to better define the detection thresholds.

- The indirect estimates of the long-period 50 percent detection threshold agree quite well with the direct estimates except at MAIO, where the indirect estimate is 0.22 m_b units higher than the direct estimate.

- The direct estimates of the long-period 50 percent detection threshold are 4.57 m_b units for ANMO, 4.51 m_b units for GUMO, 4.34 m_b units for MAIO, 4.66 m_b units for NWAO, and 4.60 m_b units for SNZO. These estimates were made using a data set from which all presumed explosions and known deep events had been deleted.

- Based on extremely limited presumed explosion data, the M_s-m_b discriminant works for presumed explosions from the Eurasian landmass but breaks down for presumed explosions from Nevada.

Future work on the evaluation of the SRO stations should be directed toward the following points:

- Evaluating all SRO stations as they become operational.
- Expanding the short-period and long-period noise data base so that one year of data is available. This will permit study of long-term noise trends. It is recommended that short-period noise trends be computed on a ten-day basis rather than a monthly basis.
- Building into the Interactive Seismic Processing System the capability to make instrument response corrections.
- Determining the detection threshold for the automatic detector at each of the SRO stations.
- Expanding the signal data base so that detection and discrimination results can be regionalized.
- Expanding the presumed explosion data base to improve estimates of discrimination capability.
- Obtaining depth information so that deep earthquakes can be deleted from the data base. This will improve estimates of long-period discrimination capability.

SECTION VIII
REFERENCES

Ringdal, F., 1974, VLPE Network Evaluation and Automatic Processing Research, Technical Report No. 2, Texas Instruments Report No. ALEX(01)-TR-74-02, AFTAC Contract Number F08606-74-C-0033, Texas Instruments Incorporated, Dallas, Texas.

Ringdal, F., J. Shaub, and D. Black, 1975, Documentation of the Interactive Seismic Processing System (ISPS), Software Documentation Report No. 1, Texas Instruments Report No. ALEX(01)-SD-75-01, AFTAC Contract Number F08606-75-C-0029, Texas Instruments Incorporated, Dallas, Texas.

Unger, R., 1974, Estimating a Seismic Station's Detection Capability from Noise, Application to VLPE Stations, Technical Report No. 4, Texas Instruments Report No. ALEX(01)-TR-74-04, AFTAC Contract Number F08606-74-C-0033, Texas Instruments Incorporated, Dallas, Texas.

APPENDIX A

LIST OF EVENTS USED IN PROCESSING

The following event list was compiled from the Norwegian Seismic Array event lists. The column headed "EVNO" gives the number we assigned to each event. The columns headed "DATE" and "TIME" give the date and origin time of the event. The epicentral coordinates are listed under "LAT" and "LONG" for latitude in degrees north and longitude in degrees east. The bodywave magnitude is listed under the heading "MB." The seismic source area is listed under "LOCATION."

EVNO	DATE	TIME	LAT.	LONG.	MB	LOCATION
0001	11/29/75	14.47.37	19.0	-156.0	5.5	HAWAII
0002	11/29/75	15.42.33	24.0	124.0	3.8	SW RYUKYU IS.
0003	11/29/75	16.17.51	7.0	-78.0	4.9	NWC OF COLOMBIA
0004	11/29/75	17.46.12	40.0	139.0	4.1	NWC OF HONSHU
0005	12/23/75	0.40.48	-25.0	180.0	3.7	SOUTH OF FIJI IS.
0006	12/23/75	6.32.21	29.0	139.0	4.1	SOUTH OF HONSHU
0007	12/23/75	10.42. 5	49.0	51.0	3.7	WESTERN KAZAKH
0008	12/23/75	12. 9.54	-32.0	-179.0	4.6	KERMADEC ISLANDS REG
0009	12/23/75	14.16. 8	39.0	73.0	4.0	TADZHIK-SINKIANG
0010	12/23/75	20.13.21	6.0	-73.0	4.5	NORTHERN COLOMBIA
0011	12/23/75	23.55. 0	33.0	88.0	3.9	TIBET
0012	12/24/75	1.28.22	55.0	148.0	4.1	SEA OF OKHOTSK
0013	12/24/75	4.36. 1	-12.0	166.0	4.6	SANTA CRUZ IS.
0014	12/24/75	5.25.36	-59.0	-26.0	5.3	S. SANDWICH IS. REG.
0015	12/24/75	8.39.29	32.0	59.0	3.6	IRAN
0016	12/24/75	11.48.58	27.0	56.0	5.6	SOUTHERN IRAN
0017	12/24/75	12. 2.35	27.0	56.0	3.8	SOUTHERN IRAN
0018	12/24/75	14.57.22	-17.0	170.0	5.4	NEW HEBRIDES IS.
0019	12/24/75	16.29.42	-14.0	167.0	4.9	NEW HEBRIDES IS.
0020	12/24/75	17. 4.29	35.0	24.0	4.5	CRETE
0021	12/24/75	18.48. 1	45.0	152.0	5.4	KURILE ISLANDS REG.
0022	12/24/75	18.49.34	46.0	152.0	4.8	KURILE ISLANDS
0023	12/24/75	19.55.17	28.0	55.0	5.0	SOUTHERN IRAN
0024	12/24/75	21. 4.20	28.0	55.0	4.5	SOUTHERN IRAN
0025	12/24/75	22.34.38	45.0	152.0	4.0	KURILE ISLANDS REG.
0026	12/24/75	23.32.44	53.0	-168.0	4.8	ALEUTIAN ISLANDS
0027	12/25/75	0.51. 1	51.0	159.0	4.0	OEC KAMCHATKA
0028	12/25/75	1.55. 2	46.0	152.0	4.3	KURILE ISLANDS
0029	12/25/75	3. 4.52	27.0	56.0	4.1	SOUTHERN IRAN
0030	12/25/75	5.17. 3	50.0	78.0	6.3	EASTERN KAZAKH SSR
0031	12/25/75	8.31.48	55.0	166.0	3.9	KOMANDORSKY ISLANDS
0032	12/25/75	15. 6.35	46.0	152.0	4.0	KURILE ISLANDS
0033	12/25/75	15.36.29	45.0	152.0	5.3	KURILE ISLANDS REG.
0034	12/25/75	16. 0.13	45.0	152.0	5.5	KURILE ISLANDS
0035	12/25/75	17. 6.30	46.0	152.0	4.2	KURILE ISLANDS
0036	12/25/75	17.31.17	-26.0	179.0	4.8	SOUTH OF FIJI IS.
0037	12/25/75	18.50.49	37.0	139.0	3.9	HONSHU, JAPAN
0038	12/25/75	19.59.40	55.0	-162.0	4.4	ALASKAN PENINSULA
0039	12/25/75	21.38.17	43.0	147.0	5.1	OFF COAST HOKKAIDO
0040	12/25/75	22.21. 5	43.0	149.0	3.6	KURILE ISLANDS REG.
0041	12/25/75	23.22.14	-2.0	145.0	6.2	ADMIRALTY ISLANDS
0042	12/25/75	23.46.22	28.0	55.0	3.9	SOUTHERN IRAN
0043	12/26/75	5.46.59	28.0	55.0	4.4	SOUTHERN IRAN
0044	12/26/75	7.17. 2	42.0	146.0	4.2	OFF COAST HOKKAIDO
0045	12/26/75	15.56.45	-15.0	-173.0	6.6	SAMOA ISLANDS REGION
0046	12/26/75	21.48.14	-25.0	-180.0	4.2	SOUTH OF FIJI ISLAND
0047	12/26/75	22. 2.39	28.0	55.0	3.8	SOUTHERN IRAN
0048	12/27/75	2.25.34	28.0	55.0	3.6	SOUTHERN IRAN
0049	12/27/75	3.16.45	32.0	142.0	4.1	S. OF HONSHU, JAPAN
0050	12/27/75	4.31.51	44.0	12.0	3.8	CENTRAL ITALY

EVNO	DATE	TIME	LAT.	LONG.	MB	LOCATION
0051	12/27/75	5.25.30	43.0	147.0	4.9	OFF COAST HOKKAIDO
0052	12/27/75	5.33.10	40.0	142.0	4.6	NEC HONSHU, JAPAN
0053	12/27/75	5.47.24	37.0	73.0	4.4	AFGHAN-USSR BORDER
0054	12/27/75	12.50.51	44.0	147.0	4.6	KURILE ISLANDS
0055	12/27/75	13.15.34	-23.0	169.0	4.8	LOYALTY ISLANDS REG.
0056	12/27/75	14. 9.46	44.0	149.0	3.9	KURILE ISLANDS REG.
0057	12/27/75	16.14.42	43.0	147.0	3.8	KURILE ISLANDS
0058	12/27/75	16.23.41	-26.0	-180.0	3.9	S. OF FIJI IS.
0059	12/27/75	17. 3.48	44.0	147.0	4.7	KURILE ISLANDS
0060	12/27/75	20.43.27	43.0	147.0	4.5	OFF COAST HOKKAIDO
0061	12/27/75	22.21.29	28.0	55.0	4.1	SOUTHERN IRAN
0062	12/27/75	23.33. 1	-16.0	-173.0	5.0	SAMOA ISLANDS REGION
0063	12/27/75	23.34.40	-16.0	-172.0	5.2	SAMOA ISLANDS REGION
0064	12/28/75	2.34.25	34.0	133.0	4.1	S. HONSHU, JAPAN
0065	12/28/75	3. 9.43	43.0	147.0	3.9	OFF COAST HOKKAIDO
0066	12/28/75	6.12.10	31.0	50.0	3.5	IRAN
0067	12/28/75	9. 6. 3	33.0	62.0	3.8	NW AFGHANISTAN
0068	12/28/75	13.49.28	34.0	85.0	4.6	TIBET
0069	12/28/75	15. 6.40	53.0	-168.0	4.5	FOX IS., ALEUTIANS
0070	12/28/75	15.20.41	51.0	-170.0	4.5	ALEUTIAN IS. REG.
0071	12/28/75	15.24.29	-7.0	119.0	6.1	FLORES SEA
0072	12/28/75	16.29.34	37.0	142.0	4.8	NEC HONSHU, JAPAN
0073	12/29/75	0. 1.49	36.0	20.0	3.5	MEDITERRANEAN SEA
0074	12/29/75	1.20. 3	27.0	97.0	4.5	BURMA
0075	12/29/75	2.34.48	-26.0	180.0	4.5	S. OF FIJI ISLANDS
0076	12/29/75	3.39.46	-58.0	-66.0	6.1	DRAKE PASSAGE
0077	12/29/75	5. 8. 2	27.0	96.0	5.7	BURMA-INDIA BORDER
0078	12/29/75	6.26.29	28.0	96.0	4.1	INDIA-CHINA BORDER
0079	12/29/75	12.33.30	53.0	-164.0	3.9	SOUTH OF ALASKA
0080	12/30/75	14.34.54	31.0	46.0	4.4	IRAQ
0081	12/30/75	15.59.43	35.0	44.0	4.3	IRAQ
0082	12/30/75	16.36.30	35.0	72.0	4.2	PAKISTAN
0083	12/30/75	23.23. 6	54.0	161.0	4.2	NEC KAMCHATKA
0084	12/31/75	1. 9. 0	16.0	121.0	4.6	LUZON, PHILIPPINE IS
0085	12/31/75	6.34.33	41.0	21.0	3.8	GREECE-ALBANIA BOR.
0086	12/31/75	9.46.16	41.0	21.0	5.0	GREECE-ALBANIA BOR.
0087	12/31/75	12.19.45	42.0	20.0	3.3	YUGOSLAVIA
0088	12/31/75	13. 2.37	41.0	21.0	3.8	GREECE-ALBANIA BOR.
0089	12/31/75	14.12.24	40.0	143.0	5.3	NEC HONSHU, JAPAN
0090	12/31/75	14.54. 8	41.0	21.0	4.3	GREECE-ALBANIA BOR.
0091	12/31/75	17. 7.48	41.0	21.0	3.7	GREECE-ALBANIA BOR.
0092	12/31/75	17.37.19	41.0	21.0	3.5	GREECE-ALBANIA BOR.
0093	12/31/75	22.55.14	41.0	20.0	3.9	GREECE-ALBANIA BOR.
0094	12/31/75	23.55.51	23.0	143.0	4.8	VOLCANO ISLANDS REG.
0095	1/ 1/76	0. 4.35	41.0	21.0	4.6	GREECE-ALBANIA BOR.
0096	1/ 1/76	1.29.47	-25.0	-178.0	5.9	S. OF FIJI IS.
0097	1/ 1/76	1.45.33	-25.0	-177.0	5.1	S. OF FIJI IS.
0098	1/ 1/76	1.49.34	-25.0	-178.0	5.0	S. OF FIJI IS.
0099	1/ 1/76	1.56. [illegible]	-25.0	-177.0	5.1	S. OF FIJI IS.
0100	1/ 1/76	1.59.25	-25.0	-178.0	4.7	S. OF FIJI IS.

EVNO	DATE	TIME	LAT.	LONG.	MB	LOCATION
0101	1/ 1/76	2. 2.55	-32.0	-176.0	3.8	KERMADEC ISLANDS REG
0102	1/ 1/76	2. 6.47	-25.0	-177.0	5.0	S. OF FIJI ISLANDS
0103	1/ 1/76	2.19.48	41.0	21.0	3.7	GREECE-ALBANIA BOR.
0104	1/ 1/76	2.21. 7	-30.0	-177.0	5.2	KERMADEC ISLANDS
0105	1/ 1/76	3.10. 6	-25.0	-179.0	3.7	S. OF FIJI ISLANDS
0106	1/ 1/76	4. 9.12	-27.0	-176.0	3.7	S. OF FIJI ISLANDS
0107	1/ 1/76	4.11.46	50.0	-128.0	4.7	VANCOUVER IS. REG.
0108	1/ 1/76	4.29.48	-25.0	-178.0	4.0	S. OF FIJI ISLANDS
0109	1/ 1/76	5.54.26	-27.0	-176.0	3.6	S. OF FIJI ISLANDS-
0110	1/ 1/76	6.20. 0	-25.0	-178.0	3.9	S. OF FIJI ISLANDS
0111	1/ 1/76	6.34. 1	-25.0	-176.0	3.7	S. OF FIJI ISLANDS
0112	1/ 1/76	6.37.58	-25.0	-178.0	4.2	S. OF FIJI ISLANDS
0113	1/ 1/76	7. 3. 4	-25.0	-178.0	4.9	S. OF FIJI ISLANDS
0114	1/ 1/76	7.51. 5	-25.0	-177.0	4.1	S. OF FIJI IS.
0115	1/ 1/76	7.56.32	41.0	21.0	3.4	GREECE-ALBANIA BOR.
0116	1/ 1/76	8.27.23	-25.0	-178.0	4.0	S. OF FIJI IS.
0117	1/ 1/76	8.36.39	-25.0	-177.0	3.8	S. OF FIJI IS.
0118	1/ 1/76	8.55. 2	51.0	-167.0	4.0	ALEUTIAN IS. REG.
0119	1/ 1/76	9. 5.24	-25.0	-178.0	4.1	S. OF FIJI ISLANDS
0120	1/ 1/76	9.34. 9	-25.0	-178.0	5.0	S. OF FIJI ISLANDS
0121	1/ 1/76	10.43. 0	49.0	47.0	3.3	WESTERN KAZAKH
0122	1/ 1/76	11.24.56	10.0	125.0	4.2	MINDANAO, PHIL. IS.
0123	1/ 1/76	13.34.16	40.0	29.0	3.2	TURKEY
0124	1/ 1/76	14.27.19	-25.0	-178.0	4.6	S. OF FIJI ISLANDS
0125	1/ 1/76	15.32.47	30.0	139.0	4.9	S. OF HONSHU, JAPAN
0126	1/ 1/76	16.15.25	-24.0	-176.0	5.6	S. OF FIJI ISLANDS
0127	1/ 1/76	18.43.49	-17.0	170.0	4.9	NEW HEBRIDES IS.
0128	1/ 1/76	19. 2.20	-29.0	-180.0	3.5	KERMADEC IS. REG.
0129	1/ 1/76	19. 3.38	-25.0	-178.0	5.3	S. OF FIJI ISLANDS
0130	1/ 1/76	20. 1.16	36.0	22.0	3.3	SOUTHERN GREECE
0131	1/ 1/76	20. 6.14	40.0	21.0	3.2	GREECE
0132	1/ 1/76	20. 9.54	40.0	20.0	3.5	GREECE-ALBANIA BOR.
0133	1/ 1/76	20.22.16	-25.0	-177.0	3.8	S. OF FIJI ISLANDS
0134	1/ 1/76	20.42.27	-25.0	-177.0	3.7	S. OF FIJI ISLANDS
0135	1/ 1/76	22.22. 1	49.0	154.0	3.7	KURILE ISLANDS
0136	1/ 2/76	1. 8.44	-25.0	-178.0	5.2	SOUTH OF FIJI IS.
0137	1/ 2/76	2.19.17	-25.0	-178.0	4.2	SOUTH OF FIJI IS.
0138	1/ 2/76	2.46.36	46.0	153.0	4.8	KURILE ISLANDS REG.
0139	1/ 2/76	2.48.19	41.0	21.0	3.3	GREECE-ALBANIA BOR.
0140	1/ 2/76	3.30.42	-14.0	167.0	4.4	NEW HEBRIDES IS.
0141	1/ 2/76	3.36.21	50.0	-130.0	4.6	VANCOUVER IS. REG.
0142	1/ 2/76	4.10.24	-25.0	-178.0	4.6	SOUTH OF FIJI IS.
0143	1/ 2/76	4.30.56	31.0	47.0	4.1	IRAN-IRAQ BOR. REG.
0144	1/ 2/76	5.48.31	-30.0	-176.0	4.8	KERMADEC IS. REG.
0145	1/ 2/76	6.47.58	43.0	147.0	5.6	OFF COAST HOKKAIDO
0146	1/ 2/76	8.38.55	-29.0	-177.0	4.4	KERMADEC IS. REG.
0147	1/ 2/76	9.51. 2	23.0	143.0	4.6	VOLCANO IS. REG.
0148	1/ 2/76	9.55.58	53.0	171.0	4.3	NEAR IS., ALEUTIANS
0149	1/ 2/76	10.41.14	-26.0	-176.0	4.7	SOUTH OF TONGA IS.
0150	1/ 2/76	11.52. 6	-28.0	-178.0	3.9	KERMADEC IS. REG.

EVNO	DATE	TIME	LAT.	LONG.	MB	LOCATION
0151	1/ 2/76	13.46.47	39.0	73.0	4.1	TADZHIK-SINKIANG BOR
0152	1/ 2/76	14.29.16	28.0	55.0	3.9	SOUTHERN IRAN
0153	1/ 2/76	15. 8.59	28.0	55.0	4.1	SOUTHERN IRAN
0154	1/ 2/76	16.29.36	-20.0	67.0	5.0	MASCARENE IS. REG.
0155	1/ 2/76	18.46.47	-25.0	-178.0	4.2	SOUTH OF FIJI IS.
0156	1/ 2/76	20.14.51	-25.0	-177.0	3.9	SOUTH OF FIJI IS.
0157	1/ 2/76	21.36.44	52.0	160.0	4.7	OEC KAMCHATKA
0158	1/ 2/76	21.56.45	-25.0	-178.0	5.0	SOUTH OF FIJI IS.
0159	1/ 2/76	22.45.13	41.0	21.0	4.2	GREECE-ALBANIA BOR.
0160	1/ 3/76	1.33.55	8.0	122.0	4.8	MINDANAO, PHIL. IS.
0161	1/ 3/76	2.58.27	26.0	130.0	5.2	RYUKYU ISLANDS
0162	1/ 3/76	4.44. 3	-25.0	-177.0	4.2	SOUTH OF FIJI IS.
0163	1/ 3/76	5.43.27	-25.0	-178.0	4.3	SOUTH OF FIJI IS.
0164	1/ 3/76	6.54. 5	-25.0	-178.0	3.9	SOUTH OF FIJI IS.
0165	1/ 3/76	6.57.14	-25.0	-176.0	4.0	SOUTH OF TONGA IS.
0166	1/ 3/76	8.22.27	21.0	-83.0	4.4	CUBA REGION
0167	1/ 3/76	9.39.42	35.0	69.0	3.8	HINDU KUSH REGION
0168	1/ 3/76	10.56. 8	23.0	143.0	4.3	VOLCANO IS. REG.
0169	1/ 3/76	12.33.29	14.0	-94.0	4.8	NC CHIAPAS, MEXICO
0170	1/ 3/76	12.38.20	-25.0	-179.0	3.8	SOUTH OF FIJI IS.
0171	1/ 3/76	13.16.58	41.0	21.0	4.3	GREECE-ALBANIA BOR.
0172	1/ 3/76	15. 4.12	40.0	22.0	4.2	GREECE
0173	1/ 3/76	15.45. 5	-25.0	-177.0	4.2	SOUTH OF FIJI IS.
0174	1/ 3/76	17. 0. 1	40.0	22.0	3.5	GREECE
0175	1/ 3/76	18. 8.57	-25.0	-178.0	4.5	SOUTH OF FIJI IS.
0176	1/ 3/76	19.15. 5	38.0	-116.0	5.9	NEVADA
0177	1/ 3/76	20.26. 8	35.0	81.0	3.7	TIBET
0178	1/ 3/76	22. 5.27	51.0	175.0	4.0	ALEUTIAN IS. REG.
0179	1/ 3/76	22.45.52	41.0	21.0	3.5	GREECE-ALBANIA BOR.
0180	1/ 4/76	0.18.41	-33.0	-180.0	4.0	SOUTH OF KERMADEC IS
0181	1/ 4/76	0.57.11	37.0	72.0	3.8	AFGHAN-USSR BORDER
0182	1/ 4/76	3.57. 4	-6.0	114.0	5.3	JAVA
0183	1/ 4/76	7.51.44	-25.0	180.0	3.8	SOUTH OF FIJI IS.
0184	1/ 4/76	10. 9.36	-25.0	-177.0	3.6	SOUTH OF FIJI IS.
0185	1/ 4/76	11.34.42	10.0	-86.0	4.4	OC COSTA RICA
0186	1/ 4/76	11.40. 3	-25.0	-179.0	3.6	SOUTH OF FIJI IS.
0187	1/ 4/76	12.45.49	-25.0	-178.0	3.3	SOUTH OF FIJI IS.
0188	1/ 4/76	13.17.28	-25.0	-176.0	3.6	SOUTH OF TONGA IS.
0189	1/ 4/76	15.13.17	-25.0	-178.0	4.4	SOUTH OF FIJI IS.
0190	1/ 4/76	16.40. 7	45.0	147.0	4.1	KURILE ISLANDS
0191	1/ 4/76	20.28. 4	-28.0	-177.0	3.6	KERMADEC IS. REG.
0192	1/ 4/76	21.14.57	42.0	18.0	3.1	ADRIATIC SEA
0193	1/ 4/76	22.11. 3	-25.0	-178.0	4.3	SOUTH OF FIJI IS.
0194	1/ 5/76	0. 3.20	52.0	162.0	4.6	OEC KAMCHATKA
0195	1/ 5/76	2. 5.18	54.0	159.0	4.3	KAMCHATKA
0196	1/ 5/76	2.31.27	-14.0	-74.0	6.0	PERU
0197	1/ 5/76	2.59.55	-25.0	-177.0	4.3	SOUTH OF FIJI IS.
0198	1/ 5/76	6.24. 5	40.0	-105.0	4.5	COLORADO
0199	1/ 5/76	7. 3. 0	52.0	162.0	4.1	OFC KAMCHATKA
0200	1/ 5/76	10.19.32	-25.0	-177.0	3.8	SOUTH OF FIJI IS.

EVNO	DATE	TIME	LAT.	LONG.	MB	LOCATION
0201	1/ 5/76	11.17.35	-25.0	-178.0	4.3	SOUTH OF FIJI IS.
0202	1/ 5/76	11.20.38	-25.0	-178.0	4.3	SOUTH OF FIJI IS.
0203	1/ 5/76	12.38.15	23.0	123.0	4.6	SOUTHEAST OF TAIWAN
0204	1/ 5/76	12.42.24	50.0	-179.0	3.8	ANDREANOF IS. ALEUT.
0205	1/ 5/76	15.16.44	-32.0	-177.0	3.8	KERMADEC IS. REG.
0206	1/ 5/76	20. 6.57	28.0	129.0	4.4	RYUKYU IS.
0207	1/ 5/76	23.33.23	39.0	74.0	3.8	S. SINKIANG PROV.
0208	1/ 6/76	2. 4. 3	0.0	122.0	5.1	NORTHERN CELEBES IS.
0209	1/ 6/76	7.46.49	-27.0	-176.0	3.6	SOUTH OF FIJI IS.
0210	1/ 6/76	8.30.45	18.0	121.0	4.1	LUZON, PHILIPPINE IS
0211	1/ 6/76	10.16.43	-26.0	-176.0	4.4	SOUTH OF TONGA IS.
0212	1/ 6/76	11. 7.48	-25.0	-176.0	3.8	SOUTH OF TONGA IS.
0213	1/ 6/76	16.40.40	41.0	20.0	3.0	ALBANIA
0214	1/ 6/76	17. 6. 4	-25.0	-176.0	3.6	SOUTH OF TONGA IS.
0215	1/ 6/76	19.28.49	56.0	162.0	4.8	NEC KAMCHATKA
0216	1/ 6/76	19.51.50	54.0	163.0	4.9	OEC KAMCHATKA
0217	1/ 6/76	20.11.52	40.0	20.0	3.4	GREECE-ALBANIA BOR.
0218	1/ 6/76	20.57.12	51.0	159.0	5.2	NEC KAMCHATKA
0219	1/ 6/76	21. 8.28	53.0	158.0	5.5	NEC KAMCHATKA
0220	1/ 6/76	21.14.47	48.0	152.0	4.3	KURILE ISLANDS
0221	1/ 6/76	21.23.56	53.0	157.0	4.9	KAMCHATKA
0222	1/ 6/76	21.32.16	52.0	158.0	4.1	NEC KAMCHATKA
0223	1/ 6/76	21.35.33	53.0	157.0	4.6	KAMCHATKA
0224	1/ 6/76	21.42.19	53.0	157.0	3.9	KAMCHATKA
0225	1/ 6/76	21.45.33	53.0	158.0	5.7	NEC KAMCHATKA
0226	1/ 6/76	21.54.15	-27.0	-177.0	4.7	KERMADEC IS. REG.
0227	1/ 6/76	22. 7. 5	-27.0	-176.0	3.5	SOUTH OF FIJI IS.
0228	1/ 6/76	22.10. 5	53.0	157.0	4.1	KAMCHATKA
0229	1/ 6/76	22.17.59	53.0	157.0	5.9	KAMCHATKA
0230	1/ 6/76	22.24.25	53.0	157.0	4.7	KAMCHATKA
0231	1/ 6/76	23.54.21	-17.0	-70.0	5.6	PERU-BOLIVIA BORDER
0232	1/ 7/76	0.10.43	10.0	119.0	5.1	PALAWAN, PHIL. IS.
0233	1/ 7/76	0.24.51	32.0	76.0	5.3	KASHMIR-INDIA BORDER
0234	1/ 7/76	1.30.59	53.0	158.0	4.1	NEC KAMCHATKA
0235	1/ 7/76	1.57. 8	53.0	158.0	5.5	NEC KAMCHATKA
0236	1/ 7/76	2.18.29	29.0	58.0	3.7	SOUTHERN IRAN
0237	1/ 7/76	3.54.58	-30.0	-175.0	3.8	KERMADEC IS. REG.
0238	1/ 7/76	4.33. 4	53.0	158.0	5.3	NEC KAMCHATKA
0239	1/ 7/76	5.10.41	48.0	120.0	3.5	NORTHEASTERN CHINA
0240	1/ 7/76	6.22.38	9.0	-85.0	4.5	COSTA RICA
0241	1/ 7/76	6.59. 8	-47.0	166.0	5.0	OWC SOUTH IS., N.Z.
0242	1/ 7/76	7.50.43	40.0	142.0	5.1	NEC HONSHU, JAPAN
0243	1/ 7/76	8.53. 2	35.0	140.0	4.5	NEC HONSHU, JAPAN
0244	1/ 7/76	8.56.13	29.0	128.0	4.7	RYUKYU ISLANDS
0245	1/ 7/76	10. 6.43	38.0	140.0	4.4	HONSHU, JAPAN
0246	1/ 7/76	10.46.29	52.0	160.0	4.9	OEC KAMCHATKA
0247	1/ 7/76	11.38.31	51.0	159.0	4.4	OEC KAMCHATKA
0248	1/ 7/76	11.51.12	39.0	142.0	4.2	NEC HONSHU, JAPAN
0249	1/ 7/76	12.58.26	53.0	157.0	4.4	KAMCHATKA
0250	1/ 7/76	18.32. 6	26.0	128.0	5.0	RYUKYU ISLANDS

EVNO	DATE	TIME	LAT.	LONG.	MB	LOCATION
0251	1/ 7/76	21.27.42	36.0	139.0	4.2	HONSHU, JAPAN
0252	1/ 7/76	23.34.32	53.0	158.0	5.8	NEC KAMCHATKA
0253	1/ 8/76	1.17. 4	54.0	161.0	4.2	NEC KAMCHATKA
0254	1/ 8/76	3.34.28	51.0	159.0	4.5	OEC KAMCHATKA
0255	1/ 8/76	5.32. 9	-25.0	-177.0	4.1	S. OF FIJI ISLANDS
0256	1/ 8/76	6.24.55	35.0	72.0	5.1	PAKISTAN
0257	1/ 8/76	8. 3.29	25.0	123.0	4.3	SW RYUKYU ISLANDS
0258	1/ 8/76	8.40.25	41.0	21.0	3.6	GREECE-ALBANIA BOR.
0259	1/ 8/76	9. 3.23	53.0	157.0	4.0	KAMCHATKA
0260	1/ 8/76	10.30.41	51.0	160.0	5.9	OEC KAMCHATKA
0261	1/ 8/76	11.55.30	51.0	-179.0	4.1	ANDREANOF IS.
0262	1/ 8/76	12. 4.15	-25.0	-177.0	4.1	SOUTH OF FIJI IS.
0263	1/ 8/76	13.25.31	53.0	158.0	4.2	KAMCHATKA
0264	1/ 8/76	13.26.44	58.0	-156.0	4.2	ALASKA PENINSULA
0265	1/ 8/76	14.19.54	51.0	159.0	4.5	OEC KAMCHATKA
0266	1/ 8/76	15.50.22	53.0	158.0	5.3	NEC KAMCHATKA
0267	1/ 8/76	16. 1.19	-2.0	123.0	5.0	CELEBES
0268	1/ 8/76	17.54.39	52.0	159.0	3.8	NEC KAMCHATKA
0269	1/ 8/76	19.32.49	53.0	158.0	4.2	NEC KAMCHATKA
0270	1/ 8/76	19.53. 7	-12.0	166.0	4.8	SANTA CRUZ ISLANDS
0271	1/ 8/76	22.34.27	33.0	76.0	4.8	KASHMIR-INDIA BORDER
0272	1/ 8/76	23.48.23	33.0	76.0	3.6	KASHMIR-INDIA BORDER
0273	1/ 9/76	1.20.21	53.0	158.0	4.4	NEC KAMCHATKA
0274	1/ 9/76	2.19.28	35.0	24.0	3.6	CRETE
0275	1/ 9/76	2.51.35	5.0	97.0	4.1	NORTHERN SUMATRA
0276	1/ 9/76	6.48. 8	-29.0	-180.0	3.8	KERMADEC IS. REG.
0277	1/ 9/76	9. 9.24	37.0	69.0	3.8	AFGHANISTAN-USSR BOR
0278	1/ 9/76	9.41.50	17.0	120.0	4.0	LUZON, PHILIPPINES
0279	1/ 9/76	15.48.13	37.0	70.0	3.7	HINDU KUSH REGION
0280	1/ 9/76	19.11.11	37.0	70.0	4.0	HINDU KUSH REGION
0281	1/ 9/76	21.32. 7	-3.0	116.0	5.7	BORNEO
0282	1/ 9/76	21.49. 2	-8.0	-81.0	5.0	OFF COAST OF PERU
0283	1/ 9/76	23.50.22	33.0	74.0	4.2	SOUTHWESTERN KASHMIR
0284	1/10/76	1.52.18	11.0	118.0	4.3	PALAWAN, PHILIPPINES
0285	1/10/76	3.37.23	51.0	159.0	5.0	OEC KAMCHATKA
0286	1/10/76	3.50.34	39.0	73.0	3.3	KIRGHIZ SSR
0287	1/10/76	5.42. 1	25.0	96.0	3.9	BURMA
0288	1/10/76	6.10. 8	-25.0	-178.0	3.5	SOUTH OF FIJI IS.
0289	1/10/76	7.11.43	40.0	29.0	3.8	TURKEY
0290	1/10/76	8.58.46	43.0	-127.0	5.6	OFF COAST OF OREGON
0291	1/10/76	10.50.11	54.0	62.0	3.6	URAL MOUNTAINS REG.
0292	1/10/76	11.58.30	45.0	149.0	3.6	KURILE ISLANDS
0293	1/10/76	12.51.39	44.0	82.0	5.4	NORTHERN SINKIANG
0294	1/10/76	13.25.20	-25.0	-178.0	5.3	SOUTH OF FIJI IS.
0295	1/10/76	17. 9.59	17.0	145.0	4.2	MARIANA ISLANDS
0296	1/10/76	21.40. 6	41.0	21.0	3.4	GREECE-ALBANIA BOR.
0297	1/11/76	3.59. 9	38.0	21.0	3.7	IONIAN SEA
0298	1/11/76	4.55.32	38.0	21.0	3.6	IONIAN SEA
0299	1/11/76	10. 7.38	-25.0	-179.0	3.9	SOUTH OF FIJI IS.
0300	1/11/76	10.49. 7	53.0	158.0	4.8	NEC KAMCHATKA

EVNO	DATE	TIME	LAT.	LONG.	MB	LOCATION
0301	1/11/76	16.10.39	32.0	140.0	4.1	SOUTH OF HONSHU
0302	1/14/76	15.56.13	-32.0	-176.0	6.5	KERMADEC IS. REG.
0303	1/14/76	21.43.56	36.0	-121.0	4.4	CENTRAL CALIFORNIA
0304	1/15/76	4.46.47	49.0	80.0	5.0	EASTERN KAZAKH SSR
0305	1/16/76	5.36.31	32.0	51.0	4.5	IRAN
0306	1/16/76	8.32.19	50.0	158.0	5.1	KURILE ISLANDS
0307	1/16/76	10.45. 8	41.0	68.0	4.1	CENTRAL KAZAKH SSR
0308	1/16/76	17.10. 6	37.0	72.0	4.6	AFGHAN.-USSR BORDER
0309	1/16/76	21.21. 5	32.0	74.0	3.8	INDIA-PAK. BORDER
0310	1/16/76	21.46.22	-30.0	-177.0	5.5	KERMADEC IS.
0311	1/17/76	6.22.45	52.0	79.0	3.4	EASTERN KAZAKH SSR
0312	1/17/76	9.56.40	-25.0	-178.0	4.8	SOUTH OF FIJI IS.
0313	1/20/76	0. 3.25	41.0	21.0	3.5	GREECE-ALBANIA BOR.
0314	1/20/76	1.25.26	41.0	22.0	3.2	GREECE
0315	1/20/76	6.42.34	53.0	158.0	4.5	NEC KAMCHATKA
0316	1/20/76	7.57. 6	33.0	80.0	3.9	TIBET
0317	1/20/76	10.13.29	23.0	-113.0	4.9	OWC BAJA, CALIF.
0318	1/20/76	13.31.31	40.0	19.0	3.2	ALBANIA
0319	1/20/76	14. 0.46	31.0	95.0	4.2	TIBET
0320	1/20/76	23.18. 0	34.0	142.0	4.1	OEC HONSHU, JAPAN
0321	1/21/76	6. 1.28	65.0	142.0	4.8	EASTERN SIBERIA
0322	1/21/76	10. 5.14	43.0	149.0	6.4	KURILE ISLANDS
0323	1/21/76	18. 1.54	57.0	163.0	5.4	NEC KAMCHATKA
0324	1/22/76	2. 9.38	43.0	149.0	4.4	KURILE ISLANDS REG.
0325	1/22/76	9.39. 7	43.0	149.0	4.6	KURILE ISLANDS REG.
0326	1/22/76	10.50.36	53.0	158.0	4.8	NEC KAMCHATKA
0327	1/22/76	14.51.10	40.0	29.0	3.3	TURKEY
0328	1/22/76	21.45.41	23.0	101.0	3.9	YUNNAN PROV., CHINA
0329	1/22/76	23.53.28	18.0	-93.0	4.2	CHIAPAS, MEXICO
0330	1/23/76	0.41. 2	46.0	153.0	4.4	KURILE ISLANDS REG.
0331	1/23/76	1.26. 8	37.0	70.0	5.0	HINDU KUSH REGION
0332	1/23/76	5.44.27	-6.0	123.0	6.5	CELEBES
0333	1/23/76	8. 4. 5	44.0	153.0	4.1	KURILE ISLANDS REG.
0334	1/23/76	9.16.33	44.0	46.0	3.5	EASTERN CAUCASUS
0335	1/23/76	11.54.23	40.0	69.0	4.3	SOUTHEAST UZBEK SSR
0336	1/24/76	17.16.38	40.0	40.0	3.6	TURKEY
0337	1/25/76	1.11.38	12.0	121.0	5.0	PALAWAN, PHILIPPINES
0338	1/25/76	10.59.50	15.0	-90.0	4.3	GUATEMALA
0339	1/25/76	11.51.51	57.0	58.0	3.4	URAL MTNS. REGION
0340	1/26/76	3.17.47	15.0	-91.0	4.4	GUATEMALA
0341	1/26/76	22.55.41	33.0	49.0	3.2	WESTERN IRAN
0342	1/27/76	0.24.30	33.0	96.0	3.8	TSINGHAI, CHINA
0343	1/27/76	9. 0. 0	31.0	51.0	3.6	IRAN
0344	1/27/76	19.23.18	32.0	76.0	4.4	KASHMIR-INDIA BOR.
0345	1/27/76	21.34.42	36.0	75.0	3.6	EASTERN KASHMIR
0346	1/28/76	11. 4. 7	45.0	45.0	3.2	SOUTHWESTERN RUSSIA
0347	1/28/76	13.41.42	32.0	49.0	3.6	WESTERN IRAN
0348	1/29/76	4.19.49	40.0	46.0	4.0	IRAN-USSR BORDER
0349	1/29/76	10. 9.28	36.0	71.0	3.7	PAKISTAN
0350	1/29/76	13.39.30	41.0	21.0	3.3	GREECE-ALBANIA BOR.

EVNO	DATE	TIME	LAT.	LONG.	MB	LOCATION
0351	1/29/76	18.45.56	43.0	-127.0	4.4	OFF COAST OF OREGON
0352	2/ 1/76	3. 3.32	-2.0	-77.0	4.6	ECUADOR
0353	2/ 1/76	11.14.55	18.0	-102.0	5.6	MICHOACAN, MEX.
0354	2/ 1/76	20.28.15	33.0	80.0	3.7	KASHMIR-TIBET BORDER
0355	2/ 2/76	3. 0.16	51.0	159.0	5.6	OEC KAMCHATKA
0356	2/ 3/76	10. 3.21	36.0	70.0	4.2	HINDU KUSH REGION
0357	2/ 3/76	16.39.47	34.0	51.0	5.1	IRAN
0358	2/ 4/76	9. 1.52	16.0	-90.0	6.5	GUATEMALA
0359	2/ 4/76	11.24.57	13.0	-91.0	4.3	NC OF GUATEMALA
0360	2/ 5/76	4. 8.48	22.0	125.0	5.2	SOUTHEAST OF TAIWAN
0361	2/ 5/76	19.38.29	40.0	29.0	3.4	TURKEY
0362	2/ 6/76	13. 4.32	36.0	51.0	3.2	IRAN
0363	2/ 6/76	18.19.25	15.0	-91.0	6.2	GUATEMALA
0364	2/ 6/76	19.37.22	31.0	97.0	3.9	TIBET
0365	2/ 7/76	3.37.31	36.0	53.0	4.6	IRAN
0366	2/ 7/76	8.41.24	41.0	75.0	4.0	KIRGIZ-SINKIANG BOR.
0367	2/ 7/76	14. 4.40	35.0	27.0	3.8	CRETE
0368	2/ 7/76	14.47.52	54.0	60.0	3.5	URAL MTNS. REGION
0369	2/ 7/76	15.54.15	33.0	89.0	4.1	TIBET
0370	2/ 8/76	8.13.48	15.0	-89.0	4.8	HONDURAS
0371	2/ 9/76	6.30.20	31.0	49.0	3.4	WESTERN IRAN
0372	2/ 9/76	18.59. 5	55.0	162.0	4.5	NEC KAMCHATKA
0373	2/10/76	6.17.47	15.0	-91.0	4.9	GUATEMALA
0374	2/10/76	17.53.12	45.0	151.0	4.1	KURILE ISLANDS
0375	2/11/76	7.36.39	51.0	159.0	4.6	OEC KAMCHATKA
0376	2/12/76	1.44.35	47.0	154.0	4.4	KURILE ISLANDS
0377	2/12/76	6.55.51	37.0	69.0	3.8	AFGHAN.-USSR BORDER
0378	2/12/76	14.45. 6	38.0	-116.0	5.9	NEVADA
0379	2/13/76	5.39.43	53.0	159.0	3.4	NEC KAMCHATKA
0380	2/13/76	9.14.57	47.0	40.0	3.4	SOUTHWESTERN RUSSIA
0381	2/14/76	11.30. 4	38.0	-115.0	5.6	SOUTHERN NEVADA
0382	2/15/76	5.47.36	33.0	48.0	3.9	WESTERN IRAN
0383	2/15/76	21. 0.56	31.0	49.0	3.4	WESTERN IRAN
0384	2/16/76	14.45.46	23.0	101.0	5.0	YUNNAN PROV., CHINA
0385	2/16/76	23.41.40	52.0	160.0	4.2	OEC KAMCHATKA
0386	2/18/76	10.29.49	59.0	51.0	3.4	WESTERN RUSSIA
0387	2/18/76	13.17.30	47.0	44.0	3.2	SOUTHWESTERN RUSSIA
0388	2/19/76	9.38.40	23.0	100.0	4.8	BURMA-CHINA BORDER
0389	2/19/76	11.45.34	23.0	101.0	3.7	YUNNAN PROV., CHINA
0390	2/19/76	22.52. 8	47.0	75.0	3.4	CENTRAL KAZAKH SSR
0391	2/20/76	0.32.36	53.0	157.0	3.8	KAMCHATKA
0392	2/20/76	10.58.39	55.0	80.0	3.2	CENTRAL RUSSIA
0393	2/20/76	23. 5.33	38.0	74.0	4.5	TADZHIK-SINKIANG BOR
0394	2/20/76	23.12.24	38.0	74.0	4.4	TADZHIK-SINKIANG BOR
0395	2/20/76	23.19.36	38.0	74.0	4.2	TADZHIK-SINKIANG BOR
0396	2/21/76	17.38.38	38.0	75.0	3.5	SOUTHERN SINKIANG
0397	2/24/76	6.25.30	14.0	-92.0	4.3	GUATEMALA
0398	2/24/76	21.57.59	35.0	81.0	4.2	TIBET
0399	2/26/76	3.23.46	36.0	76.0	4.0	EASTERN KASHMIR
0400	2/26/76	11.19. 0	35.0	72.0	5.4	PAKISTAN

EVNO	DATE	TIME	LAT.	LONG.	MB	LOCATION
0401	2/26/76	13.46.28	-33.0	-179.0	4.6	S. OF KERMADEC IS.
0402	2/26/76	21.38.34	40.0	69.0	3.8	SE UZBEK SSR
0403	2/26/76	23. 8. 9	-23.0	170.0	4.4	LOYALTY IS. REG.
0404	2/27/76	3.36.15	-20.0	-68.0	5.6	CHILE-BOLIVIA BOR.
0405	2/27/76	3.51.20	-31.0	-178.0	4.6	KERMADEC IS. REG.
0406	2/27/76	5.37.49	51.0	179.0	4.1	RAT IS., ALEUTIANS
0407	2/27/76	11. 0.55	-25.0	-178.0	4.8	S. OF FIJI ISLANDS
0408	2/27/76	16.40.36	-31.0	178.0	3.7	KERMADEC IS. REG.
0409	2/28/76	3. 1.55	44.0	85.0	3.5	NORTHERN SINKIANG
0410	2/28/76	4.24.24	-25.0	-178.0	4.7	S. OF FIJI ISLANDS
0411	2/28/76	5.22.56	-32.0	-176.0	3.8	KERMADEC IS. REG.
0412	2/28/76	5.35. 2	-25.0	-178.0	4.7	S. OF FIJI ISLANDS
0413	2/28/76	7.15. 5	51.0	-170.0	3.8	ALEUTIAN ISLANDS
0414	2/28/76	11.25.35	-28.0	-176.0	4.8	KERMADEC IS. REG.
0415	2/28/76	12.43.31	-14.0	167.0	4.8	NEW HEBRIDES IS.
0416	2/28/76	14. 0.13	-32.0	-179.0	4.1	KERMADEC IS. REG.
0417	2/28/76	16.27.12	-40.0	-77.0	5.6	OC OF C. CHILE
0418	2/28/76	18. 2. 5	27.0	105.0	3.8	YUNNAN PROV., CHINA
0419	2/29/76	3.19. 1	21.0	122.0	3.9	PHILIPPINE IS. REG.
0420	2/29/76	3.45.29	31.0	50.0	3.6	IRAN
0421	2/29/76	5.58. 4	-10.0	-71.0	4.9	PERU-BRAZIL BOR. REG
0422	2/29/76	7.23.42	38.0	21.0	2.9	IONIAN SEA
0423	2/29/76	9.27.13	36.0	140.0	4.9	HONSHU, JAPAN
0424	2/29/76	12.49.38	46.0	150.0	3.8	KURILE ISLANDS
0425	2/29/76	13.14.23	-25.0	-178.0	3.8	S. OF FIJI ISLANDS
0426	2/29/76	16.49.58	-25.0	-178.0	3.6	S. OF FIJI ISLANDS
0427	2/29/76	19.33.28	-16.0	-174.0	4.7	TONGA ISLANDS
0428	2/29/76	20.23.18	44.0	142.0	3.9	HOKKAIDO, JAPAN
0429	2/29/76	20.34.13	36.0	22.0	3.9	MEDITERRANEAN SEA
0430	2/29/76	22.50.29	-25.0	-177.0	5.1	S. OF FIJI ISLANDS
0431	2/29/76	23.18.12	37.0	69.0	3.4	AFGHANISTAN-USSR BOR
0432	3/ 1/76	7.41.38	32.0	137.0	3.9	S. OF HONSHU, JAPAN
0433	3/ 1/76	9.42.34	-10.0	28.0	4.6	ZAIRE
0434	3/ 1/76	18.58.49	27.0	140.0	5.0	BONIN ISLANDS REG.
0435	3/ 2/76	6. 7.44	2.0	103.0	4.4	MALAY PENINSULA
0436	3/ 2/76	6.47.53	35.0	134.0	4.5	S. HONSHU, JAPAN
0437	3/ 2/76	10.51. 6	-6.0	155.0	5.2	SOLOMON ISLANDS
0438	3/ 2/76	15.46.26	-33.0	-179.0	4.8	S. OF KERMADEC IS.
0439	3/ 2/76	21.59.30	28.0	140.0	4.4	BONIN IS. REGION
0440	3/ 3/76	0.32.44	33.0	131.0	4.6	KYUSHU, JAPAN
0441	3/ 3/76	0.33.54	-25.0	-177.0	4.0	S. OF FIJI ISLANDS
0442	3/ 3/76	2.50.15	34.0	142.0	4.2	OEC HONSHU, JAPAN
0443	3/ 3/76	13.30.12	51.0	158.0	3.8	KURILE ISLANDS
0444	3/ 3/76	18.54. 8	35.0	72.0	3.6	PAKISTAN
0445	3/ 3/76	19.24.34	-23.0	173.0	4.1	LOYALTY IS. REG.
0446	3/ 3/76	22.50. 7	-7.0	124.0	5.3	BANDA SEA
0447	3/ 3/76	23.14. 1	9.0	-76.0	3.9	NC OF N. COLOMBIA
0448	3/ 4/76	1. 6. 9	-31.0	-180.0	3.4	MERMADEC IS. REG.
0449	3/ 4/76	1.52. 9	-12.0	166.0	4.6	SANTA CRUZ ISLANDS
0450	3/ 4/76	2.50.16	-15.0	167.0	6.3	NEW HEBRIDES IS.

EVNO	DATE	TIME	LAT.	LONG.	MB	LOCATION
0451	3/ 4/76	3.14. 4	6.0	-73.0	4.2	NORTHERN COLOMBIA
0452	3/ 4/76	4.52.11	30.0	130.0	4.6	KYUSHU, JAPAN
0453	3/ 4/76	5.44.17	30.0	143.0	3.8	S. OF HONSHU, JAPAN
0454	3/ 4/76	6.12.48	43.0	149.0	4.0	KURILE ISLANDS REG.
0455	3/ 4/76	9.42.14	44.0	148.0	3.8	KURILE ISLANDS
0456	3/ 4/76	16. 9.14	53.0	146.0	4.2	SEA OF OKHOTSK
0457	3/ 4/76	18.45.39	33.0	76.0	3.7	EASTERN KASHMIR
0458	3/ 4/76	18.47.16	-17.0	166.0	4.4	NEW HEBRIDES IS.
0459	3/ 4/76	19.35.56	-25.0	-177.0	3.6	S. OF FIJI IS.
0460	3/ 4/76	22.37.10	-26.0	-176.0	3.6	SOUTH OF TONGA IS.
0461	3/ 4/76	23.57.49	49.0	156.0	3.7	KURILE ISLANDS
0462	3/ 5/76	0. 9.15	-25.0	-174.0	4.0	SOUTH OF TONGA IS.
0463	3/ 5/76	5.10.25	-17.0	170.0	4.2	NEW HEBRIDES IS.
0464	3/ 5/76	6. 4.26	-34.0	-177.0	4.2	S. OF KERMADEC IS.
0465	3/ 5/76	7.58.52	-25.0	-178.0	4.3	S. OF FIJI ISLANDS
0466	3/ 5/76	10.24.50	-33.0	-179.0	4.0	S. OF KERMADEC IS.
0467	3/ 5/76	10.34.51	46.0	79.0	3.6	EASTERN KAZAKH SSR
0468	3/ 5/76	11.50.41	44.0	148.0	3.8	KURILE ISLANDS
0469	3/ 5/76	18.26.59	-26.0	180.0	4.9	S. OF FIJI ISLANDS
0470	3/ 5/76	20.49. 3	41.0	21.0	3.5	GREECE-ALBANIA BOR.
0471	3/ 6/76	1.16.18	35.0	137.0	3.6	SOUTHERN HONSHU
0472	3/ 6/76	1.52.23	46.0	154.0	3.8	KURILE ISLANDS REG.
0473	3/ 6/76	11. 7. 9	0.0	122.0	5.8	NORTHERN CELEBES
0474	3/ 6/76	12.21.43	58.0	-157.0	4.4	ALASKA PENINSULA
0475	3/ 6/76	13.35.42	33.0	48.0	4.1	IRAN-IRAQ BORDER
0476	3/ 6/76	15. 6.35	-7.0	155.0	5.3	SOLOMON ISLANDS
0477	3/ 6/76	16.54.39	34.0	135.0	4.5	NSC OF S. HONSHU
0478	3/ 6/76	17.47.31	52.0	-170.0	4.2	FOX IS., ALEUTIANS
0479	3/ 7/76	0.33.13	54.0	-168.0	3.6	FOX IS., ALEUTIANS
0480	3/ 7/76	0.42.22	27.0	59.0	4.0	SOUTHERN IRAN
0481	3/ 7/76	2. 6.20	31.0	130.0	3.7	KYUSHU, JAPAN
0482	3/ 7/76	2.54. 7	15.0	-92.0	4.9	NC OF CHIAPAS, MEX
0483	3/ 7/76	8.23.27	-26.0	-180.0	3.5	S. OF FIJI ISLANDS
0484	3/ 7/76	9.43.16	44.0	-131.0	4.8	OFF OREGON COAST
0485	3/ 7/76	11.37.21	1.0	-29.0	3.7	MID-ATLANTIC TIDGE
0486	3/ 7/76	12.19.19	36.0	68.0	4.2	HINDU KUSH REGION
0487	3/ 7/76	15.10.43	29.0	130.0	3.7	RYUKYU ISLANDS
0488	3/ 7/76	21.48.15	16.0	-109.0	5.0	OC OF MEXICO
0489	3/ 7/76	21.53.52	40.0	19.0	3.4	ALBANIA
0490	3/ 7/76	23.52.41	-32.0	-176.0	4.6	KERMADEC IS. REG.
0491	3/ 8/76	0.48.47	41.0	16.0	3.4	SOUTHERN ITALY
0492	3/ 8/76	2.59. 1	-25.0	-177.0	4.1	S. OF FIJI ISLANDS
0493	3/ 8/76	3.17.11	-25.0	-178.0	4.3	S. OF FIJI ISLANDS
0494	3/ 8/76	9.37.39	30.0	141.0	3.9	S. OF HONSHU, JAPAN
0495	3/ 8/76	9.57.29	35.0	72.0	3.7	PAKISTAN
0496	3/ 8/76	13.45.14	13.0	121.0	4.2	MINDORO, PHIL. IS.
0497	3/ 8/76	14.38. 5	-33.0	-180.0	4.5	S. OF KERMADEC IS.
0498	3/ 8/76	16.48.51	-25.0	-178.0	5.1	S. OF FIJI ISLANDS
0499	3/ 8/76	17. 3. 7	46.0	152.0	3.4	KURILE ISLANDS
0500	3/ 8/76	18.52.28	-25.0	-177.0	4.6	S. OF FIJI ISLANDS

EVNO	DATE	TIME	LAT.	LONG.	MB	LOCATION
0501	3/ 8/76	20. 6.18	-17.0	170.0	5.3	NEW HEBRIDES IS.
0502	3/ 8/76	22. 6.57	-25.0	-177.0	3.5	S. OF FIJI IS.
0503	3/ 8/76	22.35.38	-25.0	-178.0	4.5	S. OF FIJI ISLANDS
0504	3/ 8/76	23. 4.43	-25.0	-178.0	3.7	S. OF FIJI ISLANDS
0505	3/ 9/76	0.46.31	-49.0	164.0	4.3	OWC S. IS., N.Z.
0506	3/ 9/76	1. 9.48	46.0	87.0	3.9	NORTHERN SINKIANG
0507	3/ 9/76	5.23.47	-25.0	-177.0	4.4	S. OF FIJI ISLANDS
0508	3/ 9/76	5.26.47	38.0	21.0	2.9	IONIAN SEA
0509	3/ 9/76	6.33.28	43.0	146.0	3.9	HOKKAIDO, JAPAN
0510	3/ 9/76	7.42.38	14.0	-91.0	5.0	NC OF GUATEMALA
0511	3/ 9/76	10.16. 3	-28.0	-176.0	5.2	KERMADEC IS. REG.
0512	3/ 9/76	14. 0.11	38.0	-116.0	5.4	NEVADA
0513	3/ 9/76	17.36.26	33.0	47.0	3.7	IRAN-IRAQ BORDER REG
0514	3/ 9/76	22.56.41	12.0	92.0	3.9	ANDAMAN IS. REG.
0515	3/10/76	1. 0. 1	-2.0	101.0	4.3	SOUTHERN SUMATRA
0516	3/10/76	1.41.40	4.0	100.0	4.6	NORTHERN SUMATRA
0517	3/10/76	3.13.41	-26.0	-180.0	4.1	S. OF FIJI ISLANDS
0518	3/10/76	4.39.12	28.0	58.0	4.1	SOUTHERN IRAN
0519	3/10/76	5. 0.54	6.0	-73.0	3.8	NORTHERN COLOMBIA
0520	3/10/76	6.29.54	50.0	-179.0	4.9	ANDREANOF IS., ALEU.
0521	3/10/76	7.51.49	38.0	21.0	3.3	IONIAN SEA
0522	3/10/76	8.57.26	50.0	-179.0	4.5	ANDREANOF IS., ALEU.
0523	3/10/76	9. 4.46	14.0	-61.0	5.6	WINDWARD ISLANDS
0524	3/10/76	12.43. 3	44.0	150.0	4.4	KURILE ISLANDS
0525	3/10/76	13.27.46	-25.0	-176.0	4.0	S. OF TONGA ISLANDS
0526	3/10/76	15.50.45	23.0	123.0	4.2	SE OF TAIWAN
0527	3/10/76	20.41.22	-1.0	103.0	4.9	SOUTHERN SUMATRA
0528	3/10/76	21. 6.56	45.0	151.0	3.9	KURILE ISLANDS REG.
0529	3/10/76	22.30.49	55.0	161.0	3.6	NEC KAMCHATKA
0530	3/10/76	22.58.48	0.0	-30.0	3.6	MID-ATLANTIC RIDGE
0531	3/11/76	1.30. 1	64.0	-157.0	3.5	CENTRAL ALASKA
0532	3/11/76	12.25.40	14.0	-91.0	3.8	NC OF GUATEMALA
0533	3/11/76	14.55.46	24.0	124.0	4.5	SW RYUKYU IS.
0534	3/11/76	17.58.41	30.0	129.0	3.6	EAST CHINA SEA
0535	3/11/76	18.51.41	38.0	73.0	4.7	TADZHIK SSR
0536	3/11/76	20. 7.39	-32.0	-176.0	4.1	KERMADEC ISLANDS REG
0537	3/11/76	20.29.21	-30.0	-178.0	3.4	KERMADEC ISLANDS
0538	3/11/76	22.31.38	40.0	40.0	3.8	TURKEY
0539	3/12/76	4.35.14	13.0	127.0	4.3	PHILIPPINE IS. REG.
0540	3/12/76	5.50. 8	50.0	-179.0	4.3	ANDREANOF IS, ALEU.
0541	3/12/76	12.11.52	-25.0	179.0	3.8	S. OF FIJI ISLANDS
0542	3/12/76	15.59.14	-1.0	9.0	5.1	S. ATLANTIC OCEAN
0543	3/12/76	16.54.17	23.0	143.0	4.4	VOLCANO IS. REG.
0544	3/12/76	18.59.41	9.0	39.0	3.7	ETHIOPIA
0545	3/12/76	20.26.51	-33.0	-179.0	4.3	S. OF KERMADEC IS.
0546	3/13/76	5.22.41	-7.0	155.0	5.4	SOLOMON ISLANDS
0547	3/13/76	9.31.40	39.0	48.0	3.9	NORTHWESTERN IRAN
0548	3/13/76	11.27.20	35.0	27.0	3.7	CRETE
0549	3/13/76	13.52.38	49.0	152.0	3.9	KURILE ISLANDS
0550	3/13/76	14.33.54	64.0	-150.0	3.6	CENTRAL ALASKA

EVNO	DATE	TIME	LAT.	LONG.	MB	LOCATION
0551	3/13/76	16.30.42	14.0	-91.0	5.4	NC OF GUATEMALA
0552	3/13/76	18.42. 8	14.0	-90.0	4.1	GUATEMALA
0553	3/13/76	20.17. 1	30.0	130.0	3.7	KYUSHU, JAPAN
0554	3/13/76	21.44.26	6.0	-73.0	5.0	NORTHERN COLOMBIA
0555	3/14/76	2. 0.11	39.0	73.0	3.7	TADZHIK-SINKIANG BOR
0556	3/14/76	2.49.44	36.0	136.0	3.6	NWC HONSHU, JAPAN
0557	3/14/76	4.10. 4	36.0	73.0	3.5	AFGHAN.-USSR BORDER
0558	3/14/76	6.44.54	52.0	-175.0	4.5	ANDREANOF IS., ALEU.
0559	3/14/76	7.44.55	32.0	142.0	4.2	S. OF HONSHU, JAPAN
0560	3/14/76	7.57. 1	43.0	145.0	4.2	HOKKAIDO, JAPAN REG.
0561	3/14/76	12.30. 6	38.0	-116.0	5.9	NEVADA
0562	3/14/76	15.43.34	-18.0	180.0	4.5	FIJI ISLANDS
0563	3/14/76	16.13.31	-10.0	-10.0	3.7	ASCENSION IS. REG.
0564	3/14/76	19.42.46	38.0	75.0	4.2	TADZHIK-SINKIANG BOR
0565	3/14/76	20.22.47	44.0	149.0	4.8	KURILE ISLANDS
0566	3/14/76	21.52.22	-35.0	-106.0	4.7	EASTER IS. CORD.
0567	3/14/76	23. 4.38	27.0	138.0	4.5	BONIN IS. REG.
0568	3/14/76	23.54.10	51.0	158.0	3.4	KURILE ISLANDS
0569	3/15/76	1.11.28	45.0	144.0	3.9	HOKKAIDO, JAPAN REG.
0570	3/15/76	2.36.36	40.0	143.0	4.3	NEC HONSHU, JAPAN
0571	3/15/76	3.29.39	11.0	130.0	4.6	E. OF PHILIPPINE IS.
0572	3/15/76	3.57.23	42.0	142.0	4.3	HOKKAIDO, JAPAN REG.
0573	3/15/76	7. 2.44	36.0	138.0	3.9	HONSHU, JAPAN
0574	3/15/76	11.21.45	29.0	130.0	3.8	RYUKYU ISLANDS
0575	3/15/76	12.40.41	8.0	125.0	4.5	MINDANAO, PHIL. IS.
0576	3/15/76	13.48.29	41.0	142.0	4.5	NEC HONSHU, JAPAN
0577	3/15/76	15.16.14	21.0	38.0	4.0	SUDAN
0578	3/15/76	18.50.15	28.0	129.0	3.8	RYUKYU ISLANDS
0579	3/15/76	20. 1.54	38.0	21.0	3.1	IONIAN SEA
0580	3/15/76	23.25. 6	-25.0	180.0	3.7	S. OF FIJI ISLANDS
0581	3/16/76	1.51.45	6.0	126.0	4.5	MINDANAO, PHIL. IS.
0582	3/16/76	4.55.54	25.0	93.0	3.8	BURMA-INDIA BOR. REG
0583	3/16/76	5.18. 6	45.0	151.0	3.7	KURILE ISLANDS
0584	3/16/76	5.59.31	-38.0	-180.0	4.4	E. OF N. ISLAND, N.Z
0585	3/16/76	6.19. 9	41.0	77.0	5.2	KIRGIZ-SINKIANG BOR.
0586	3/16/76	8.42.50	41.0	77.0	3.6	KIRGIZ-SINKIANG BOR.
0587	3/16/76	12.46.34	35.0	27.0	3.6	CRETE
0588	3/16/76	14.15.58	38.0	21.0	3.0	IONIAN SEA
0589	3/16/76	15.33.10	1.0	-28.0	4.5	MID-ATLANTIC RIDGE
0590	3/16/76	17.28.36	27.0	55.0	3.6	SOUTHERN IRAN
0591	3/16/76	22.19.13	-25.0	-178.0	4.5	S. OF FIJI ISLANDS
0592	3/16/76	22.51.35	26.0	56.0	3.5	E. ARABIAN PENINSULA
0593	3/17/76	4.25.56	24.0	142.0	3.9	VOLCANO IS. REG.
0594	3/17/76	4.32.49	27.0	56.0	3.6	SOUTHERN IRAN
0595	3/17/76	14.15. 4	38.0	-115.0	5.7	SOUTHERN NEVADA
0596	3/17/76	14.45. 6	38.0	-116.0	5.6	NEVADA
0597	3/17/76	18.51. 7	35.0	72.0	3.5	PAKISTAN
0598	3/17/76	21.45. 5	-25.0	179.0	4.6	S. OF FIJI ISLANDS
0599	3/18/76	3.35.39	-26.0	179.0	4.2	S. OF FIJI ISLANDS
0600	3/18/76	5.56. 9	28.0	55.0	4.2	SOUTHERN IRAN

EVNO	DATE	TIME	LAT.	LONG.	MB	LOCATION
0601	3/18/76	7.26.17	24.0	94.0	3.6	BURMA-INDIA BOR. REG
0602	3/18/76	11. 6.56	-31.0	-178.0	4.8	KERMADEC IS. REG.
0603	3/18/76	11.30.28	-25.0	-178.0	4.0	S. OF FIJI ISLANDS
0604	3/18/76	15.12. 7	-26.0	-176.0	3.5	S. OF TONGA ISLANDS
0605	3/18/76	19.45.14	-25.0	179.0	5.2	S. OF FIJI ISLANDS
0606	3/18/76	22.51.44	36.0	71.0	3.6	PAKISTAN
0607	3/18/76	23.38.48	-25.0	-177.0	3.3	S. OF FIJI ISLANDS
0608	3/19/76	0.50.34	23.0	37.0	4.1	RED SEA
0609	3/19/76	2.18.20	-28.0	-176.0	4.8	KERMADEC IS. REG.
0610	3/19/76	3.31.26	37.0	87.0	4.1	S. SINKIANG PROV.
0611	3/19/76	3.36. 1	52.0	-168.0	3.9	FOX IS., ALEUTIANS
0612	3/19/76	9.40.56	-22.0	-178.0	4.3	S. OF FIJI ISLANDS
0613	3/19/76	11.30.21	10.0	123.0	4.0	NEGROS, PHIL. IS.
0614	3/19/76	11.49. 5	46.0	43.0	3.0	SOUTHWEST RUSSIA
0615	3/19/76	13. 3.52	38.0	67.0	6.5	AFGHAN.-USSR BORDER
0616	3/19/76	13.48.25	27.0	55.0	3.6	SOUTHERN IRAN
0617	3/19/76	15.54.23	3.0	-83.0	3.9	SOUTH OF PANAMA
0618	3/19/76	17.12. 2	40.0	143.0	3.6	NEC HONSHU, JAPAN
0619	3/19/76	17.42.50	39.0	74.0	3.2	S. SINKIANG PROV.
0620	3/19/76	18.35.51	39.0	73.0	3.3	TADZHIK-SINKIANG BOR
0621	3/19/76	21. 7.10	-28.0	-179.0	4.2	KERMADEC IS. REG.
0622	3/20/76	1. 6.56	24.0	122.0	5.1	TAIWAN
0623	3/20/76	3. 3.55	11.0	-44.0	4.6	N. ATLANTIC RIDGE
0624	3/20/76	3.11.58	4.0	123.0	4.8	CELEBES SEA
0625	3/20/76	4. 3.33	49.0	79.0	4.8	EASTERN KAZAKH SSR
0626	3/20/76	4.33.53	41.0	91.0	4.9	S. SINKIANG PROV.
0627	3/20/76	4.53.26	20.0	95.0	4.2	BURMA
0628	3/20/76	9.24. 3	28.0	55.0	4.6	SOUTHERN IRAN
0629	3/20/76	10.29.20	51.0	51.0	2.9	WESTERN KAZAKH SSR
0630	3/20/76	13.47.38	-21.0	179.0	4.5	S. OF FIJI ISLANDS
0631	3/20/76	18.39. 0	-39.0	178.0	5.2	N. IS., N.Z.
0632	3/20/76	18.52.37	36.0	71.0	4.4	PAKISTAN
0633	3/21/76	5.48. 0	-28.0	-176.0	4.2	KERMADEC IS. REG.
0634	3/21/76	8.22.20	7.0	126.0	4.7	MINDANAO, PJIL. IS.
0635	3/21/76	9.22.56	52.0	179.0	3.9	RAT IS., ALEUTIANS
0636	3/21/76	9.53.43	48.0	66.0	3.5	CENTRAL KAZAKH SSR
0637	3/21/76	10.32.20	42.0	146.0	4.7	OC HOKKAIDO, JAPAN
0638	3/21/76	11. 9.57	-32.0	180.0	3.8	KERMADEC IS. REG.
0639	3/21/76	12. 3.13	41.0	70.0	4.0	TADZHIK SSR
0640	3/21/76	15. 5.31	-25.0	-177.0	3.9	S. OF FIJI ISLANDS
0641	3/21/76	17.33.29	53.0	-168.0	4.7	FOX IS., ALEUTIANS
0642	3/21/76	19.59.28	43.0	144.0	4.1	HOKKAIDO, JAPAN REG.
0643	3/21/76	23.10.23	24.0	124.0	4.9	SW RYUKYU ISLANDS
0644	3/22/76	2.42.52	28.0	55.0	3.8	SOUTHERN IRAN
0645	3/22/76	5. 8.58	53.0	-167.0	4.6	FOX IS., ALEUTIANS
0646	3/22/76	6.15.33	36.0	73.0	4.4	AFGHAN.-USSR BORDER
0647	3/22/76	7.51.50	-25.0	-177.0	3.7	S. OF FIJI ISLANDS
0648	3/22/76	8.13.35	28.0	55.0	3.7	SOUTHERN IRAN
0649	3/22/76	9.14. 3	-28.0	-176.0	4.6	KERMADEC IS. REG.
0650	3/22/76	11.50. 7	51.0	156.0	4.2	KURILE ISLANDS

EVNO	DATE	TIME	LAT.	LONG.	MB	LOCATION
0651	3/22/76	16.56.16	-25.0	-178.0	3.7	S. OF FIJI ISLANDS
0652	3/22/76	19.50.23	47.0	154.0	4.5	KURILE ISLANDS
0653	3/22/76	20.52.35	35.0	71.0	4.3	PAKISTAN
0654	3/22/76	21.42.13	35.0	72.0	4.1	PAKISTAN
0655	3/22/76	21.58.40	42.0	145.0	3.6	HOKKAIDO, JAPAN REG.
0656	3/23/76	4.17.51	23.0	143.0	4.1	VOLCANO IS. REG.
0657	3/23/76	4.44.32	61.0	4.0	4.3	SOUTHERN NORWAY
0658	3/23/76	10. 8.12	38.0	143.0	4.1	NEC HONSHU, JAPAN
0659	3/23/76	11.31.30	30.0	142.0	4.8	SOUTH OF HONSHU
0660	3/23/76	11.58.40	31.0	143.0	4.1	SOUTH OF HONSHU
0661	3/23/76	12.33.44	35.0	68.0	4.3	HINDU KUSH REG.
0662	3/23/76	14.26.21	1.0	-85.0	4.1	OC OF ECUADOR
0663	3/23/76	14.36.42	-3.0	156.0	4.8	N. OF SOLOMON IS.
0664	3/23/76	21.43.37	-25.0	-177.0	4.3	SOUTH OF FIJI IS.
0665	3/23/76	23.47. 4	44.0	150.0	4.1	KURILE ISLANDS
0666	3/24/76	0.52.57	30.0	139.0	4.2	SOUTH OF HONSHU
0667	3/24/76	4.45.59	-29.0	-178.0	6.8	KERMADEC ISLANDS
0668	3/24/76	5.51. 7	-25.0	-179.0	4.1	SOUTH OF FIJI IS.
0669	3/24/76	6.25. 8	-30.0	-177.0	4.4	KERMADEC ISLANDS
0670	3/24/76	6.59.21	-26.0	-178.0	4.5	SOUTH OF FIJI IS.
0671	3/24/76	8.14.37	-30.0	-177.0	4.8	KERMADEC ISLANDS
0672	3/24/76	14.53. 8	51.0	160.0	4.5	OEC KAMCHATKA
0673	3/24/76	15.44.50	53.0	-168.0	4.5	FOX IS., ALEUTIANS
0674	3/24/76	17.58. 5	35.0	71.0	4.5	PAKISTAN
0675	3/24/76	19. 3.23	22.0	121.0	4.0	TAIWAN REGION
0676	3/24/76	20.44. 1	9.0	95.0	4.1	NICOBAR IS. REG.
0677	3/25/76	0.19.25	-24.0	-177.0	5.0	SOUTH OF FIJI IS.
0678	3/25/76	0.41.45	38.0	-89.0	4.2	SOUTHERN ILLINOIS
0679	3/25/76	1.48. 7	46.0	152.0	4.3	KURILE ISLANDS
0680	3/25/76	4. 3.36	9.0	95.0	4.1	NICOBAR ISLANDS REG.
0681	3/25/76	6.17.43	10.0	93.0	4.5	NICOBAR ISLANDS REG.
0682	3/25/76	6.33. 8	35.0	72.0	4.0	PAKISTAN
0683	3/25/76	8.16.31	8.0	95.0	5.1	NICOBAR ISLANDS REG.
0684	3/25/76	8.41.58	14.0	123.0	4.8	LUZON, PHILIPPINES
0685	3/25/76	11.54.27	34.0	48.0	4.4	WESTERN IRAN
0686	3/25/76	12.22. 1	15.0	-94.0	5.0	NC OF CHIAPAS MEXICO
0687	3/25/76	12.41. 4	-25.0	-179.0	4.4	SOUTH OF FIJI IS.
0688	3/25/76	16.58.28	8.0	94.0	4.5	NICOBAR ISLANDS REG.
0689	3/25/76	22. 1. 8	24.0	122.0	4.1	TAIWAN
0690	3/25/76	22.16.26	2.0	-86.0	5.2	GALAPAGOS IS. REG.
0691	3/25/76	23. 5. 2	20.0	-101.0	5.4	MICHOACAN, MEXICO
0692	3/26/76	2. 0. 5	72.0	-3.0	4.2	JAN MAYEN IS. REG.
0693	3/26/76	3.16.12	3.0	97.0	4.6	NORTHERN SUMATRA
0694	3/26/76	13.15.49	-29.0	-180.0	4.3	KERMADEC IS. REG.
0695	3/26/76	14.56. 2	-23.0	179.0	4.5	SOUTH OF FIJI IS.
0696	3/26/76	20.15.27	-59.0	-18.0	4.9	SW ATLANTIC OCEAN
0697	3/27/76	2.35. 4	-31.0	-178.0	5.4	KERMADEC ISLANDS
0698	3/27/76	19.41.46	-33.0	-177.0	5.8	S. OF KERMADEC IS.
0699	3/27/76	21.21. 3	6.0	126.0	4.6	MINDANAO, PHIL. IS.
0700	3/27/76	23.14.21	3.0	-83.0	4.5	SOUTH OF PANAMA

EVNO	DATE	TIME	LAT.	LONG.	MB	LOCATION
0701	3/28/76	1.42.18	14.0	144.0	5.5	S. OF MARIANA IS.
0702	3/29/76	6.19. 9	38.0	139.0	4.1	HONSHU, JAPAN
0703	3/28/76	6.55.17	53.0	-168.0	4.9	FOX IS. ALEUTIANS
0704	3/28/76	7.56.11	52.0	-168.0	4.1	FOX IS. ALEUTIANS
0705	3/28/76	8.48.51	41.0	81.0	4.7	SOUTHERN SINKIANG
0706	3/28/76	15. 1.17	-2.0	103.0	4.2	SOUTHERN SUMATRA
0707	3/28/76	16.49.40	39.0	140.0	4.2	HONSHU, JAPAN
0708	3/28/76	18. 2.24	8.0	-102.0	5.1	OFF COAST OF MEXICO
0709	3/28/76	18.11.32	25.0	123.0	4.1	SW RYUKYU ISLANDS
0710	3/28/76	20.19.29	32.0	-40.0	5.1	N. ATLANTIC RIDGE
0711	3/28/76	22.20. 7	42.0	142.0	5.2	HOKKAIDO, JAPAN
0712	3/28/76	22.33. 6	-25.0	-178.0	4.8	SOUTH OF FIJI IS.
0713	3/28/76	23.52. 8	14.0	123.0	4.5	LUZON, PHILIPPINES
0714	3/29/76	5.39.26	0.0	-84.0	6.0	OFF COAST ECUADOR
0715	3/29/76	6.59.50	46.0	48.0	4.5	SOUTHWESTERN RUSSIA
0716	3/29/76	8.21.59	22.0	122.0	4.5	TAIWAN REGION
0717	3/29/76	11.52.20	-19.0	180.0	5.1	FIJI ISLANDS
0718	3/29/76	14.58.40	28.0	55.0	4.0	SOUTHERN IRAN
0719	3/29/76	18.34.18	-28.0	179.0	4.2	KERMADEC IS. REG.
0720	3/29/76	19.48.24	46.0	151.0	5.5	KURILE ISLANDS
0721	3/29/76	20.29.29	51.0	-177.0	4.2	ALEUTIAN ISLANDS
0722	3/29/76	21.25. 4	14.0	-94.0	4.3	NC OF CHIAPAS MEXICO
0723	3/30/76	3.32.44	41.0	143.0	4.3	NEC HONSHU, JAPAN
0724	3/30/76	5.53.16	40.0	142.0	5.5	NEC HONSHU, JAPAN
0725	3/30/76	6. 4.18	40.0	142.0	5.6	NEC HONSHU, JAPAN
0726	3/30/76	6.48.27	24.0	94.0	4.3	BURMA-INDIA BOR. REG
0727	3/30/76	8. 7.54	20.0	136.0	4.3	PHILIPPINE SEA
0728	3/30/76	9. 9.25	40.0	141.0	5.1	HONSHU, JAPAN
0729	3/30/76	9.24.51	37.0	142.0	5.2	OEC HONSHU JAPAN
0730	3/30/76	11.23.18	35.0	140.0	4.2	NEC HONSHU JAPAN
0731	3/30/76	14.32.25	-25.0	-178.0	4.1	S. OF FIJI ISLANDS
0732	3/30/76	16. 0.25	-15.0	-178.0	4.7	FIJI ISLANDS REGION
0733	3/30/76	22.58.53	-15.0	-174.0	4.5	SAMOA ISLANDS REGION
0734	3/30/76	23.53. 2	39.0	142.0	4.3	NEC HONSHU, JAPAN
0735	3/31/76	0. 0.59	59.0	-33.0	4.9	NORTH ATLANTIC OCEAN
0736	3/31/76	2.34.33	30.0	56.0	4.4	SOUTHERN IRAN
0737	3/31/76	10.35.44	54.0	161.0	4.0	NEC KAMCHATKA
0738	3/31/76	21. 9.22	35.0	72.0	4.9	PAKISTAN
0739	3/31/76	23.38.38	32.0	58.0	4.5	IRAN
0740	3/31/76	23.49.37	58.0	-36.0	5.1	NORTH ATLANTIC OCEAN
0741	4/ 1/76	3.36.51	10.0	124.0	4.8	PHILIPPINE ISLANDS
0742	4/ 1/76	4.31. 3	51.0	101.0	4.8	MONGOLIA
0743	4/ 1/76	6.18.25	-15.0	-174.0	5.1	SAMOA ISLANDS REGION
0744	4/ 1/76	7.53.43	35.0	72.0	4.2	PAKISTAN
0745	4/ 1/76	19.21. 4	7.0	-73.0	5.1	NORTHERN COLOMBIA
0746	4/ 1/76	21. 3.46	-16.0	167.0	5.4	NEW HEBRIDES IS.
0747	4/ 2/76	5.25.31	44.0	149.0	4.4	KURILE ISLANDS
0748	4/ 2/76	8.31.16	4.0	-83.0	5.5	SOUTH OF PANAMA
0749	4/ 2/76	10.23.57	-29.0	-178.0	4.9	KERMADEC IS. REG.
0750	4/ 2/76	12.49.16	-4.0	105.0	4.2	SOUTHERN SUMATRA

EVNO	DATE	TIME	LAT.	LONG.	MB	LOCATION
0751	4/ 2/76	15.49.46	-33.0	-178.0	5.0	S. OF KERMADEC IS.
0752	4/ 2/76	17. 8. 1	37.0	141.0	5.6	NEC HONSHU, JAPAN
0753	4/ 2/76	17.52.55	44.0	41.0	4.1	WESTERN CAUCASUS
0754	4/ 2/76	20.33. 6	-58.0	-25.0	5.1	S. SANDWICH IS. REG.
0755	4/ 3/76	0.26.55	52.0	-170.0	5.0	ALEUTIAN ISLANDS
0756	4/ 3/76	0.56.10	52.0	-170.0	4.2	FOX IS., ALEUTIANS
0757	4/ 3/76	2.56.41	52.0	-170.0	4.2	FOX IS., ALEUTIANS
0758	4/ 3/76	3.50.44	16.0	-93.0	4.0	NC OF CHIAPAS MEXICO
0759	4/ 3/76	8.51.57	32.0	140.0	4.1	S. OF HONSHU, JAPAN
0760	4/ 3/76	10. 6.48	44.0	149.0	4.2	KURILE ISLANDS
0761	4/ 3/76	10.49.28	52.0	-170.0	4.3	FOX IS., ALEUTIANS
0762	4/ 3/76	12.34.20	-32.0	-179.0	4.4	KERMADEC IS. REG.
0763	4/ 3/76	19.14.17	45.0	149.0	4.9	KURILE ISLANDS
0764	4/ 3/76	21.42. 7	3.0	-83.0	4.1	SOUTH OF PANAMA
0765	4/ 3/76	23.19.41	11.0	122.0	4.4	PHILIPPINE ISLANDS
0766	4/ 4/76	1.30. 0	52.0	-170.0	4.3	FOX IS., ALEUTIANS
0767	4/ 4/76	11. 7. 4	52.0	-170.0	4.0	FOX IS., ALEUTIANS
0768	4/ 4/76	15.40. 4	-20.0	179.0	4.4	SOUTH OF FIJI IS.
0769	4/ 4/76	17.55.20	13.0	-86.0	4.6	NICARAGUA
0770	4/ 4/76	21.15.39	40.0	142.0	4.7	NEC HONSHU, JAPAN
0771	4/ 4/76	22.38. 1	50.0	150.0	4.9	NW OF KURILE ISLANDS
0772	4/ 4/76	23.11.24	-20.0	179.0	4.5	SOUTH OF FIJI IS.